ISBN 978-3-902842-22-0

International Commission on Illumination
Commission Internationale de l'Eclairage
Internationale Beleuchtungskommission

PROCEEDINGS of CIE Expert Symposium on Measurement Uncertainties in Photometry and Radiometry for Industry

12 September 2014

Vienna, Austria

CIE x040:2014

UDC:	535.24	Descriptor:	Photometry
	535.241.5		Quantities related to photometric and other measurements
	535.241.535		Calibration

THE INTERNATIONAL COMMISSION ON ILLUMINATION

The International Commission on Illumination (CIE) is an organization devoted to international co-operation and exchange of information among its member countries on all matters relating to the art and science of lighting. Its membership consists of the National Committees in about 40 countries.

The objectives of the CIE are:

1. To provide an international forum for the discussion of all matters relating to the science, technology and art in the fields of light and lighting and for the interchange of information in these fields between countries.
2. To develop basic standards and procedures of metrology in the fields of light and lighting.
3. To provide guidance in the application of principles and procedures in the development of international and national standards in the fields of light and lighting.
4. To prepare and publish standards, reports and other publications concerned with all matters relating to the science, technology and art in the fields of light and lighting.
5. To maintain liaison and technical interaction with other international organizations concerned with matters related to the science, technology, standardization and art in the fields of light and lighting.

The work of the CIE is carried on by seven Divisions each with about 20 Technical Committees. This work covers subjects ranging from fundamental matters to all types of lighting applications. The standards and technical reports developed by these international Divisions of the CIE are accepted throughout the world.
A plenary session is held every four years at which the work of the Divisions and Technical Committees is reported and reviewed, and plans are made for the future. The CIE is recognized as the authority on all aspects of light and lighting. As such it occupies an important position among international organizations.

LA COMMISSION INTERNATIONALE DE L'ECLAIRAGE

La Commission Internationale de l'Eclairage (CIE) est une organisation qui se donne pour but la coopération internationale et l'échange d'informations entre les Pays membres sur toutes les questions relatives à l'art et à la science de l'éclairage. Elle est composée de Comités Nationaux représentant environ 40 pays.

Les objectifs de la CIE sont :

1. De constituer un centre d'étude international pour toute matière relevant de la science, de la technologie et de l'art de la lumière et de l'éclairage et pour l'échange entre pays d'informations dans ces domaines.
2. D'élaborer des normes et des méthodes de base pour la métrologie dans les domaines de la lumière et de l'éclairage.
3. De donner des directives pour l'application des principes et des méthodes d'élaboration de normes internationales et nationales dans les domaines de la lumière et de l'éclairage.
4. De préparer et publier des normes, rapports et autres textes, concernant toutes matières relatives à la science, la technologie et l'art dans les domaines de la lumière et de l'éclairage.
5. De maintenir une liaison et une collaboration technique avec les autres organisations internationales concernées par des sujets relatifs à la science, la technologie, la normalisation et l'art dans les domaines de la lumière et de l'éclairage.

Les travaux de la CIE sont effectués par sept Divisions, ayant chacune environ 20 Comités Techniques. Les sujets d'études s'étendent des questions fondamentales, à tous les types d'applications de l'éclairage. Les normes et les rapports techniques élaborés par ces Divisions Internationales de la CIE sont reconnus dans le monde entier.
Tous les quatre ans, une Session plénière passe en revue le travail des Divisions et des Comités Techniques, en fait rapport et établit les projets de travaux pour l'avenir. La CIE est reconnue comme la plus haute autorité en ce qui concerne tous les aspects de la lumière et de l'éclairage. Elle occupe comme telle une position importante parmi les organisations internationales.

DIE INTERNATIONALE BELEUCHTUNGSKOMMISSION

Die Internationale Beleuchtungskommission (CIE) ist eine Organisation, die sich der internationalen Zusammenarbeit und dem Austausch von Informationen zwischen ihren Mitgliedsländern bezüglich der Kunst und Wissenschaft der Lichttechnik widmet. Die Mitgliedschaft besteht aus den Nationalen Komitees in rund 40 Ländern.

Die Ziele der CIE sind:

1. Ein internationales Forum für Diskussionen aller Fragen auf dem Gebiet der Wissenschaft, Technik und Kunst der Lichttechnik und für den Informationsaustausch auf diesen Gebieten zwischen den einzelnen Ländern zu sein.
2. Grundnormen und Verfahren der Messtechnik auf dem Gebiet der Lichttechnik zu entwickeln.
3. Richtlinien für die Anwendung von Prinzipien und Vorgängen in der Entwicklung internationaler und nationaler Normen auf dem Gebiet der Lichttechnik zu erstellen.
4. Normen, Berichte und andere Publikationen zu erstellen und zu veröffentlichen, die alle Fragen auf dem Gebiet der Wissenschaft, Technik und Kunst der Lichttechnik betreffen.
5. Liaison und technische Zusammenarbeit mit anderen internationalen Organisationen zu unterhalten, die mit Fragen der Wissenschaft, Technik, Normung und Kunst auf dem Gebiet der Lichttechnik zu tun haben.

Die Arbeit der CIE wird in sieben Divisionen, jede mit etwa 20 Technischen Komitees, geleistet. Diese Arbeit betrifft Gebiete mit grundlegendem Inhalt bis zu allen Arten der Lichtanwendung. Die Normen und Technischen Berichte, die von diesen international zusammengesetzten Divisionen ausgearbeitet werden, sind auf der ganzen Welt anerkannt.
Alle vier Jahre findet eine Session statt, in der die Arbeiten der Divisionen berichtet und überprüft werden, sowie neue Pläne für die Zukunft ausgearbeitet werden. Die CIE wird als höchste Autorität für alle Aspekte des Lichtes und der Beleuchtung angesehen. Auf diese Weise unterhält sie eine bedeutende Stellung unter den internationalen Organisationen.

Published by the

COMMISSION INTERNATIONALE DE L'ECLAIRAGE
CIE Central Bureau
Babenbergerstrasse 9, A-1010 Vienna, AUSTRIA
Tel: +43(1)714 31 87
e-mail: ciecb@cie.co.at
www.cie.co.at

ISBN 978-3-902842-22-0

International Commission on Illumination
Commission Internationale de l'Eclairage
Internationale Beleuchtungskommission

PROCEEDINGS of CIE Expert Symposium on Measurement Uncertainties in Photometry and Radiometry for Industry

12 September 2014

Vienna, Austria

CIE x040:2014

UDC:	535.24	Descriptor:	Photometry
	535.241.5		Quantities related to photometric and other measurements
	535.241.535		Calibration

Any mention of organizations or products does not imply endorsement by the CIE. Whilst every care has been taken in the compilation of any lists, up to the time of going to press, these may not be comprehensive.

The following table provides an overview of the papers presented at the symposium. They are published in the proccedings in consecutive order of presentation. Contributions that have not been submitted are marked as such (“n.s.”).

The authors are responsible for the contents of their papers.

Please note: For direct access of a paper click on the respective page number.

UNCERTAINTIES IN ELECTRICAL POWER MEASUREMENT OF SOLID-STATE LIGHTING PRODUCTS

Tuomas Poikonen
Centre for Metrology and Accreditation (MIKES), P.O. Box 9, FI-02151 Espoo, FINLAND
tuomas.poikonen@mikes.fi

Abstract

As incandescent lamps for general lighting are being phased out, consumers buy more energy-efficient lighting products based on their specifications. The various optical designs and built-in power converters of energy-saving lamps bring challenges to test laboratories, as well as NMIs, and often lead to increased measurement uncertainties. Characterization of compact-fluorescent lamps (CFLs) and solid-state lamps based on light-emitting diodes (LEDs) with low uncertainty requires understanding of both optical and electrical properties of the lamps, as well as of the measurement equipment. Due to the problematic behaviour of some lamp electronics, and underlying systematic errors, electrical power measurement may be the major source of uncertainty in measurement of luminous efficacy. This paper focuses on electrical power measurements of solid-state lighting products on a general level, and identifies different sources of uncertainties that need to be evaluated for each measurement system in order to determine the total uncertainty of electrical power measurement.

Keywords: Luminous efficacy, solid-state lighting, LED, CFL, electrical power, uncertainty

1 Background

Luminous efficacy (lm/W) of a light source is defined as the luminous flux (lm) produced by the source divided by its active electrical power consumption (W) [1]. Luminous efficacy measurement of incandescent lamps operated with stable laboratory power supplies is quite straightforward due to well-known photometric and electrical properties of the lamps. Often, the measurement of DC-current and AC-voltage at 50/60 Hz fundamental frequency can be carried out with uncertainty much lower than that of luminous flux measurement. Incandescent lamps used for general lighting are being replaced by energy-efficient lighting products, such as CFLs and LED-lamps. Electrical power measurement of these lamps, operated with AC-voltage, is much more challenging because the lamps contain small built-in AC-DC power converters that draw non-sinusoidal current, and may have an influence on the stability of the measurement [2-4]. Figure 1 shows an example of power converters used in LED-lamps, as well as a distorted current waveform measured for a 6.5-W LED-lamp. Measurements carried out for a larger group of lamps have shown that the total harmonic distortion (THD) and power factor of LED-lamps can vary in a wide range of 30 – 280 % and 0.2 – 1.0, respectively [5].

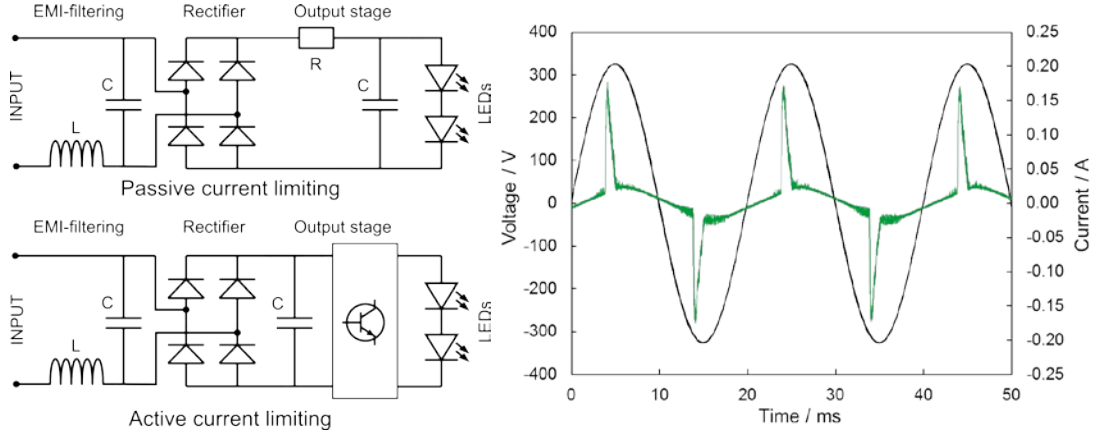

Figure 1 – Simple built-in power converter electronics used in LED-lamps, and a heavily distorted current waveform measured for an LED-lamp.

2 Sources of uncertainty

2.1 Quality of the AC-voltage source

Due to the instability and distortion characteristics of a typical low-voltage power system, luminous efficacy measurement of CFLs and LED-lamps requires using of regulated AC-voltage sources [1,5,6]. Figure 2 shows a comparison of two luminous efficacy measurements carried out for the same LED-lamp using voltage directly from the AC-line, as well as using a programmable AC-voltage source. The stabilization time in both cases is approximately the same, but the difference in the voltage fluctuation between the two methods is clear. The voltage of the AC-line changes nearly 2 volts during the 1-hour measurement, whereas the programmable AC-voltage source manages to regulate the load voltage within ± 0.03 %. By coincidence, the voltages and efficacies recorded at the end of these two measurements are nearly the same, but the standard deviation of luminous efficacy is reduced approximately by a factor of 15, when using the regulated AC-voltage source.

The influence of the AC-voltage to the measured efficacy also depends on the built-in power converter of the lamp. Some lamps are designed to produce the same luminous output with input voltages of 110 – 230 VAC, whereas lamps with passive current limiting are typically affected by the changes in the AC-voltage. In addition to the voltage and frequency regulation capabilities, the distortion characteristics of the AC-voltage source should be taken into account. IES LM-79 recommends AC-sources with better than ±0.2 % voltage regulation, and THD less than 3 % [1]. If the AC-voltage is distorted, the active power is carried not only by the 50/60 Hz fundamental frequency, but also by the harmonic frequencies. Depending on the power measurement equipment, this can lead to increased measurement uncertainty [6-8].

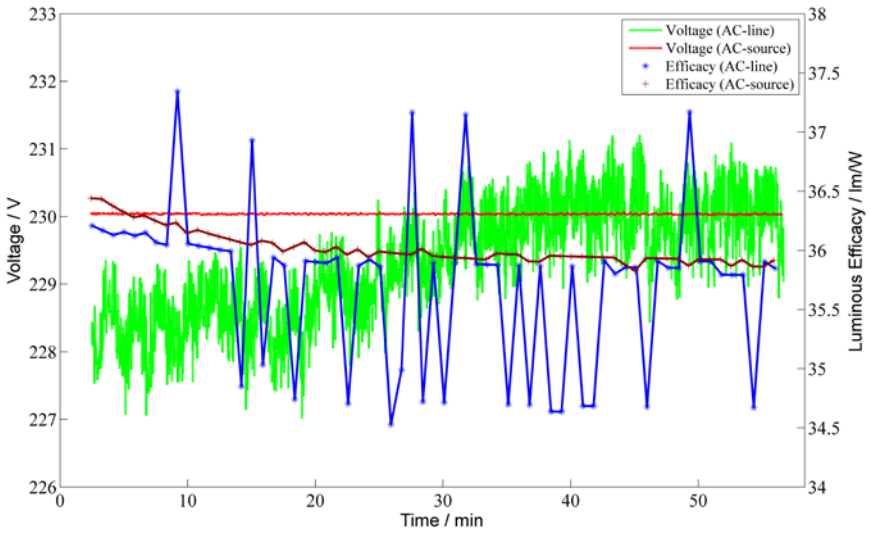

Figure 2 – Stabilization of luminous efficacy of an LED-lamp with regulated (AC-source) and unregulated (AC-line) voltage sourcing.

2.2 Influence of wiring configuration

The input impedance Z_V of high quality digital voltmeters (DVMs), used in laboratories for measurements of DC-voltage and current, often have input impedances larger than 10 GΩ. As a result, such meters do not load the circuit under measurement, such as DC-source feeding an incandescent lamp. Typically, a 4-wire measurement configuration is used in DC-measurements, where 2 wires feed the current to the lamp, and another 2 wires are connected parallel to the lamp to measure its voltage. The current is measured using a shunt resistor R_s, and another DVM. Due to the high input impedance Z_V of the DC-voltage measurement, the current flowing through the voltage measurement circuit is negligible.

The situation is different, when measuring lamps that are operated using AC-voltage (Figure 3 - left side). The typical input impedance Z_V of a high-quality DVM or a power meter in AC-mode is no longer 10 GΩ, but closer to 1 – 2 MΩ. Now, a current i_{VD} flows through Z_V, and is measured together with the current of the LED-lamp i_{SSL}. As a result, the measured RMS-

current and the shape of the current waveform contain errors. This is problematic also, because the waveform is used for calculating further parameters, such as THD and power factor of the lamp. Another thing to consider is that the Z_V of the voltage input depends on frequency, and if connected parallel to the lamp, may pass some of the high frequency harmonic currents through, and cause further errors in the measured current waveform. With a supply voltage of 230 V and the wiring configuration optimized for high currents, a Z_V of 1 MΩ would pass a current of i_{VD} = 230 V / 1 MΩ = 0.23 mA. If the current consumption of a 7-W LED-lamp was approximately 30.4 mA, the relative error caused by the current i_{VD} flowing through the current input terminal of the power meter would be 0.76 %.

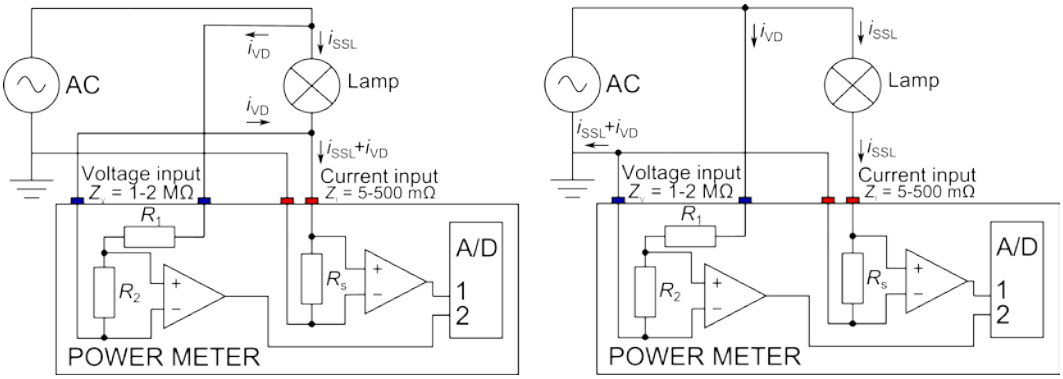

Figure 3 – Two power meter wiring configurations optimized for measurement of high currents (left) and for small currents (right).

These errors can be avoided by using the measurement configuration optimized for small currents (Figure 3 – right side). In this method, the voltage is measured over the AC-voltage source. This ensures that the current measured by the power meter is the current of the lamp. However, a small error is made in the voltage measurement that can be corrected for. If we consider the same 7-W LED-lamp, and a shunt resistor size of R_s = 100 mΩ, the error made in the voltage measurement is only 3 mV that is less than 0.002 % of 230 V. In addition to the two wiring configurations, the cable length and its effect on the results need to be evaluated.

2.3 Stabilization of the lamp

Due to the differences in electrical and thermal designs of lamps, the stabilization times required by different products vary a lot, from 30 min to several hours [1,5,8]. IES LM-79 suggests that final values of the flux and electrical power can be recorded, if the changes in these parameters have been less than 0.5 % within a time window of 30 min [1]. This is a good solution for well-behaving lamps, whose stabilization follows typical exponential decay, as shown for the LED-lamp of Figure 4.

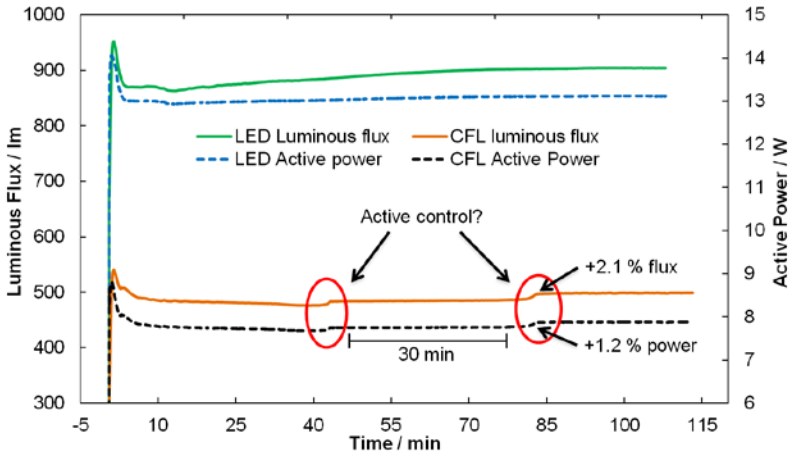

Figure 4 – Stabilization time of luminous flux and active electrical power consumption of an LED-lamp and a CFL.

If the recommendation of LM-79 is followed, the uncertainty due to the stabilization is less than 0.1 % for the LED-lamp. This value was obtained as the relative difference between two flux values recorded for the lamp, the first value according to the LM-79 recommendation, and the second after 4 hours of operation, when nearly no change in the flux was observed.

However, some CFLs and LED-lamps have shown signs of active electronic control of their luminous output. Figure 4 shows such stabilization data measured for a CFL. This particular lamp is very peculiar, as it changes its operation approximately every 45 min. As a result, it is possible to find time windows longer than 30 min, in which it is possible to record the final values according to the LM-79 recommendation. For this lamp, it would be possible to record the final values around 70 min of operation, but around 82 min, the built-in electronics cause a change of +2.1 % in flux, and +1.2 % in electrical power. This equals +0.96 % change in the measured luminous efficacy. For this kind of lamps, much longer stabilization times are needed. However, increasing the stabilization time does not always help, as some lamps have shown that their electrical power and luminous flux follow a certain pattern that repeats randomly, and no equilibrium is ever reached. For such lamps, the uncertainty due to stabilization is inevitably higher.

2.4 Frequency response and traceability of the power meter

Due to the high harmonic content of CFLs and LED-lamps, a power meter or analyzer with frequency range up to several hundred kHz or 1 MHz should be used [2-9]. The effective frequency response of the electrical power measurements is affected by several different factors. If we consider the current measurement alone, the performance of the power meter is influenced by the size and construction of the shunt resistor, as well as the noise and nonlineariy of the analog amplifiers and A/D-converters. Selecting a proper shunt resistor size for the measurement can have an important role in both the noise performane and the frequency response of the measurement. A larger shunt resistor will provide better signal-to-noise ratio, but also adds to the effective impedance seen by the lamp. Also, no shunt resistor is purely resistive in nature, but has inductance and capacitance as well. Often, the effect of shunt capacitance can be reduced to a negligible level by manufacturing choices, but the remaining inductance causes the frequency response of the shunt to deviate from unity at high frequencies, causing error to the measured current waveform.

Another thing to consider when estimating the measurement uncertainty of a commercial power meter or analyzer is what kind of signal processing is carried out inside the equipment? It is often unknown whether a power meter corrects for the deviations of its response, or not. This is problematic also, because not all power meters allow saving of the raw waveform data for analysis, or the resolution and sample rate of the saved data is drastically reduced. Another problem is the traceability of calibration at high frequencies. Many power meter and analyzer manufacturers report values for current, voltage and power measured at individual frequencies up to 1 MHz, but do not provide information on traceability for the measurements. Also, there is currently no commonly accepted method for calibration of power meters or analyzers with non-sinusoidal waveforms, such as those found in many CFLs and LED-lamps.

2.5 Effect of source impedance

Test laboratories use regulated AC-voltage sources from different manufacturers to operate lamps in efficacy measurements. Depending on the manufacturer, the output impedance of the AC-voltage source can be different at two different test laboratories. A problem arises, when the impedance of the AC-voltage source is coupled with the power converter of the lamp. The operation of the lamp electronics may thus depend on the effective impedance, and differences of several percents in the measured luminous flux and power can occur depending on the lamp type and the measurement equipment used [6-8]. In addition to the output impedance of the AC-voltage source, the impedance of the shunt resistor used in the power meter or analyzer, as well as the impedance of the cables all affect the operation of the lamp, and the measured values.

To overcome this problem, an impedance stabilization network needs to be developed for measurements of energy-saving lighting products [6,8,9]. Impedance stabilization networks for measurement of electromagnetic compatibility (EMC) are commercially available, but they are not directly suitable for measurements of energy-saving lamps, for which the most

interesting frequency range is 50 Hz – 200 kHz. Zhao *et al.* [6] have developed a prototype of such network that is connected between the AC-voltage source and the lamp, in order to reduce the effect of source impedance seen directly by the lamp. MIKES has developed an adjustable power line impedance emulator (APLIE) [9] based on publications of power system impedance, and using a modified version of the stabilization network published by Zhao *et al.*

The power consumption of the APLIE is 4 W of active and 100 var of reactive power that is compatible with most AC-voltage sources used in test laboratories. Due to adjustability, the APLIE can be used for testing the sensitivity of lamps to various source impedances as well. Test measurements with APLIE have shown to improve the stability of the measurements, and reducing the high frequency harmonic content of lamps. Figure 5 shows an example of current waveforms measured for an LED-lamp in two conditions. On the left side (blue), the measured current of the LED-lamp was measured without the stabilization network, and is therefore rich in harmonics up to several hundred kHz. On the right side (red), the stabilization network is connected between the AC-voltage source and the LED-lamp, significantly reducing the high frequency harmonic components.

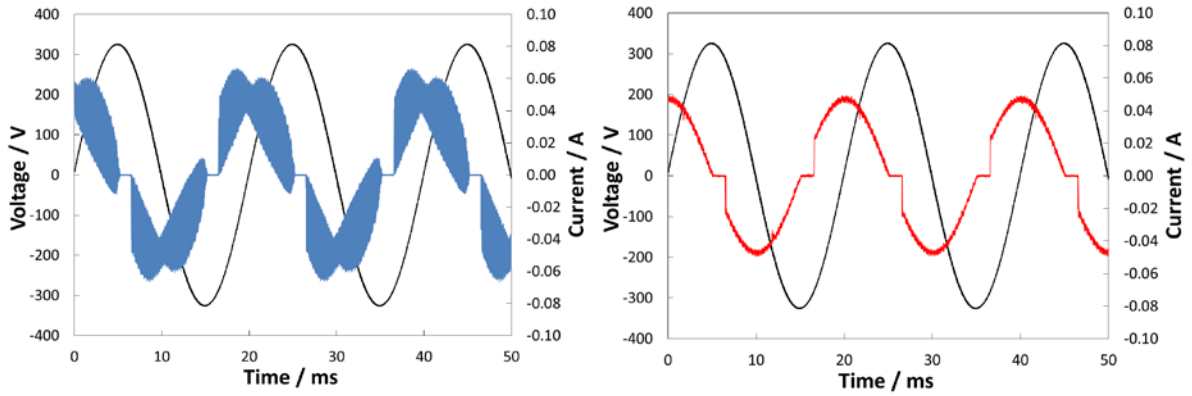

Figure 5 – Current waveform of an LED-lamp with direct connection to the AC-voltage source (left) and with an impedance stabilization network with maximum impedance setting (right).

In addition to these findings, some lamps have shown changes in measured efficacy, up to 1.2 %, depending on the impedance setting in use [9]. The test measurements carried out with the APLIE show the importance of further developing such a network that could be eventually standardized, and used by test laboratories to overcome the problems caused by the built-in electronics of energy-saving lighting products.

3 Conclusions

Uncertainties involved in electrical power measurement of AC-operated energy-saving lighting products are often underestimated. Analysis of the uncertainties requires understanding of the characteristics of the lamps under measurement, as well as of the equipment used for the AC-voltage supply and power measurement. Special attention should be given to the wiring of the equipment, distortion and stability of the AC-voltage source, and the frequency response of the power meter. The problem of source impedance and methods to implement a fixed stabilization network for measurements of energy-saving lighting products are currently being investigated in a project ENG62 Metrology for Efficient and Safe Innovative Lighting (MESaIL), funded by the European Metrology Research Programme (EMRP). The outcome of the project will be shared with CIE and other standardization bodies, when it is available.

References

1. IES 2008 IES LM-79-08. Approved Method: Electrical and Photometric Measurements of Solid-State Lighting Products. New York: IES.
2. VAN DER BROECK, H. 2007. Power driver topologies and control schemes for LEDs. In Proceedings of IEEE Applied Power Electronics Conference APEC, Anaheim, US, 1319-1325.
3. YE, Z. et al. 2008. A topology study of single-phase offline AC/DC converters for high brightness white LED lighting with power factor pre-regulation and brightness dimmable. In Proceedings of IEEE Industrial Electronics Conference IECON, Orlando, US, 1961–1967.
4. LINLIN, G. et al. 2009. Means of eliminating electrolytic capacitor in AC/DC power supplies for LED lightings. *Trans. Power Elec.* 24, 1399-1408.
5. POIKONEN, T. et al. 2012. Luminous efficacy measurement of solid-state lamps. *Metrologia*, 49, S135–S140.
6. ZHAO, D. et al. 2012. The influence of source impedance in electrical characterizationof solid state lighting sources. In Proceedings of IEEE Precision Electromagnetic Measurements Conference CPEM 2012, Washington DC, US, 300-301.
7. MARTINSONS, C. et al. 2013. Influence of current and voltage harmonic distortion on the power measurement of LED lamps and luminaires. In Proceedings of CIE Centenary Conference Towards a new century of light, Paris, France, 290-299.
8. ZHAO, D. et al. 2014. Traceable measurement of the electrical parameters of solid-state lighting products. In Proceedings of IEEE Precision Electromagnetic Measurements Conference CPEM 2014, Rio de Janeiro, Brazil, 650-651.
9. POIKONEN, T. et al. 2014. Adjustable power line impedance emulator for characterization of energy-saving lamps. In Proceedings of NEWRAD 2014 conference, Espoo, Finland, 348-349.

A PRACTICAL METHOD OF EVALUATING UNCERTAINTIES IN CHROMATICITY VALUES DERIVED FROM SPECTRAL MEASUREMENTS

Bergen, A.S.J.
Photometric Solutions International, Melbourne, AUSTRALIA
tonyb@photometricsolutions.com

Abstract

In the world of spectroradiometry, a common task is to take a measured spectrum and derive chromaticity data. However many industrial testing and calibration laboratories do not have the know-how or confidence to approach the determination of uncertainties for the derived data.

This paper outlines the methods developed for calculating uncertainty for derived quantities in spectroradiometry in the author's photometric testing laboratory. An Excel spreadsheet is used to model the various contributions to the measurement uncertainty on a wavelength-by-wavelength basis. This enables the easy assessment of uncertainties for individual measurements or for typical spectral data for types of light sources.

Keywords: measurement uncertainty, uncertainty budget, chromaticity

1 Introduction

Many testing and calibration laboratories will perform spectral measurements on light sources and use the measured spectra to calculate derived data. Commonly calculated properties include chromaticity coordinates (x, y) and (u', v'); correlated colour temperature; D_{uv}; and colour rendering indices. The equipment used may be a simple CCD array spectroradiometer or may be a monochromator- or double-monochromator-based spectroradiometer. There is much literature covering the characterisation and calibration of these devices. However the laboratory staff may not always perform a detailed analysis of the uncertainty of measurement of the measured spectra and on the associated derived quantities.

It has historically been quite common for laboratories to assign an uncertainty value based on a rough estimate or based on an industry practice, eg: 0.003 in x and y coordinates, without making a rigorous evaluation or allowing for the specific properties of individual DUTs. While this may sometimes be because of convention or because a more rigorous approach is not enforced by an accreditation body, it is also often because the laboratory does not have the knowledge or experience to perform such a task. Moreover, they may not have the mathematical inclination to meticulously follow the methods of CIE 198:2011 (CIE, 2011).

A simple and practical way to approach this is to consider the various aspects of measurement that have an influence on the uncertainty of measurement and deal with each separately. Where it is not possible to make a direct statistical analysis of the uncertainty, it may be possible to model the effect or to perform some simple experiments to estimate the magnitude of errors which may be present. These separate components can then be combined in a spreadsheet and added in quadrature in the traditional manner.

It is important to note that this method may not be strictly mathematically rigorous, because it does not make allowances for correlations between the different uncertainty contributions. It also ignores the fact that some of the uncertainty contributions will have asymmetrical probability distributions. However it is easy and practical to implement and is certainly more rigorous than simply using the same default value of uncertainty for every measurement. Furthermore, when performing this analysis it is possible to see which components have a higher contribution to the uncertainty budget and which therefore may require further study to improve the measurement and reduce the uncertainty for future measurements.

In this paper, the focus of the discussion is on the uncertainty in x and y chromaticity coordinates measured using a CCD array spectrometer, but the principle can easily be transferred to the other derived quantities and other types of instruments. It should also be noted that the methods described here are in no way the only way to perform this analysis and individual laboratories may determine other methods more appropriate to their equipment or otherwise more superior to the methods offered here.

2 Common Sources of Error and How to Model Them

In this section some of the main contributions to uncertainty in spectral measurements and the derivation of chromaticity coordinates are discussed and ways to measure or model them are suggested.

2.1 Wavelength error

For strongly coloured light sources, wavelength error can be a significant source of uncertainty, and it will often be quite different for the x and y chromaticity coordinates. Take the three points marked on the CIE 1931 (x, y) chromaticity chart shown in Figure 1: green, blue-green and red.

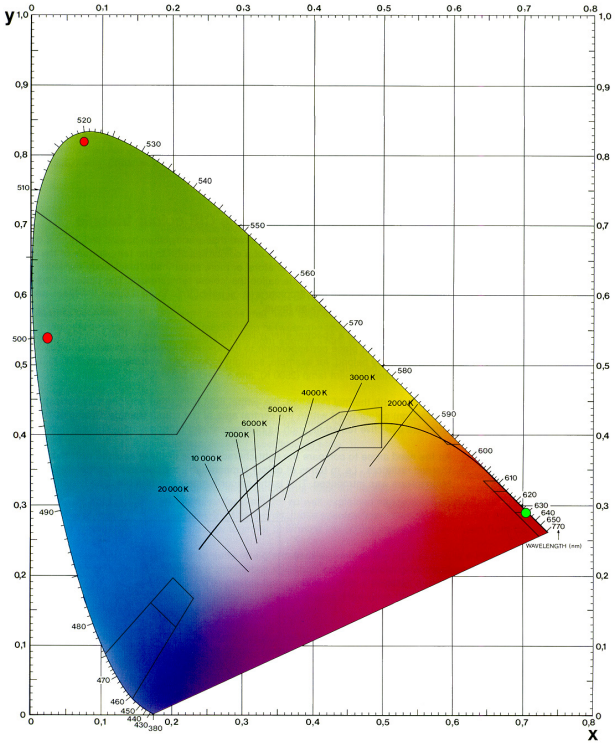

Figure 1 – CIE 1931 chromaticity chart with three colours marked

2.1.1 Green signal

The green point marked in Figure 1 is enlarged in Figure 2.

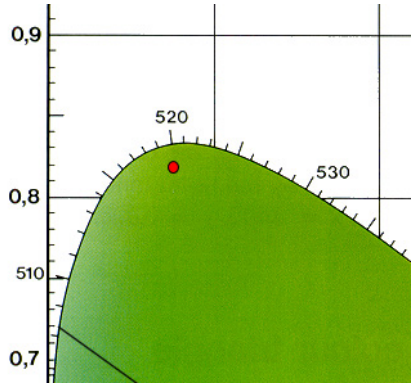

Figure 2 – Green signal

The wavelength scale is shown around the boundary of the colour space; here the wavelengths 510 nm, 520 nm and 530 nm can be seen. The green signal is close to the 520 nm point. A change in wavelength from 520 nm to 521 nm involves a large shift in the x coordinate, but only a small shift in the y coordinate. For monochromatic radiation the shift in the x coordinate is nearly 0.008, while for a narrow width LED the shift might be around 0.006 (the actual shift depends on the LED spectrum).

The ramification of this is that a spectrometer with a wavelength uncertainty of 0.5 nm may have a contribution to the x coordinate uncertainty of around 0.003 due to wavelength uncertainty alone when measuring a 520 nm green LED.

2.1.2 Blue-green signal

The blue-green point marked in Figure 1 is enlarged in Figure 3.

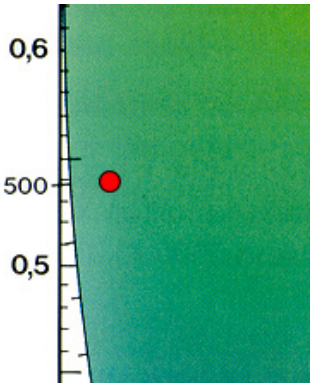

Figure 3 – Blue-green signal

In this case, the wavelength scale is roughly aligned with the y axis. For monochromatic radiation a change in wavelength of 1 nm results in a change in the y coordinate of around 0.025, while for an LED it may be around 0.020. An uncertainty in wavelength of 0.5 nm therefore may result in an uncertainty in the y coordinate of around 0.010 due to wavelength uncertainty alone when measuring a 500 nm blue-green LED.

2.1.3 Red signal

The red point marked in Figure 1 is enlarged in Figure 4.

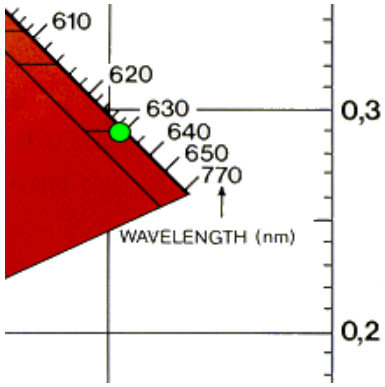

Figure 4 – Red signal

Here the wavelength scale is much narrower and is equal between the x and y coordinates. For monochromatic radiation a change in wavelength of 1 nm results in a change in the x and y coordinates of around 0.0013, while for an LED it may be around 0.0017. An uncertainty in wavelength of 0.5 nm therefore may result in an uncertainty in the x and y coordinates of around 0.0008 due to wavelength uncertainty alone when measuring a 630 nm red LED. Clearly this a less significant contribution to the uncertainty budget for a red LED compared with a green LED.

2.1.4 How to model

It is quite straightforward in a spreadsheet to simulate the effects of a shift in the wavelength scale on the chromaticity coordinates: one possible way to do so is given here for example.

The spectrum is pasted into a spreadsheet and interpolated to 0.1 nm intervals. The CIE 1931 colour matching functions are also inserted into the spreadsheet and interpolated to 0.1 nm intervals. The x and y coordinates are then calculated according to CIE 15 (CIE, 2004). The spectrum is then shifted by n rows corresponding to a wavelength uncertainty of 0.n: so for a wavelength uncertainty of 0.3 nm the spectrum is shifted by 3 rows. The chromaticity coordinates are calculated again and the differences in x and y from the original coordinates are noted. The spectrum is then shifted negatively by n rows; the coordinates calculated again and the differences again noted. The larger of the differences in both x and y are then taken as the uncertainty contribution due to wavelength shift.

Note 1: This process assumes a uniform shift in wavelength scale across the spectrum, whereas in practice it is likely that wavelength errors may change across the spectrum. It is always preferable to model the wavelength scale more precisely and correct it better (thus reducing the uncertainty). But where this is not possible or practical then it is possible to estimate the maximum error and use this as a uniform shift.

Note 2: Here the effect is being analysed for the measured spectrum only. But the effect will also have a bearing on the calibration of the instrument with a reference lamp. This needs also to be modelled, taking into account both random (the wavelength shift will be different for the calibration and the measurement) and systematic (the wavelength shift will be the same for the calibration and the measurement) effects.

2.2 Nonlinearity error

Nonlinearity effects result in a distorted measured spectrum. For the measurement of phosphor-type white LEDs, this can result in an error in the measured height of the blue peak compared with the height of the photoluminescent part of the spectrum. One possible way of estimating the magnitude of this error in a CCD array spectrometer system is described here.

The equipment is set up to measure the source with the integration time set so that the peak signal is near full scale. A measurement is taken and the measured chromaticity coordinates are noted. The integration time is then reduced without adjusting the source, so that the peak drops. The change in chromaticity coordinates are noted. This process is repeated until the peak signal is quite low in the scale. For example, if the integration time is initially 100 ms, then further measurements may be made at 90 ms, 80 ms, 70 ms, ... , 10 ms as shown in Figure 5. The largest deviation in x and y coordinates from the original value can then be taken as an estimate of the possible error in the measurement and used in the uncertainty budget.

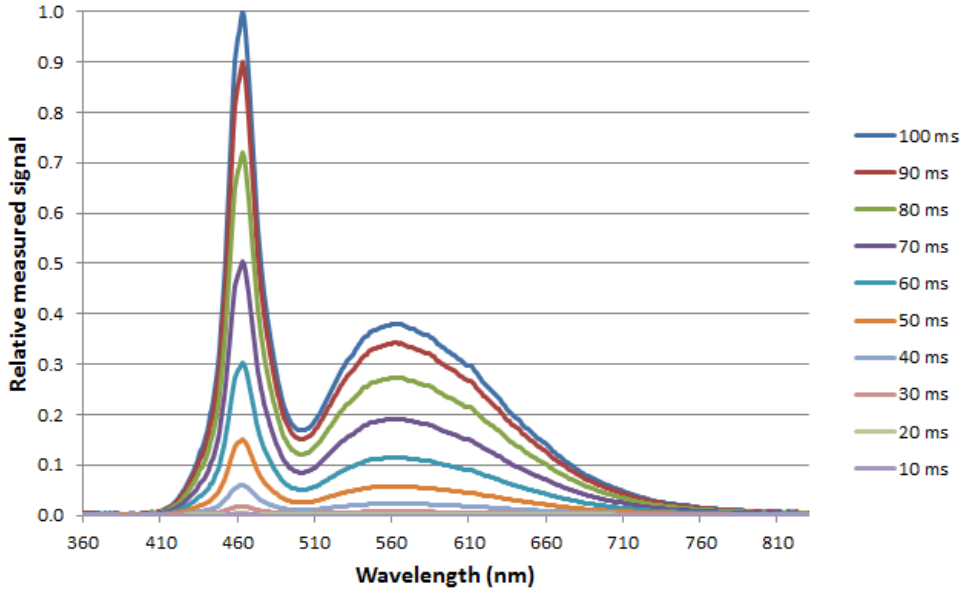

Figure 5 – Estimation of nonlinearity error

Note: By doing this experiment it may be found that the spectrometer's response becomes highly nonlinear near the CCD array's saturation level and best performance is achieved by using lower integration times.

2.3 Instrument bandpass

An important principle was learnt in CIE TC 2-60 (CIE, 2014): to estimate of the effect of instrument bandpass on the measured result, apply the bandpass again and record the differences in x and y. Applying the instrument's bandpass to the data again gives a good estimate of the effect that the instrument's bandpass had on the measured spectrum and derived quantities in the first place.

In Excel it is quite straightforward to convolve the measured spectrum with a function similar to the instrument's bandpass (eg: a 5 nm Gaussian) and note the effect that this has on the x and y coordinates.

2.4 Stray light

Take, for example, the measurement of an incandescent source with a red filter as shown in Figure 6 left, and the zoomed section in Figure 6 right.

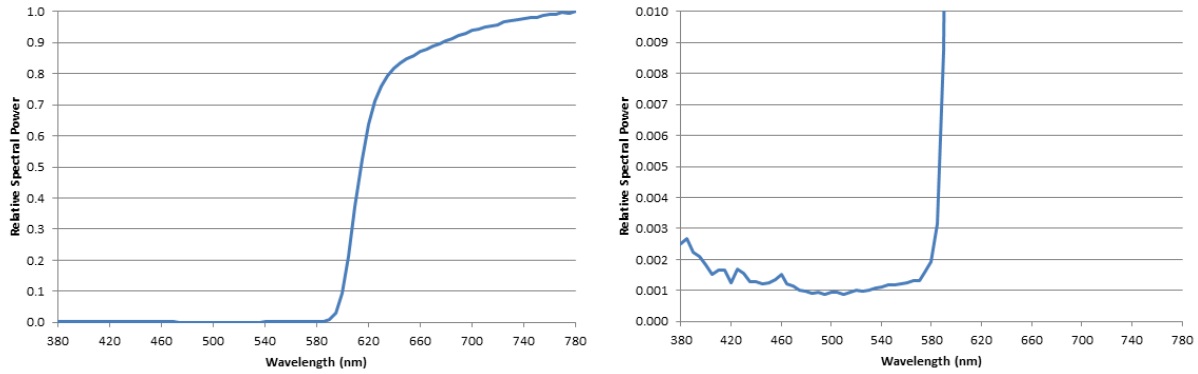

Figure 6 – Measurement of a red filter and zoomed section showing stray light

Clearly there is a large amount of stray light at the bottom end of the spectrum below 580 nm and there is also likely to be stray light in the rest of the spectrum but we can't distinguish it from the measured signal. If the stray light is spread uniformly across the spectrum then it will have the effect of shifting the chromaticity coordinates towards the equal energy point. For a red signal such as in Figure 6, this will affect the x coordinate substantially but will not affect the y coordinate much. For a green LED it will usually affect the y coordinate more than the x coordinate.

If possible it is best to minimise the stray light effect using a correction method such as that by Zong (2006). However where that is not possible, an approach like the following may be used.

- Assume that the stray light is constant across the spectrum.

  Note 1: This is not a great assumption but it is better than nothing.

  Note 2: It may be possible for the lab staff to determine a better model than this.

- Measure an incandescent source through a high-pass filter: the area below the cut-off should be effectively zero. Systematic non-zero readings in that region are likely to be attributable to stray light.

  Note: This should be separately validated to confirm that the spectral transmittance in the area below the cut-off is negligible.

- Calculate the average offset of the stray light as a proportion of the total signal area.
- Repeat for other filters with different cut-off wavelengths.
- Use these ratios to simulate artificially adding stray light to the measured spectrum: the difference is a reasonable estimate of error due to stray light.

Note 1: Stray light will also have affected the measurement of the reference lamp. The measured DUT spectrum will need to be corrected first by dividing through by the measured reference lamp spectrum and then multiplying through by the reference lamp spectrum minus stray.

Note 2: This is just a correction for estimating the stray light error. This process should not be used for correcting reported results unless it has been rigorously validated.

Note 3: If, by rigorous validation, we know that there should not be any signal measured in the area below the cut-off then it is possible to improve our estimate of the chromaticity coordinates by setting the values below the cut-off in the measured spectrum to zero. This is shown in Figure 7. In this case, setting the values below the cut-off to zero shifts the coordinates from (0.6953, 0.3007) to (0.6981, 0.3008), i.e. from z = 0.0040 to z = 0.0011. Given that we would expect the chromaticity coordinates to be very close to the z = 0 line, we can conclude that this has improved our estimate of the x and y coordinates.

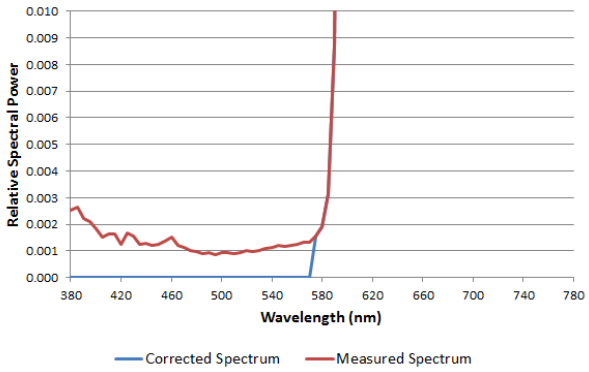

Figure 7 – Corrected stray light for red filter

2.5 Random noise

When we are taking a measurement, we will often observe the instrument readings fluctuating. Once the DUT and the instrument are warmed up and stable these fluctuations will often just be random noise, such as shown in Figure 8.

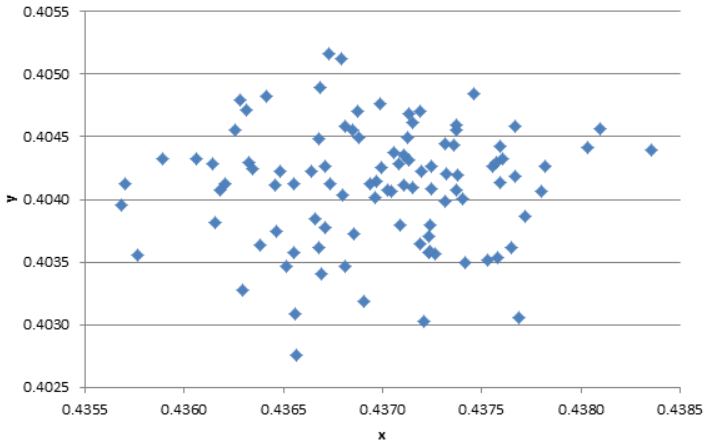

Figure 8 – Random noise in x and y coordinates

The instrument taking the readings may come with software that will enable the random noise to be assessed statistically. A large number of values can be recorded and the average and standard deviation taken. If it is genuinely a random distribution (a simple check of the correlation coefficient will determine that) then the standard deviation could be divided by the square root of the number of measurements.

If it is not possible to record the values and treat them statistically, then the data can be "eyeballed" by looking at the readings and noting the minimum and maximum observed values. Note: this will now be a rectangular distribution.

2.6 Reference lamp calibration data

The reference lamp that was used to calibrate the instrument will have uncertainties associated with its calibrated spectral data. It is possible to assess the effect this uncertainty will have on the measurement uncertainty using the following method.

- Multiply the measured spectrum by the ratio of the reference lamp data plus uncertainty to the reference lamp data for each wavelength.
- Repeat for the reference lamp data minus uncertainty.
- Observe and record the largest deviation in x and y.

2.7 Reference lamp current setting

The reference lamp data will only be valid for the current (or voltage) setting stated in the calibration report. But when the reference lamp is run there will be some uncertainty in the current that is applied. One possible way to study this is to measure the reference lamp at the rated current and then again with a shift in current equivalent to the uncertainty in the current measurement. Spectra can be recorded for both positive and negative shifts in current. The effect on the chromaticity coordinates can then be treated in the same way as in Section 2.6 above.

2.8 Reference lamp aging

If the reference lamp has been calibrated several times then it is possible to observe the change in the spectrum of the lamp as it ages. Given the time since the last calibration and the time interval between calibrations it is then possible to estimate how the spectrum of the reference lamp may have changed since it was calibrated. The effect on the chromaticity coordinates can then be treated in the same way as in Section 2.6 above.

If there is no calibration history for the lamp, i.e. it has only been calibrated once, then the calibration laboratory that calibrated the lamp may be able to provide advice on how the lamp spectrum may change over time based on their experience with similar lamps. If no other guidance is available, it may be possible to assume that the lamp spectrum changes similarly to a small change in the applied current.

2.9 Interval between instrument calibrations

The throughput of the instrument may drift between calibrations. It is possible to estimate this effect by measuring an artefact immediately before and after calibration – the difference between the measurements will be representative of how much the instrument may have drifted since the previous calibration. With knowledge of how the instrument drifts between calibrations, the time interval between calibrations and the time since the last calibration, it is possible to estimate the effect that this has on the measured spectrum and therefore on the derived chromaticity coordinates.

Reducing the interval between calibrations will reduce this uncertainty component, but will impact the aging of the reference lamp(s) used to calibrate the equipment.

2.10 Applied current/voltage error

When we measure a DUT we will usually have a requirement to run it at a given voltage or current. However there will also be some uncertainty in the applied voltage or current. It is possible to measure the DUT at the original rated voltage or current, and then to vary the voltage or current by an amount equivalent to the uncertainty in the voltage or current measurement (plus and minus) and to observe the effect that this has on the chromaticity coordinates.

3 Add in Quadrature

As mentioned in the introduction, this paper considers the different contributions to the uncertainty budget in isolation and ignores any correlations between them. Thus it is approaching the uncertainty budget by simply adding the individual components in quadrature and specifically ignoring the correlation term in the law of propagation of uncertainties from the GUM (ISO, 1995).

Not all of the contributions described in Section 2 may apply to every specific measurement situation, and there may be additional uncertainty contributions which are not covered here. Sample spreadsheets for several different types of sources are shown in Figure 9 to Figure 13. Note that they are sample data only and the values in the spreadsheets should not be used as reference values for another laboratory's uncertainty assessment.

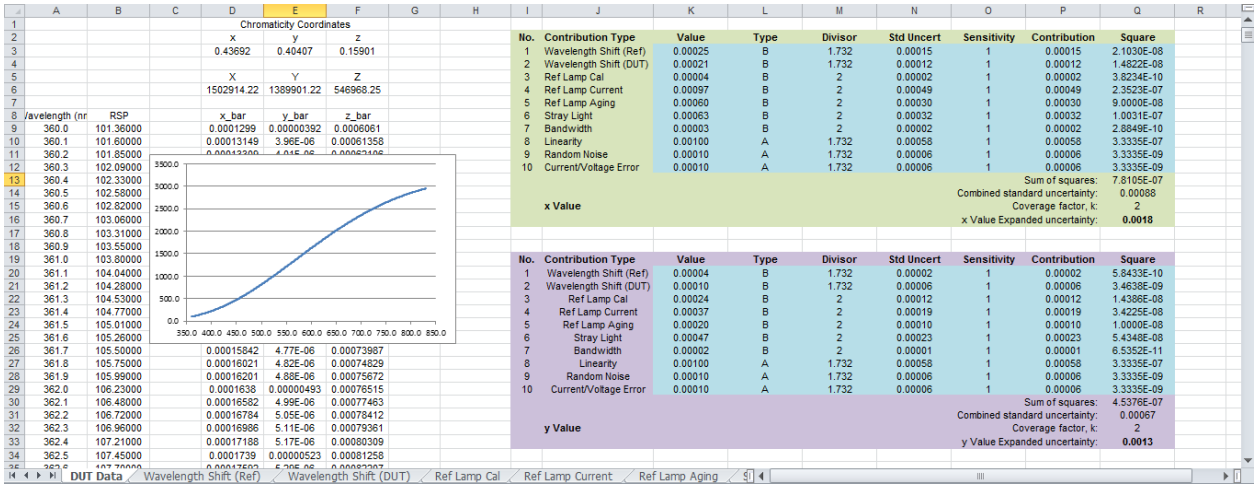

Figure 9 – Sample uncertainty spreadsheet for an incandescent lamp

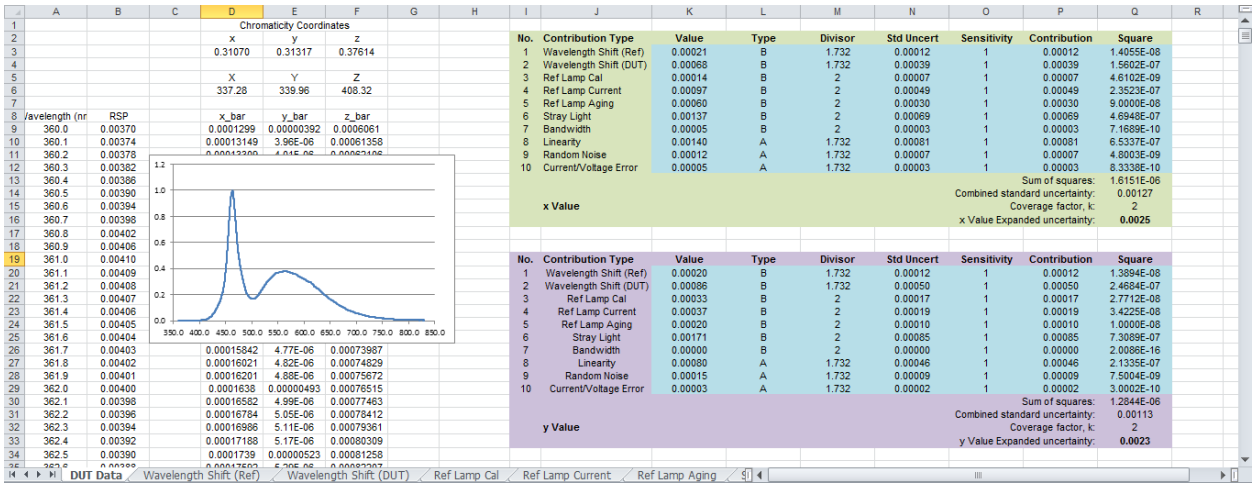

Figure 10 – Sample uncertainty spreadsheet for a white LED

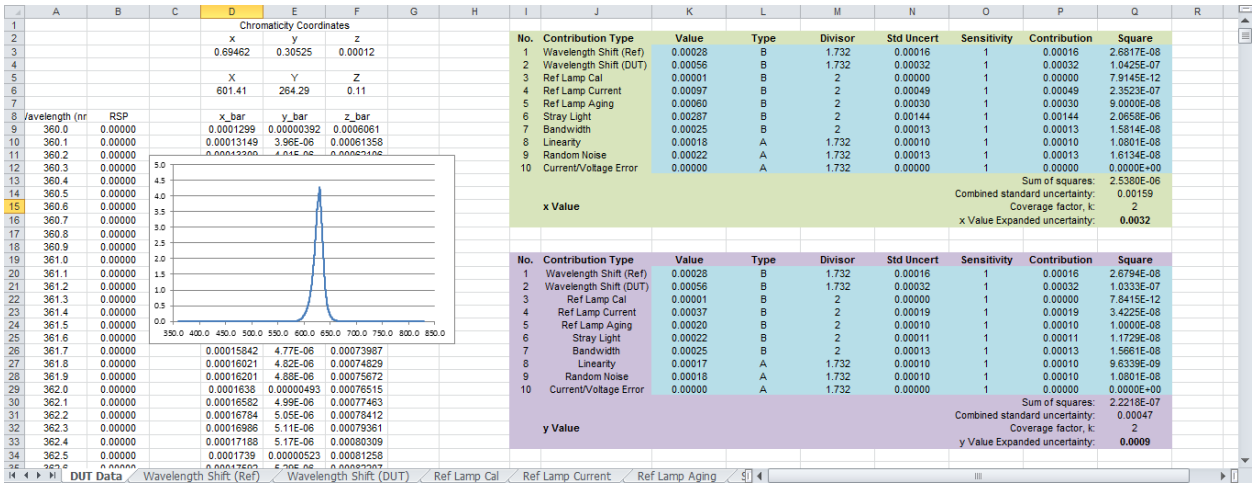

Figure 11 – Sample uncertainty spreadsheet for a red LED

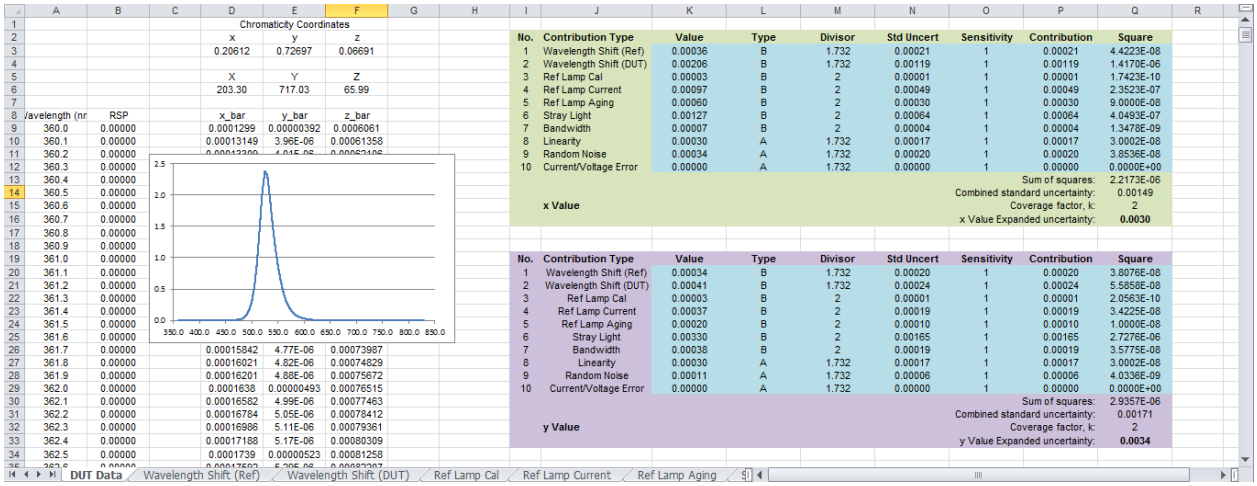

Figure 12 – Sample uncertainty spreadsheet for a green LED

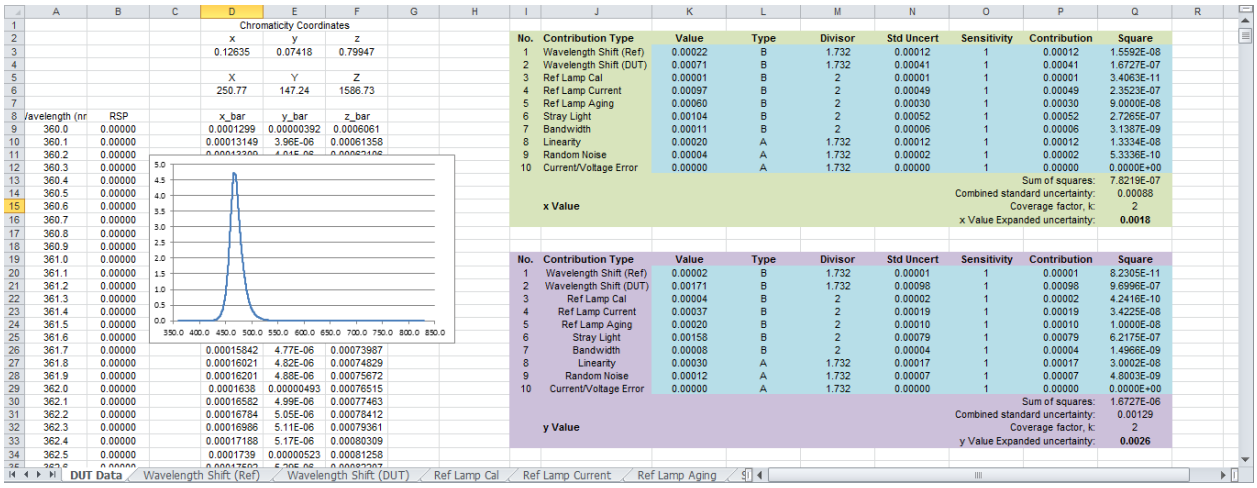

Figure 13 – Sample uncertainty spreadsheet for a blue LED

Once the spreadsheet has been initially set up, it is then a simple process of pasting in a measured spectrum and updating the DUT-specific properties such as random noise and current/voltage error. A separate spreadsheet can then be saved with the test data for each test in keeping with proper record keeping practices.

4 Conclusion

A method of determining the uncertainty in chromaticity coordinates from a spectral measurement is presented in this paper. While it has many shortfalls, it is better than the alternatives of having fixed values or purely making a guess when it is not possible to rigorously analyse a system.

Because we are working with a spectrum, the same principle can also be applied to other derived quantities. However, the modelling methods contained in this paper should not be used to correct the data unless it has been rigorously verified.

5 References

CIE, 2011. CIE 198:2011: Determination of Measurement Uncertainties in Photometry

CIE, 2004. CIE 015:2004 (3rd edition): Colorimetry

CIE, 2014. CIE TC 2-60 Effect of Instrumental Bandpass Function and Measurement Interval on Spectral Quantities, not yet published

ZONG, Y. et.al. 2006. Simple Spectral Stray Light Correction Method for Array Spectroradiometers, Applied Optics, Vol.45, Issue 6, 2006

International Organization for Standardization ISO, 1995. Guide to the Expression of Uncertainty in Measurements, Geneva, Switzerland.

UNCERTAINTY EVALUATION OF SPECTRALLY RESOLVED SOURCE OUTPUT MEASUREMENT USING ARRAY SPECTRORADIOMETER

Dubard, J.[1], Etienne, R.[1], Valin, T.[1]
[1] Laboratoire National de Métrologie et d'essais (LNE), Trappes, FRANCE
jimmy.dubard@lne.fr

Abstract

Spectrally resolved source output characterization is often performed using array spectroradiometer. Because of the properties of this type of spectroradiometer accurate measurement requires stray light correction. Therefore the measurement uncertainty evaluation must take into account this correction that involves matrix calculations. We use Monte Carlo technique to perform this uncertainty evaluation based on a measurement model that is highly non-linear and taking into account correlations between input quantities.

Keywords: Uncertainty, Monte Carlo technique, array spectroradiometer, stray light correction

1 Introduction

Array spectroradiometers are widely used in many applications because of their interesting features: portability, fast measurement (<1s), low cost. They are based on a single grating monochromator and therefore results of measurements are impaired by inherent stray light. Large improvement of the measurements is achieved when stray light correction is applied based on the characterisation of the Line Spread Function (LSF) of the spectroradiometer using tuneable laser *[1,Zong Y., 2006]*. This correction is complex and involves large matrix calculations. The measurement uncertainty evaluation must take into account the contribution of this correction process. The measurement model is nonlinear and therefore the GUM classical approach is not suitable.

We present the work that has been performed at LNE in the framework of the European Metrology Research Program EMRP-ENV03 project to evaluate the uncertainty of solar UV measurement using array spectroradiometers. Monte Carlo (MC) technique is used for that purpose and correlations between input quantities are taken into account. We described the measurement model, and how the MC technique is implemented in a software developed under Matlab.

2 Measurement using array spectroradiometer

Source spectral characterization requires the use of array spectroradiometers when short time variation of the source output is an issue, example: gas discharged lamps, flash light, natural sun light. Array spectroradiometers are made of a single monochromator and therefore they suffer from defects such as stray light.

Measurement of a source spectrum must follow two steps:

- Step 1: calibration of the spectroradiometer using a standard lamp
- Step 2: measurement of the source output

For each of these steps stray light correction should be applied on the raw data after subtraction of the dark signal. Additional signal processing can be performed prior to stray light correction such as linearity, wavelength scale correction,.

3 Uncertainty evaluation

3.1 Monte Carlo technique

Monte Carlo technique for measurement uncertainty is described in Guide for Uncertainty Measurement, supplement 1 [2,ISO/IEC Guide 98-3/Suppl. 1, (2008)]. The principle based on the propagation of probability distibution is depicted on figure 1.

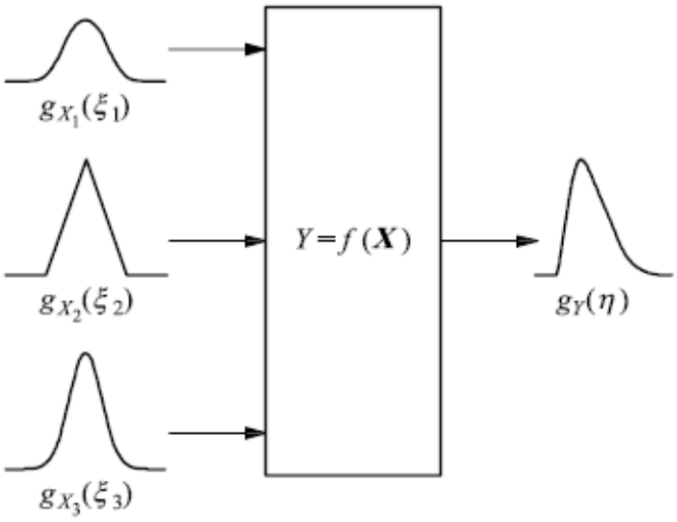

Figure 1 – Principle od uncertainty evaluation through propagation of probability didtribution

A measurand **Y** is obtained from the input quantities **Xi** through the measurement model **f** according to equation 1.

$$Y = f(X) \tag{1}$$

If gxi(ξi) is the probability distribution function PDF of the input quantities Xi, by choosing randomly a set of Xi values and by using the measurement model, we generate one Y value. By repeating this process we can generate a probability distribution function for Y from which we obtain the measurement value and the standard deviation. These information rely on an accurate definition of the measurement model.

3.2 Measurement model

As indicated in &2, prior to measure the source spectral output the array spectroradiometer must be calibrated using a standard lamp. The measured signal $S_{Std,i}$ given by the spectroradiometer corresponding to wavelength λ_i is:

$$S_{Std,i} = \frac{\left(M_{Std,i} - M_{DStd,i}\right) C_{Lin}\ C_{\lambda}}{T_{Int,Std}} \quad (counts/s) \tag{2}$$

$M_{Std,i}$, signal for pixel “i” corresponding to λi when measuring the standard lamp

$M_{DStd,i}$, measured dark signal for pixel “i” corresponding to λi when measuring the standard lamp

$T_{Int,Std}$, the integrating time when measuring the standard lamp

C_{Lin} correction due to non-linearity response of array detector of the spectroradiometer

C_{λ} correction due to wavelength accuracy

Because array spectroradiometers are based on single monochromator stray light contributes to the measured signal. Stray light correction technique is applied [1] and equation (2) can be written in matrix form as:

$$S_{Std} = S_{True} + S_{True}\ D \tag{3}$$

S_{Std} matrix representing the measured signal
S_{True} matrix representing the signal corrected from stray light
D matrix representing the stray light distribution function SDF. It is a square 2D matrix.

S_{True} can be determined from equation (3) and the spectral responsivity of the spectroradiometer SRi at wavelength λi is given by:

$$SR_i = \frac{S_{True,i}}{E_{Std,i}} \tag{4}$$

Once calibrated, source spectral output can be measured using the same process described above to correct the measured signal. Then the source spectral output S_i at λ_i is given by:

$$S_i = \frac{S_{meas,i}}{SR_i} \tag{4}$$

where $S_{meas,i}$ is the corrected signal when measuring the source.

3.3 Monte Carlo technique implementation

According to the measurement model uncertainty evaluation of source spectral output can be performed in two steps: first evaluation of the uncertainty of the spectral responsivity of the spectroradiometer, second evaluation of the uncertainty of the source spectral output.

When dealing with spectral measurements classic GUM uncertainty evaluation technique is tedious. We propose to use the Monte Carlo technique [3,*Obaton A-F*, 2007] to determine the uncertainty of source spectral output measurements.

Correlation between input quantities are taken into account. For instance uncertainty due to the stray light correction is evaluated based on equation (3) that can be written as :

$$S_{True} = \left(1 + D\right)^{-1} S_{Std} \tag{5}$$

Where “1” is the matrix unity. D contains diagonal elements set to zero and non-zero off diagonal elements that are small compare to “1”. Therefore $(1+D)^{-1}$ reduces to (1-D). Therefore each element of the column matrix S_{True} is:

$$S_{True,i} = \sum_j S_{Std,j} \left(1 - D\right)_{i,j} \tag{6}$$

(j=1 to N), where N is the number of wavelengths taken into account.

The $S_{Std,j}$ elements are correlated as well as the $(1\text{-}D)_{i,j}$ elements. The multivariate Gaussian algorithm is used to evaluate the uncertainty associated to these correlated input quantities.

A software using Matlab® has been developed to evaluate the uncertainty. The interesting feature regarding the use of Matlab is that the functions to generate random draws from the PDF are validated by the GUM supplement 1. The output is the probability distribution function (PDF) of the source spectral output at selected wavelengths from which the value of the spectral output and the associated uncertainty are obtained from respectively the average and standard deviation of the PDF. Example of user interface and PDF for the array spectroradiometer spectral responsivity is shown on figure 2.

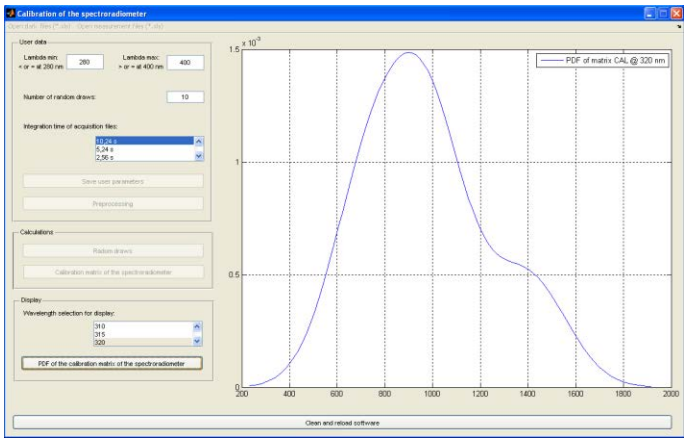

Figure 2 – PDF of the spectroradiometer responsivity

4 Conclusion

Monte Carlo technique is used to evaluate the uncertainty of source spectral output measurement using array spectroradiometer. Based on the measurement model that includes the stray light correction the uncertainty is evaluated taking into account correlations between input quantities of the stray light correction algorithm. A software using Matlab is developed to evaluate the uncertainty at selected wavelengths. This software developed in the framework of the European project EMRP ENV03 is publicly available on the web site http://projects.pmodwrc.ch/env03.

Acknowledgment

The EMRP is jointly funded by the EMRP participating countries within EURAMET and the European Union**.**

References

[1] ZONG Y., BROWN S B., JOHNSON B.C., LYKKE K R and. OHNO Y, 2006, Simple spectral stray light correction method for array spectroradiometers, *Applied Optics*, 45.

[2] ISO/IEC Guide 98-3/Suppl. 1, 2008, *Propagation of distributions using a Monte Carlo method*

[3] OBATON A F, LEBENBERG J., FISCHER N., GUIMIER S. and DUBARD J., 2007, Two procedures for the estimation of uncertainty of spectral irradiance measurement for UV source calibration, *Metrologia*, 44

CHARACTERIZATION OF ARRAY SPECTRORADIOMETERS FOR SOLAR UV MEASUREMENTS

Egli, L.[1], Nevas, S.[2], Blattner, P.[3], ElGawhary, O.[4], Kärhä, P.[5] and Gröbner, J.[1]
[1]Physikalisch-Meteorologisches Observatorium Davos (PMOD/WRC), World Radiation Center, Davos Dorf, SWITZERLAND
[2]Physikalisch-Technische Bundesanstalt, Braunschweig (PTB), GERMANY
[3]Federal Institute of Metrology, METAS, Bern, SWITZERLAND
[4]Dutch Metrology Institute (VSL), Delft, NETHERLANDS
[5]Aalto University (MIKES-Aalto), Espoo, FINLAND
luca.egli@pmodwrc.ch

Abstract

Array spectroradiometers are widely used in many applications due to their characteristics: portability, fast measurement and low cost. However, array spectroradiometers use single monochromators and therefore suffer significantly from stray light. In addition to stray light, the pixel-to-wavelength assignement and non-linearities of detectors are severe problems for measurements of solar UV radiation due to the sharp cut-off of the solar UV spectrum as a consequence of ozone absorption. Therefore, it is important to characterize and correct for straylight, to calibrate the wavelength dependency and to determine the linearity of the entire system for a correction at the post processing of the solar UV data. The characterizations described in this article were elaborated within the EMRP project “Solar UV” and firstly presented in the final EMRP project-report.

Keywords: array spectroradiometer, characterization, stray light, wavelength, linearity

1 Stray light corrections

One of the biggest uncertainty components in the measurements by array spectroradiometers in the solar UV spectral range is caused by a poor suppression of the internally created stray light. A reduction of the stray light effect by up to two orders of magnitude may be achieved using a correction matrix (Zong et al., 2006) based on line spread functions (LSFs) that can be determined with the help of spectrally tuneable lasers. However, the stray light corrections using the results of the LSF characterization are effective only as long as the spectral range of the laser covers the spectral range of the array detector, typically a silicon-based charged coupled device (CCD), in use. Array spectroradiometers for the solar UV measurements may have a narrow spectral range. The simplest way of taking care of this out-of-range (OoR) stray light would be by using bandpass filters or other spectral pre-selection techniques that prevent the OoR radiation from getting into the instrument. For certain applications, it may also be practical to subtract the OoR radiation by making an additional measurement with a long-pass filter in front of the entrance optics of the instrument. For the case that hardware modifications are not desired and feasible, an approach was implemented to characterize the response of the instrument to the OoR radiation and to take it into account by means of a matrix for the OoR responsivity (Nevas et al., 2014).

The contribution to the signal of every pixel of the CCD detector by the OoR stray light can be calculated numerically as

$$\Delta = \boldsymbol{s}_{\mathrm{OoR}} \cdot \boldsymbol{E}_{\mathrm{OoR}} \cdot \delta\lambda \tag{1}$$

provided that the responsivity of every detector pixel to the radiation from the wavelengths outside the spectral range (OoR) of the instrument, put in a matrix $\mathbf{S}_{\mathrm{OoR}}$, and the spectral irradiance outside the spectral range of the spectroradiometer, contained in a vector $\mathbf{E}_{\mathrm{OoR}}$, are known. $\delta\lambda$ represents the OoR wavelength step with which the OoR stray light data are available. The dimensions of the OoR responsivity matrix $\mathbf{s}_{\mathrm{OoR}}$ are *NxM*, where *N* is the number of pixels in the linear array detector and *M* is the number of wavelengths on a uniform

grid throughout the OoR of the instrument, say every 1 nm. Then following the matrix formalism of Zong et al. (2006) the spectroradiometer data vector corrected for both the OoR and InR spectral stray light can be obtained as

$$\boldsymbol{Y}_{\mathrm{IB}} = [\boldsymbol{I} + \boldsymbol{D}]^{-1} \cdot [\boldsymbol{Y}_{\mathrm{meas}} - \boldsymbol{\Delta}] = \boldsymbol{A}^{-1} \cdot [\boldsymbol{Y}_{\mathrm{meas}} - \boldsymbol{\Delta}] \,. \tag{2}$$

In order to calculate $\boldsymbol{\Delta}$ and to apply the correction of (2) the spectral irradiance $\mathbf{E}_{\mathrm{OoR}}$ outside the spectral range of the array spectroradiometer, up to 1100 nm in the case of silicon detectors, needs to be known for both the source used to calibrate the instrument and the source under test. For calibration sources such data is normally available. The OoR stray light estimation for a test source, i.e. the solar radiation, however, requires either measurements by an auxiliary spectroradiometer or some kind of extrapolation of the spectral content into the OoR spectral region based on the InR measurement data by the instrument. For this purpose one can use, e.g., radiative transfer model calculations or reference solar spectra normalized by the measurements in the overlapping spectral range. It can be shown, that in most cases the OoR irradiance does not need to be known very accurately.

To check the efficiency of the combined OoR and InR corrections, several solar UV instruments were characterized. One of them was of the type AvaSpec-ULS2048 (Avantes), named AVOS. The instrument has a nominal spectral range from 280 nm to 440 nm wavelength and a spectral bandpass of 0.7 nm. As a detector, a Hamamatsu back-illuminated Si CCD with 2048 pixels is used in the device. Both the InR and the OoR stray light properties of the spectroradiometer were characterized at the PLACOS setup of PTB. The InR and OoR stray light properties of the AVOS instrument are shown in Figure 1.

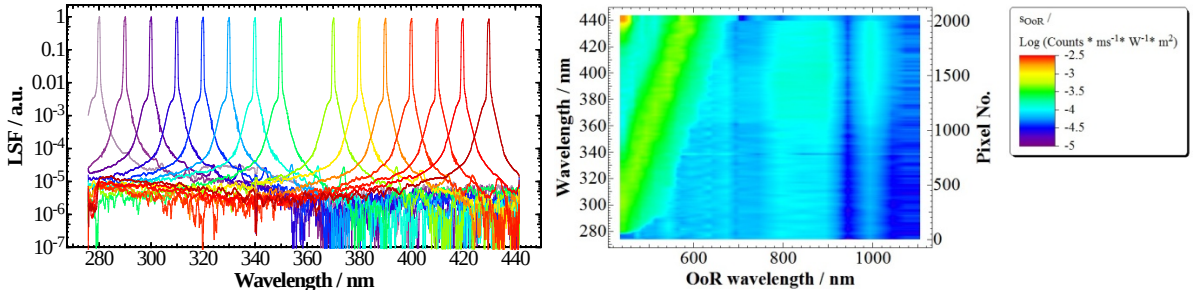

Figure 1 – a) Line spread functions of the AVOS spectroradiometer at several laser wavelengths. They are used to take into account internal stray light created within the spectral range of the instrument. b) Responsivity of the spectroradiometer with respect to irradiance at the out-of-range wavelengths, 440 nm to 1100 nm. This data was used to correct the OoR stray light contribution.

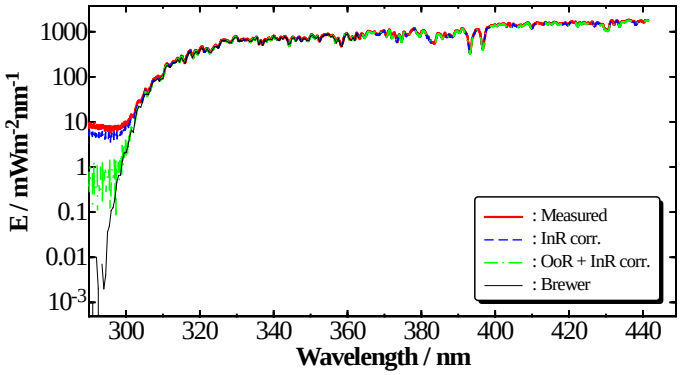

Figure 2 – Solar UV irradiance at SZA of 42° measured by the AVOS array spectroradiometer in a clear sky measurement campaign in Davos. Solid red curve is the solar spectrum without any stray light correction applied. Dashed blue and dash-dotted green curves are the solar spectra corrected for exclusively the InR and the combined OoR and InR stray light, respectively. Thin black curve shows the solar spectral irradiance measured with a Brewer spectroradiometer based on a scanning double monochromator.

Figure 2 shows the solar UV irradiance measured by the AVOS instrument, results of solely InR stray light correction, as well as the combined OoR and InR stray light corrections applied to the measurement data. For comparison purpose, the spectral irradiance measured by a reference Brewer spectroradiometer based on a double monochromator is shown as well. As can be seen, there are significant effects by stray light on measurements below 310 nm wavelength. For this instrument, the OoR stray light contribution made about 2/3 of the whole stray light in the instrument. With the help of combined OoR and InR stray light corrections, ca. 95% of the stray light contribution could be corrected.

2 Wavelength Scale device

Accurate wavelength calibration is a key parameter for solar spectral measurements. The aimed uncertainty is below 50 pm. Typically, spectrometers are calibrated with spectral emission lines. However, for small spectral ranges, only few lines are typically available. In addition, some of the spectral lines consists of multiplets (i.e. at 313 nm, 365 nm, 404 nm and 408 nm), or can have very low intensity levels (297 nm, 302 nm and 334 nm) and therefore cannot be used by typical solar UV spectrometers.

Within the EMRP project, two different approaches were realized that allow characterizing the wavelength scale accurately all over the UV (and visible) spectral ranges: METAS realized devices based on different Fabry-Perot etalons; VSL developed a wavelength ruler that is based on a one-stage Lyot filter. These devices show an oscillating transmittance behavior that can theoretically be modelled knowing the optical thicknesses of the material layers in the devices (see Figure 3 and Figure 4). If the temperature conditions are controlled (typically to better than 0,1 °C) and the geometry is fixed (angular alignment and beam divergence better than 0,5°) the devices can be used as absolute devices, and deviations of the wavelength scale can be directly identified.

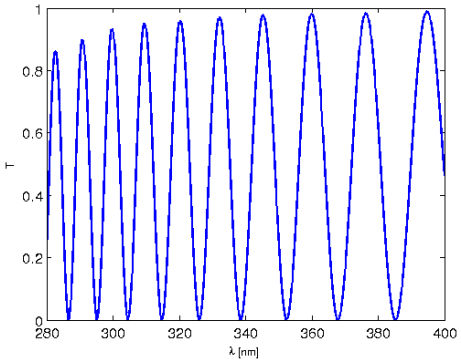

Figure 3 – Spectral transmittance of a one-stage Lyot filter.

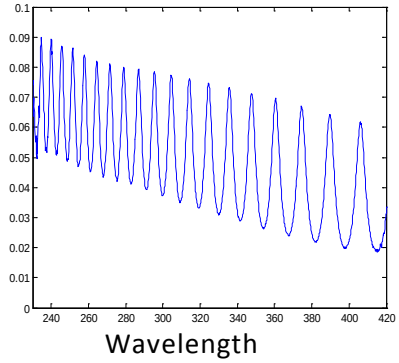

Figure 4 –Spectral transmittance of a Fabry Perot etalon.

Theoretically, the devices can be used with any kind of “white” light sources, but for best performance, i.e. to generate stable and powerful radiation in the UV range, a laser driven light source is recommended to be used. In the first step, the transmittance is experimentally determined by measuring the spectral distribution of the light source with and without the filter. This transmittance is then compared to the theoretically modeled transmittance. If the optical thicknesses of the layers in the device are not known or the setup doesn’t respect the conditions for absolute measurements, it is still possible to use the device in combination with known spectral lines of a mercury lamp or one or several lasers. In this case an optimization algorithm has to be used to retrieve the effective optical thicknesses. Both devices have there advantages: Usually the modulation depth of the one-stage Lyot filter is higher and therefore the device is less sensitive to noise, particularly for low light levels. However the setup is more bulky. The Fabry Perot etalon is a very compact optical element which can be easily integrated into an instrument, but also shows more sensitivity to noise. Both devices can reduce the uncertainty of the wavelength scale to below 50 pm. Figure 5 shows the error of the wavelength scale of a particular spectrometer obtained by using a Fabry-Perot device. After correction, the error reduces to within 20 pm as can be seen in Figure 6.

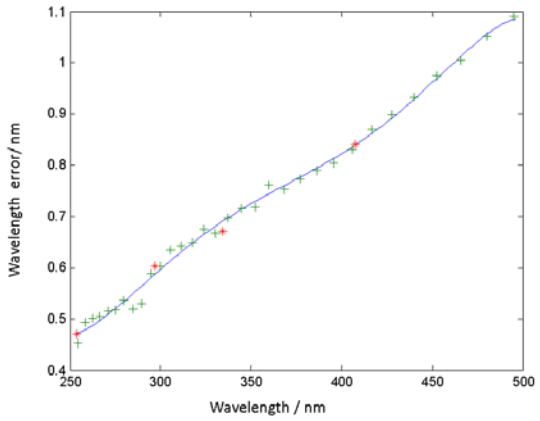

Figure 5 – measured wavelength error as a function of the wavelength prior correction.

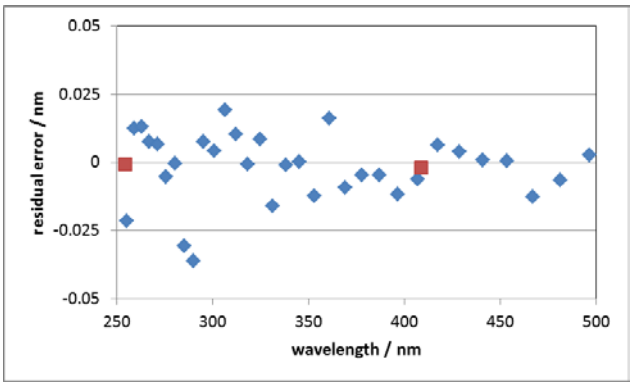

Figure 6 – Residual error after wavelength correction.

3 Linearity

Terrestrial solar UV irradiance varies within the relatively narrow spectral range, 280 – 400 nm, over a large dynamic range, about 5 to 6 orders of magnitude. Hence, the dependence between the measured solar UV irradiance values over the whole dynamic range and the respective signals of a spectroradiometer that is used for the measurements is required, i.e., the linearity of the instrument must be known. Residual deviations from the linear regime will yield errors both in absolute values as well as in relative spectral distributions of the measured solar UV irradiance.

In the case of compact array spectroradiometers, the linearity of the CCD instrument is typically characterized by exposing the instrument to the radiation of a stable source and by varying the integration time of the detector. This is a simple but by far a not complete characterization method. In fact, it accounts for the linearity of the signal processing electronics only. In principle, the linearity of such devices should also be tested by varying the spectral irradiance level over the whole dynamic range. For the radiometric characterization of the linearity of the spectroradiometers, the technical challenge consists of providing a radiation source, the spectral irradiance of which can be dynamically tuned over 5 to 6 orders of magnitude and reach the level of 1 W/m^2nm^{-1}. In the case of, e.g. halogen lamps used for the calibration of the instruments, this is difficult.

Within the framework of the EMRP project, an approach to the linearity characterization of array spectroradiometers used for the solar UV radiation measurements has been chosen based on monochromatic sources tuneable over wide dynamic range with different setups at Aalto, METAS, PTB and VSL.

MIKES-Aalto built a setup based on a single monochromator with two light sources (see Figure 7). The light exiting the monochromator is collimated and attenuated with interchangeable neutral-density filters in two consequent filter wheels. The light beam then continues to the device to be characterized through a beam splitter taking a fraction of the beam to a silicon photodiode serving as the linearity reference. PTB used for the linearity characterizations its tuneable laser source based on a frequency doubled and tripled mode-locked Ti:Sa (80 MHz repetition rate, 200 fs pulse duration) with the developed beam conditioning unit to generate high irradiance levels in the solar UV spectral range (see Figure 8). The measurements are made also relative to silicon detector. Similar laser setup was used for the measurements at METAS as well. The setup built at VSL is portable so that it can also be used outside of the VSL laboratories (see Figure 9). It uses a laser with 372 nm wavelength as a source and a crossed-polarizer attenuator. The measurements are also made relatively to a silicon photodiode.

A comparison of the linearity measurements using the setups of MIKES-Aalto, PTB and VSL was carried out in spring 2014. In this intercomparison, two different array spectroradiometers were characterized at the three institutes. The measurements in irradiance-variation mode could be carried out within a dynamic range from $1 \cdot 10^{-4}$ W/(m^{2}nm) to 2 W/(m^{2}nm). The lowest measurable irradiance was limited by the responsivity of the instruments. Results of the linearity measurements at the NMIs were in a good agreement with each other. Also, results obtained by irradiance variation were consistent with those collected by varying the integration time of the instruments. Both instruments showed significant nonlinearities that were obviously caused by signal processing electronics, i.e. the analog-to-digital converter (ADC), and could be corrected as a function of ADC counts. Having this correction applied, no additional nonlinearity for irradiances of up to 2 W/(m^2/nm) could be detected (see Figure 10).

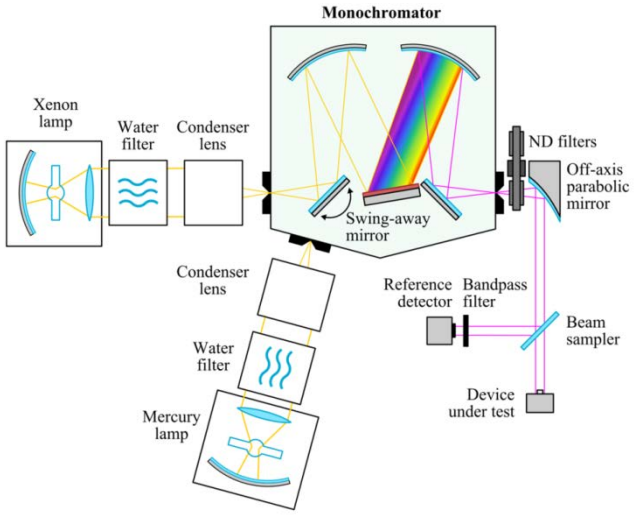

Figure 7 – Setup for linearity measurements built at MIKES-Aalto.

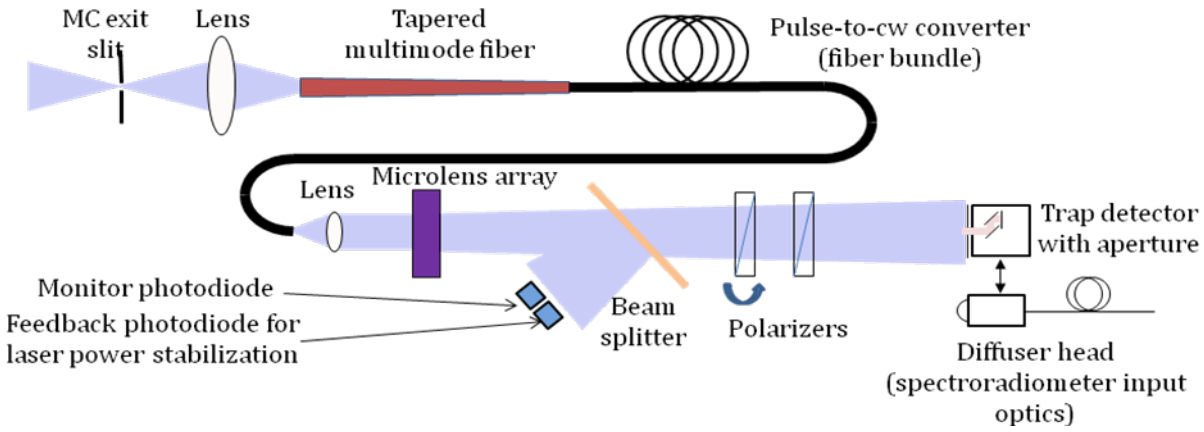

Figure 8 – Beam conditioning in the TULIP setup at PTB for linearity characterization.

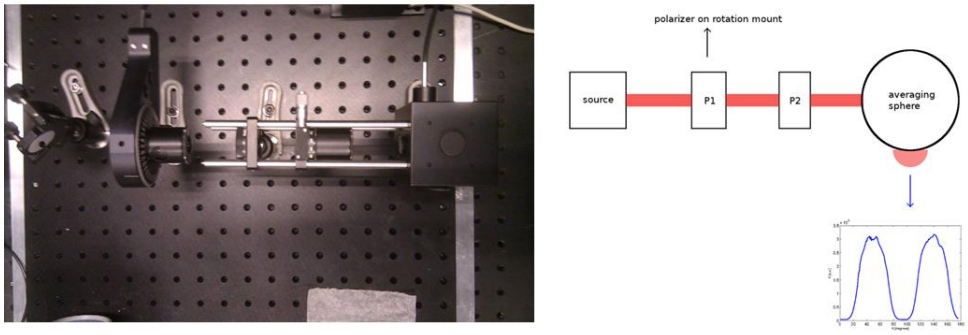

Figure 9 – Picture and schematic diagram of the setup for linearity measurements built at VSL.

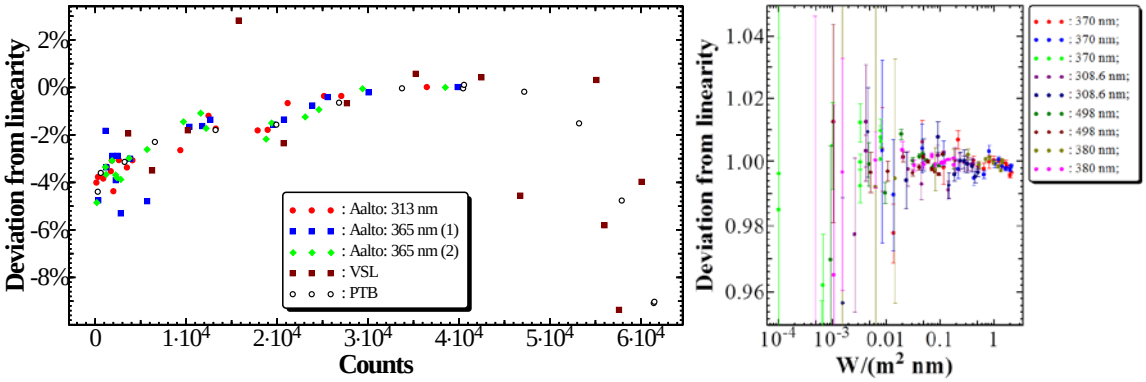

Figure 10 – Non-linearities for an AvaSpec-ULS2048LTEC-USB2 spectroradiometer measured at MIKES-Aalto, PTB and VSL and shown as a function of ADC counts. b) Residual nonlinearities of the instruments after a polynomial correction for the ADC nonlinearity. The measurements at the different wavelengths and irradiance levels were carried out at PTB.

4 Conclusions

1) Method to correct for the out-of-range stray light of solar UV array spectroradiometers has been developed and is available for the solar UV community using array spectroradiometers.
2) Based on the research and development, devices based on Fabry Perot and Lyot filters may lead to commercial products if a sufficiently stable alignment and temperature control can be provided by an interested manufacturer.
3) Array spectroradiometers must be characterized for the nonlinearity. Large nonlinearities due to the signal processing electronics may be observed for the instruments.
4) Since array spectroradiometers require substantial characterization, characterization services may be provided by national metrology institutes or private laboratories.

References

1. Zong, Y, Brown, S.W., Johnson, B. C., Lykke, K. R. and Ohno, Y., 2006, “Simple spectral stray light correction method for array spectroradiometers,” Appl. Opt. 45, 1111–1119.
2. Nevas, S., Gröbner, J., Egli, L. and Blumthaler, M, 2014, “Stray light correction of array spectroradiometers for solar UV measurements,” Appl. Opt. 53, 4313–4319.
3. Blattner, P., Foaleng, S.M., Van den Berg, S., El Gawhary, O., Blumthaler, M., Gröbner, J and Egli, L., 2014, Devices for characterizing the wavelength scale of UV spectrometers, Proceedings of NEWRAD 2014, Espoo, Finland, June 24 – 27, pp. 201 – 202.

MEASURING COLORIMETRIC QUANTITIES WITH A HYPERSPECTRAL CAMERA

Ruggaber, B. and Krueger, U.
TechnoTeam Bildverarbeitung GmbH, Ilmenau, GERMANY
Benjamin.Ruggaber@technoteam.de

Abstract

The present study investigates the use of a hyperspectral camera for spatially resolved measurements of chromaticity coordinates of light sources such as white and coloured light-emitting diodes. The chromaticity coordinates (CIExy) are treated as 2D-quanitities, therefore Supplement 2 of the Guide to the Expression of Uncertainty in Measurement (GUM) had to be used for the uncertainty statement. The GUM gives a step-by-step guide for solving such problems; this step-by-step procedure is followed throughout the whole paper, where the hyperspectral Camera is used as an example.

Keywords: Hyperspectral Camera, Colorimetry, Monte-Carlo Method, GUM Supplement 2, Liquid-Crystal Tunable Filter (LCTF)

1 Introduction

The present study investigates the use of a hyperspectral camera (HSC) for spatially resolved measurements of chromaticity coordinates. HSCs generally consist of an optical imaging system, an electrically tunable filter in addition to a detector array. The tunable bandpass shaped transmittance of the electrically tunable filter in conjunction with the imaging system enables the spatially resolved reconstruction of spectra. The spectrum is sequentially sampled by tuning the filter, which results in a shift of the bandpass-shaped transmittance of the filter, where every filter characteristic is called a channel in the field of HSCs. The transmittance for a couple of channels, over the working range of the filter, is shown in Figure 1. In the investigation a Liquid-Crystal Tunable Filter (LCTF) (Perkin Elmer 2014) is used. The bandpass-shaped transmittance of the LCTF can be displaced in 1 nm increments over the working range (400 nm - 720 nm) of the LCTF. A single channel of the HSC can be tuned with random access.

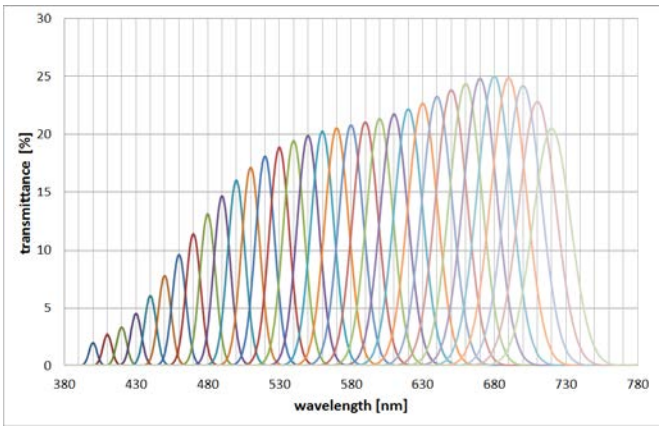

Figure 1 – Transmittances of the LCTF channels

The spectrum resulting from measurements with the HSC is used in the present work to determine chromaticity coordinates, where the chromaticity coordinates are treated as 2D-quantities for the measurement uncertainty evaluation. The focus is on the reconstruction of spectra, and the calculation of chromaticity coordinates for coloured- and white light-emitting diodes (LEDs).

2 Step-by-Step Guide according to the Guide to the Expression of Uncertainty in Measurement

For solving the problems described in paragraph 1, the Guide to the Expression of Uncertainty in Measurement (GUM) (BIPM 2014) provides a step-by-step Guide. The procedure given by GUM can be divided into three steps: modelling, propagation and summarizing.

1. Modelling
    a. Defining the measurand
    b. Establishing a measurement model (a realistic picture of the physics involved in the measurement).
    c. Modelling the state of knowledge about the model parameters by assigning probability density functions (PDFs)
2. Propagation
    a. Propagation of the PDFs through the model, using a Monte-Carlo-Method
3. Summarizing
    a. Using the resulting (bivariate) PDF to extract…

        best estimate of the measurand

        covariance matrix

        construct coverage region

The first step of the modelling process is to define the measurand. By defining the measurand it is usually possible to derive the measuring principle. In a next step, a measurement model has to be established which gives a realistic picture of the physics involved in the measurement (measuring principle). In the case of an indirect measurement, it is useful to consider the so-called signal chain first, and to invert the signal chain to get the measurement model (Sommer 2005). The signal chain constitutes the path from cause to effect where the measurement model can be considered as the inverted signal chain (see Figure 2).

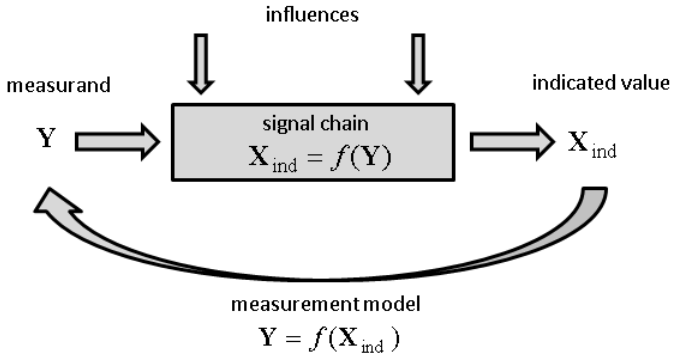

Figure 2 – Connection between signal chain and measurement model

To establish the signal chain it is good practice to model it first as ideal, and to insert imperfections afterwards. The knowledge about typical effects which should be considered can usually be obtained from the literature, from investigations of the system, and measurements made with the system. The modelling process is usually an iterative process. After modelling the signal chain, corrections have to be determined (e.g. offsets etc.) to be able to describe the signal chain as ideal again. After that, the ideal signal chain has to be inverted to get the measurement model, which is the basis for evaluating a measurement and calculating the measurement uncertainty as well. In a last step of the modelling process, our

state of knowledge about the measurement model parameters has to be modelled by assigning probability density functions (PDFs). Next, the PDFs have to be propagated through the measurement model by using a Monte-Carlo-Method. The result of the Monte-Carlo-Method is a PDF for the measurand. From this PDF the best estimate, the covariance matrix and the coverage region can be stated.

2.1 Modelling

The first step of the modelling process is to define the measurand. For this investigation, however, we have restricted ourselves to the determination of the chromaticity coordinates (CIExy). Before chromaticity coordinates can be calculated, the CIE 1931 tristimulus values X, Y and Z have to be determined. From the defining equations of the tristimulus values the evaluation process can be deduced. One way is to match the spectral responsivities of a system to the CIE1931 colour matching functions (filter-wheel systems). Another way is to measure the spectrum of the light source and to calculate tristimulus values. The latter is used in the case of HSC. Because the chromaticity coordinates are calculated from the spectrum, we can call the spectrum of the light source the actual measurand, and because a HSC is an imaging system it is useful to describe the spectrum by spectral radiance and use this quantity to model the HSC.

After defining the measurand, a measurement model has to be established which gives a realistic picture of the physics involved in the measurement. Before a measurement model can be established, the signal chain has to be modelled. This is done by using the simplified ray-path below.

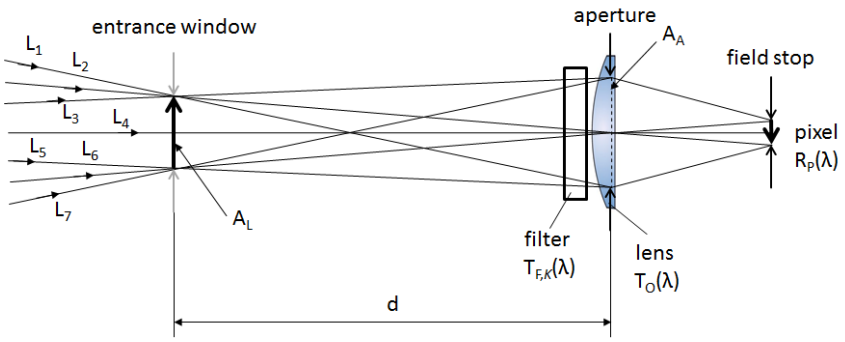

Figure 3 – Ray path for modelling the signal chain

The signal chain constitutes the path from cause to effect, in the case of a HSC this is the path from the spectrum $L_{e\lambda}(x, y, \theta, \phi, \lambda)$, which is seen by a pixel, to the resulting grey-scale value $n_{\mathrm{dig},Pixel,K}$ for a pixel and a channel *K* of the HSC.

$$n_{\mathrm{dig},Pixel,K} = \int_{\Delta\lambda_K} \int_{\Omega} \int_{A_L} L_{e\lambda}(x, y, \theta, \varphi, \lambda) \cdot \cos\theta \cdot R_{\Phi,K}(x, y, \theta, \varphi, \lambda) \cdot t_{\mathrm{int},K} \cdot \mathrm{d}A_L \cdot \mathrm{d}\omega \cdot \mathrm{d}\lambda \qquad (1)$$

Where $R_{\Phi,K}(x, y, \theta, \phi, \lambda)$ is the spectral responsivity of a channel *K* and $t_{\mathrm{int},K}$ is the integration time. The spectral responsivity contains the transmittance of the LCTF (Figure 1), which depends on the channel the LCTF is tuned to, the transmittance of the lens and the responsivity of a pixel. Usually the signal chain is modelled first as ideal (Equation 1) and imperfections are added afterwards. The system has to be checked for significant effects which influence the signal chain, these effects have to be taken into account in the ideal signal chain. In most cases, common effects are found in the literature (for example EMVA 2010). To keep the model simple only two effects, dark signal $n_{\mathrm{dig},Pixel,\mathrm{D}}(t_{\mathrm{int},K}, T)$, which depends on the integration time and the temperature, and non-linearity, which is modelled as a monotonically increasing non-linear function *G* (Equation 2), are inserted in the ideal model. Where $\hat{n}_{\mathrm{dig},Pixel,K}$ is the output signal of the non-ideal signal chain.

$$\hat{n}_{\mathrm{dig},Pixel,K} = G\left[\int_{\Delta\lambda_K}\int_{\Omega}\int_{A_L} L_{\mathrm{e}\lambda}\left(x,y,\theta,\varphi,\lambda\right)\cdot\cos\theta\cdot R_{\Phi,K}\left(x,y,\theta,\varphi,\lambda\right)\cdot t_{\mathrm{int},K}\cdot \mathrm{d}A_{\mathrm{L}}\cdot \mathrm{d}\omega\cdot \mathrm{d}\lambda + n_{\mathrm{dig},Pixel,\mathrm{D}}\left(t_{\mathrm{int},K},T\right)\right] \quad (2)$$

Usually, it is possible to correct these imperfections. To do so, it is necessary to determine offsets, correction functions etc.. After utilizing the corrections the signal chain can be described by an ideal signal chain again (Equation 3).

$$s_{Pixel,K} = \int_{\Delta\lambda_K}\int_{\Omega}\int_{A_L} L_{\mathrm{e}\lambda}\left(x,y,\theta,\varphi,\lambda\right)\cdot\cos\theta\cdot R_{\Phi,K}\left(x,y,\theta,\varphi,\lambda\right)\cdot \mathrm{d}A_{\mathrm{L}}\cdot \mathrm{d}\omega\cdot \mathrm{d}\lambda \quad (3)$$

Here, $s_{Pixel,K}$ is the corrected output signal. The resulting data of a measurement with a HSC can be visualized by a so-called hyperspectral data cube (Figure 4). Such a hyperspectral data cube consists of a number of pictures of the light source, one for every channel used during the measurement.

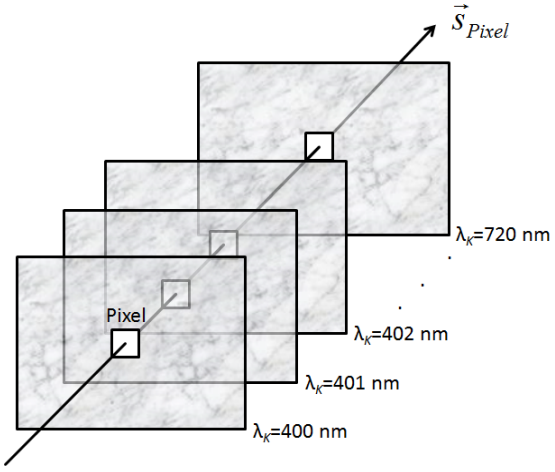

Figure 4 – Hyperspectral data cube

A grey-scale vector $\vec{s}_{Pixel}$ can be built which contains all grey-scale values of an identical pixel in the hyperspectral cube. Here, each value of the vector can be described by Equation 3. The goal is to estimate a spectrum from such grey-scale vectors. Therefore, the signal chain which leads to the so-called measurement model (see Figure 2) has to be inverted.

In this investigation, it is assumed that the spectrum which is seen by a pixel can be treated as homogeneous and lambertian. Therefore, the signal chain can be modelled by the following equation.

$$s_{Pixel,K} = \int_{\Delta\lambda_K} L_{\mathrm{e}\lambda}\left(\lambda\right)\cdot R_{\mathrm{L},Pixel,K}\left(\lambda\right)\cdot \mathrm{d}\lambda \quad (4)$$

Here, $R_{\mathrm{L},Pixel,K}\left(\lambda\right)$ corresponds to the resulting double integral as $L_{\mathrm{e}\lambda}\left(x,y,\theta,\phi,\lambda\right)$ is assumed to be constant, which leads to $L_{\mathrm{e}\lambda}\left(\lambda\right)$. To get the measurement model, the signal chain (Equation 4) has to be inverted. The signal chain contains an integral. The integration is a process where information about the integrands is lost. In order to get some information about one of the integrands ($L_{\mathrm{e}\lambda}\left(\lambda\right)$) from the result of an integration ($s_{Pixel,K}$), a so-called inverse problem has to be sloved. The method for solving this inverse problem depends on the number of channels used during the measurement. Therefore, two operating modes of the HSC are distinguished in the following: the high-dimensional sampling and the low-dimensional sampling.

1. **High-dimensional sampling:** Sampling by a large number of channels („1nm-steps"). Usually, there is no interpolation needed to determine chromaticity coordinates.

2. **Low-dimensional sampling:** Sampling by a low number of channels. Usually, there is a trade-off between measurement time and tolerable measurement deviation. Restricted to smooth spectra because of the risk of undersampling. There is some kind of interpolation needed to determine chromaticity coordinates.

A simple solution to the inverse problem in the case of high-dimensional sampling is to assume a constant spectral radiance over the bounds of integration again (similar to the assumptions resulting in Equation 4). This leads to the measurement model:

$$\hat{L}_{e\lambda}(\lambda_K) := \frac{s_{Pixel,K}}{\int_{\Delta\lambda_K} R_{L,Pixel,K}(\lambda)\cdot \mathrm{d}\lambda} \tag{5}$$

Here, a value of spectral radiance has to be assigned to a wavelength. Usually, a value of spectral radiance is assigned to the centroid wavelength λ_K of a particular channel of the HSC. In most cases, Equation 5 yields acceptable results for smooth spectra such as standard illuminant D50, D65 and A or white LEDs (Figure 5 left).

In the case of narrowband spectra such as coloured LEDs, another approach for solving the inverse problem has to be used. This is because the assumptions related to the applicability of Equation 5 are not fulfilled sufficiently well (Figure 5 right). Therefore, in the case of narrowband spectra, the measured spectra have to be deconvoluted. In this investigation, good results were achieved by using the Richardson-Lucy-Algorithm (Richardson 1972 and Lucy 1974) for deconvolution.

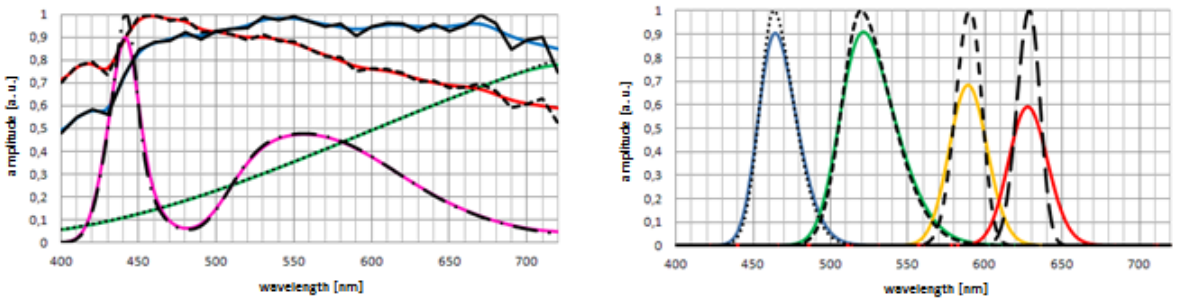

Figure 5 – Reconstructed spectra - the black graphs are the actual spectra, and the coloured ones are the reconstructed spectra

In the case of low-dimensional sampling, only a small number of channels are used for reconstruction. Therefore, some kind of interpolation is needed to be able to calculate chromaticity coordinates with small deviations.

To reconstruct spectra, either Equation 5 (Figure 6 left) could be used or the inverse problem could be treated as solving an underdetermined system (Figure 6 right). For the former option, some kind of interpolation is necessary, for example the spline interpolation. For the latter, the Wiener-Inverse (Pratt and Mancill 1976) was found to be the method of choice.

For all operating modes of the HSC (high- and low-dimensional sampling), or also for all approaches for reconstructing spectra discussed above, it is always necessary to have some knowledge of the spectral responsivity of the HSC. The spectral responsivity was determined for each position on the detector matrix of the HSC so that it was possible to use the effective spectral responsivity, depending on the position of the pixel used to evaluate the spectrum of a light source. In a last step of the modelling process, PDFs have to be assigned to all parameters of the measurement model. In order to assign meaningful PDFs which model the state of knowledge about the model parameters, simulations of the measurement have to be

performed, the determination of model parameters has to be taken into account and information from the literature (calibration certificates etc.) has to be considered.

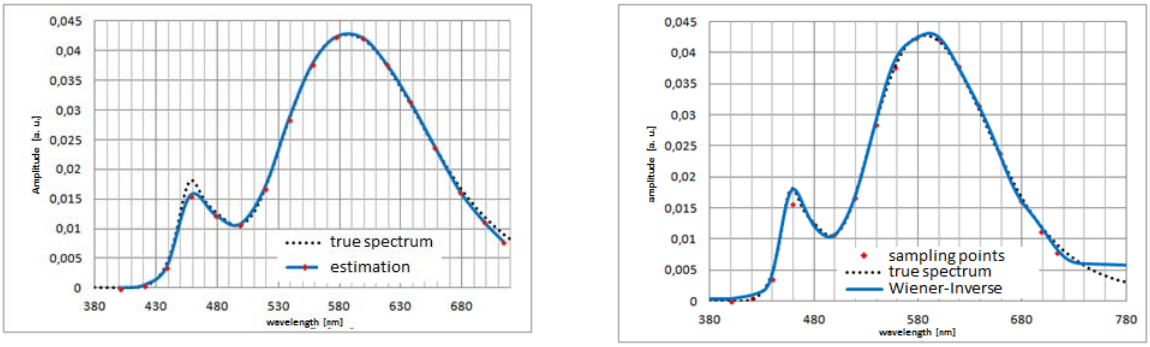

Figure 6 – Results obtained by applying spline interpolation (left) and Wiener-Inverse (right)

2.2 Propagation

In GUM Supplement 2, a Monte-Carlo-Method is used to propagate PDFs through the measurement model. Where the measurement model depends on the mode the HSC is operated in (high- or low-dimensional sampling). The Monte-Carlo-Method is based on the following procedure. During a run of the Monte-Carlo-Method, random values are generated according to the assigned PDFs for each model parameter. Those random values are inserted into the measurement model, and as a result one gets a pair of chromaticity coordinates x_i and y_i. This procedure is repeated until a meaningful statistic for the chromaticity coordinates is achieved.

2.3 Summarizing

The result of the Monte-Carlo-Method is a number of pairs of chromaticity coordinates which equal the number of the trials in this method. These pairs of chromaticity coordinates can be treated as 2D-quantities in the CIE1931 chromaticity diagram. The result is then called a bivariate PDF. The resulting bivariate PDF in the case of low-dimensional sampling using spline interpolation and the reconstruction of a warm-white LED is shown in the figure below.

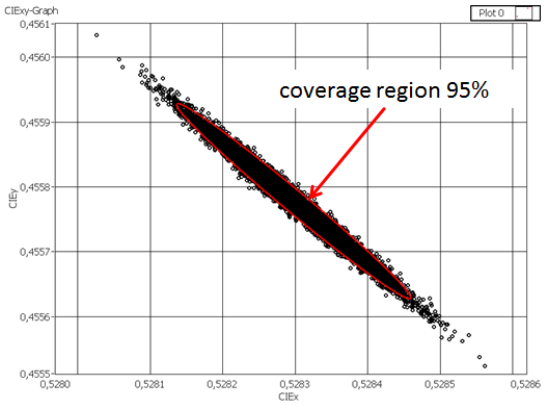

Figure 7 – Resulting bivariate PDF with elliptical coverage region

From this bivariate PDF it is possible to derive a best estimate for the chromaticity coordinates, a covariance matrix and a coverage region. Please note that, in the case of a warm-white LED, the result of the Monte-Carlo-Method corresponds to a normally distributed bivariate PDF, therefore, the coverage region is elliptical and the coverage factor is 2,45 for a 95 % coverage probability.

References

Perkin Elmer, company website. URL: http://www.perkinelmer.com/catalog/product/id/varispc. October 2014.

BIPM. URL: http://www.bipm.org/en/publications/guides/gum.html. October 2014

SOMMER, K.D. et. al.. 2005. A systematic approach to the modelling of measurements of uncertainty evaluation. *Journal of Physics: Conference Series*, 13, 224-227.

EMVA 2010. EMVA 1288. Standard for Characterization of Image Sensors and Cameras. 2010. www.emva.org.

RICHARDSON, W. H.. 1972. Bayesian-Based Iterative Method of Image Restoration. *Journal of the optical Society of America*, vol. 62, no. 1.

LUCY, L.B.. 1974. An Iterative Technique for the Rectification of Observed Distributions. *The Astronomical Journal*, vol. 79, no. 6.

PRATT, W.K. and C.E. MANCILL. Spectral Estimation Techniques for the Spectral Calibration of a Color Image Scanner. *Applied Optics*, no. 15, 73-75.

RUGGABER, B. et. al.. 2013. Characterization of a Liquid-Crystal Tunable Filter Based Hyperspectral Camera. *Proceedings of the 12th International Colour Congress*, Newcastle upon Tyne, UK.

ENVIRONMENTAL INFLUENCES ON A CALIBRATION STANDARD

Schewe, F.[1], Paulus, D.[1], **Young, R.[1]**
[1] Instrument Systems GmbH, Munich, GERMANY
young@instrumentsystems.com

Abstract

In order to evaluate environmental influences on equipment, both in transport and use, two studies were performed. The first recorded temperature, humidity and mechanical shock conditions experienced during shipping and use. The second recorded luminance changes in a calibration standard as the temperature and humidity were changed in programmed cycles.

The first study showed that temperature and humidity changes were not at all extreme but that severe mechanical shocks must be endured in transport.

The second study demonstrated the need for multi-cycle environmental testing. It showed that sensitivity coefficients for temperature and ageing effects could be readily obtained but changes due to humidity never reached equilibrium. This meant that the traditional sensitivity coefficient due to humidity could not be obtained and that a time-variant model was required.

Keywords: environmental, sensitivity, coefficient, temperature, humidity, mechanical shock, acceleration, transport, calibration, standard, instrument.

1 Introduction

Instruments are generally subjected to a wide range of environmental conditions. During transport they must survive any conditions without significant changes to their operation or calibration; during operation they must maintain their performance over a range of conditions. To assess these environmental influences on a calibrations standard, two studies were performed.

Study 1 assessed the effects of transport. Sensors were placed within the instrument giving values for temperature, humidity and acceleration (mechanical shock). The instrument was then shipped and returned to provide a record of conditions the instrument must survive.

Study 2 assessed the effects of operational environmental conditions on the performance of the standard. An environmental chamber was used to give a programmed cycle through fixed conditions in a controlled way. The program cycles were specifically aimed at providing sensitivities of the luminance value to the environmental conditions of temperature, humidity and time.

2 Study 1

A typical instrument was fitted with temperature, humidity and acceleration sensors. The values for each 10 second period were stored automatically (for shock the maximum value above a threshold was stored). The instrument was then packed as normal, including “fragile” stickers, and shipped in the usual way to Taiwan. There it was unpacked, operated as normal for approximately one week, repacked and shipped back.

2.1 Results of study 1

Results for the outward journey are shown in Figure 1. The return journey showed similar values, and the period of operation between showed more stable conditions as one would expect.

This study showed that no extreme temperatures were encountered and conditions were between 10°C and 27°C throughout the transport and use.

Humidity values were similarly over a narrow range, with 28% to 64% R.H. except when the package was opened or closed. These periods corresponded to unpacking and repacking and high values (up to 85% R.H.) may have resulted from the breath of people nearby.

Despite the “fragile” stickers, the shock values indicated the instrument was subjected to up to 10 g_n (g-force). Repeated tests on the package indicate this corresponded to being dropped from more than 1 metre height onto a concrete floor. Luckily the instrument survived intact.

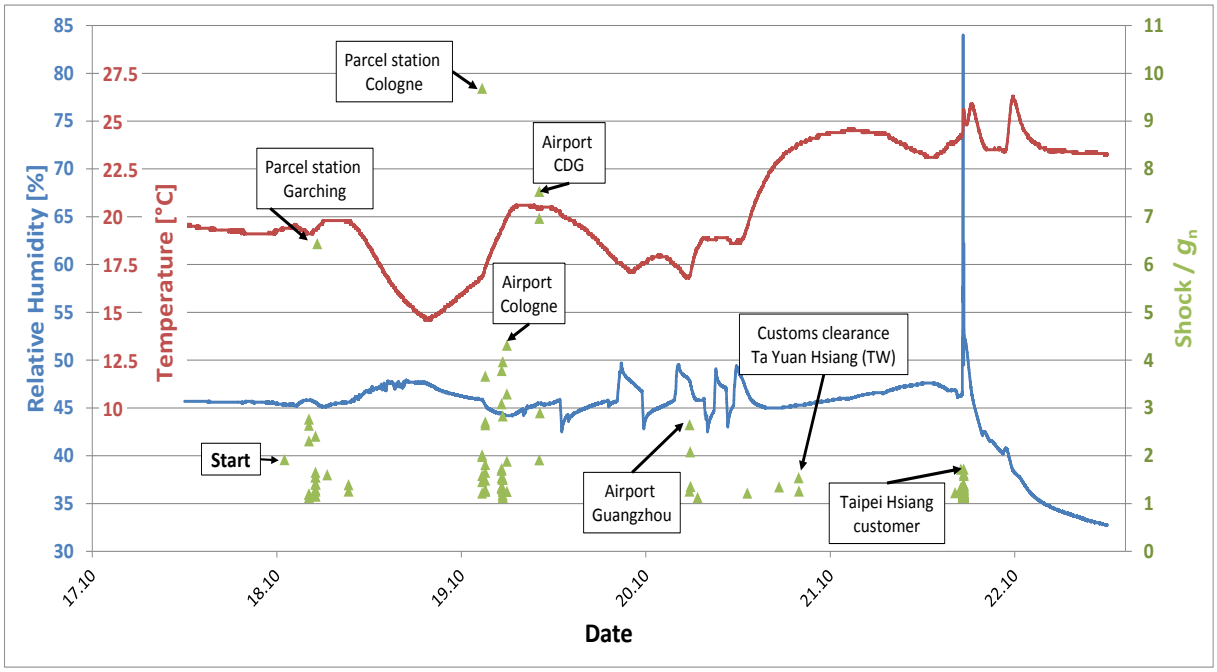

Figure 1 – Plot of the environmental conditions recorded during the outward journey

3 Study 2

The maximum rated operation conditions of the luminance standard are 40°C / 70% R.H.so the cycle is aimed at determining sensitivities relative to that condition. More “normal” conditions of 20°C and 30% R.H. were selected, sequentially, in order to assess sensitivities. The cycle is shown in Figure 2.

3.1 Single cycle tests

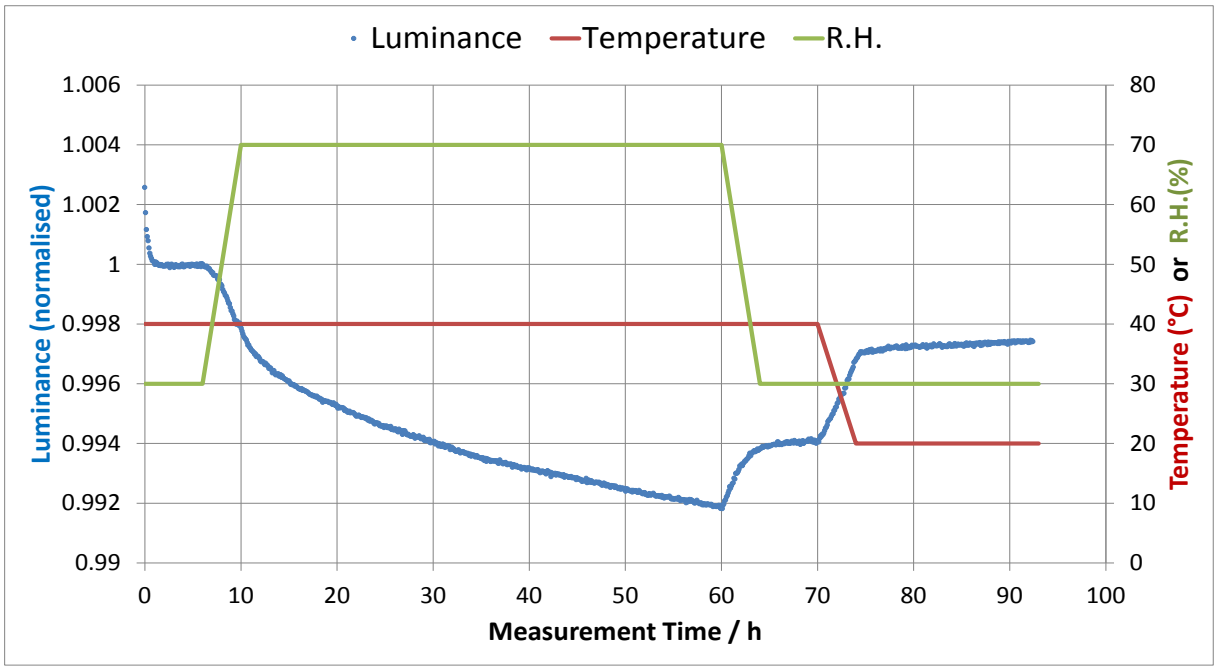

Figure 2 – Temperature and humidity cycles with corresponding luminance output with respect to time.

In this simple approach, the luminance sensitivity to temperature would be obtained from the change in luminance over the 20°C change (70 h to 74 h period); the luminance sensitivity to humidity would be obtained from the 40 %R.H. change (60 h to 64 h period); and the ageing rate would be obtained from the slope with time over the 30 h to 60 h period. However, the programmed change in environmental conditions was deliberately gradual and linear, but only the temperature change shows a corresponding linear change in luminance. This could be the result of non-linear sensitivity values or that equilibrium was not reached. A further test involving multiple environmental cycles was therefore performed.

3.2 Multiple cycle tests

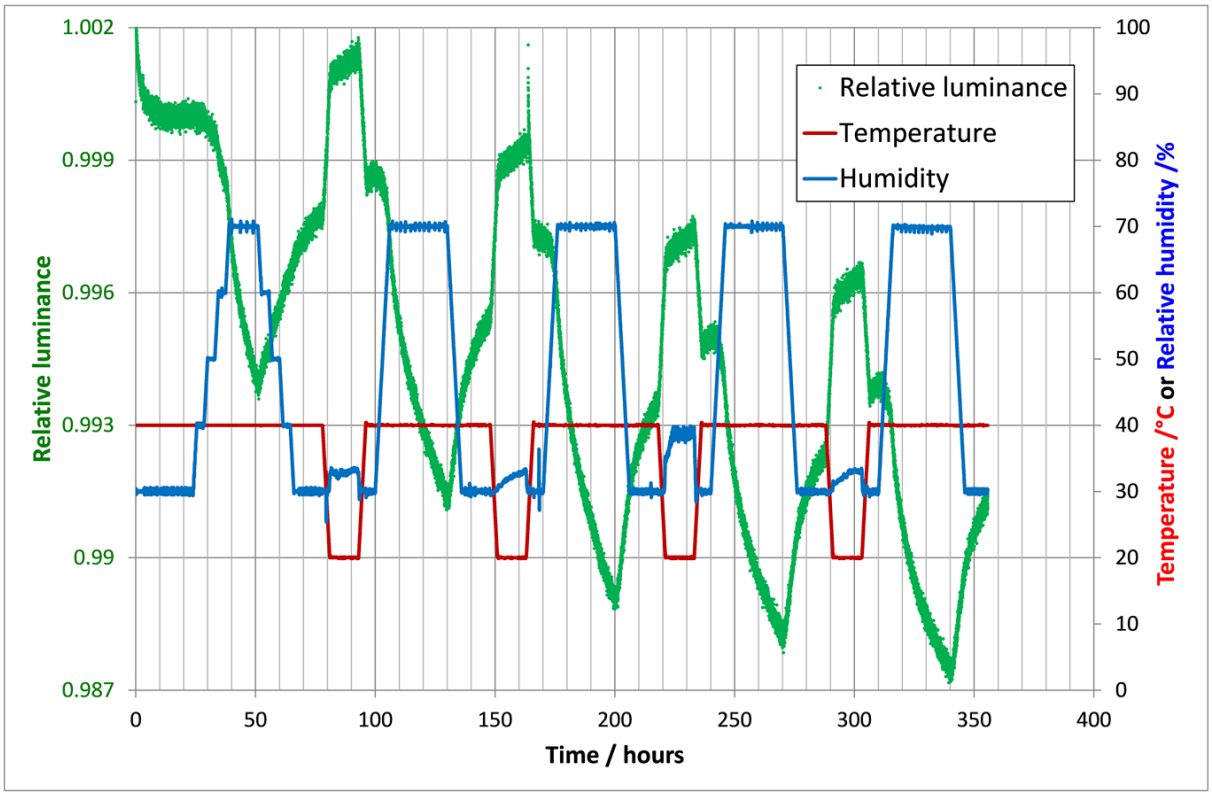

Figure 3 – Results of multiple cycle tests for a LED calibration standard with integrating sphere

In the multiple cycle tests, shown in Figure 3, the first part of the programmed changes is aimed at determining whether the luminance changes are due to non-linear sensitivity coefficients or non-equilibrium conditions. The humidity is changed in 10% R.H. steps over this 24 h to 66 h period. It is clear that corresponding steps are not seen in the luminance data so the conclusion must be that equilibrium is not achieved.

In fact it is clear that equilibrium is not achieved even over a 24 hour period (Figure 3) or 50 hour period (Figure 2) of constant environmental conditions. Using the multiple cycle technique we can however identify the temperature and ageing effects unambiguously. If we correct the luminance variation for temperature and ageing, as shown in Figure 4, we obtain the effect due to humidity alone.

Creating an uncertainty budget requires we know the uncertainty in an input parameter, in this case relative humidity, and also a sensitivity of the output luminance to the input parameter [CIE 2011],[JCGM 2008]. This assumes equilibrium conditions prevail and clearly this is not the case so another method is required to estimate uncertainty due to humidity variations. Humidity normally varies diurnally (daily cycles) and extreme values would only be seen for short periods. However, if we assume the worst case condition where it is at the extreme for 12 hours and at the calibration condition for 12 hours, we can use the maximum change over 12 hours seen with the 40 %R.H. change together with the measured humidity differences for the calibration condition. In other words, if the calibration was at 45 %R.H. and the maximum humidity seen in the period around the calibration is 55 %R.H. the uncertainty relative to the calibration is $(55-45)/\sqrt{3} = 5{,}8$ %R.H. and the sensitivity to be applied is $0{,}4/40 = 0{,}01$ %/%.

The above simplifications and assumptions can be avoided by fitting a time response function to the curves in Figure 4 and then convoluting actual humidity data measured over a long period. In fact, this is the only way to correct data as well as giving a robust estimate of uncertainties. Usually however, uncertainties due to humidity are not the most significant contributions to the uncertainty budget so a rough estimate may be sufficient.

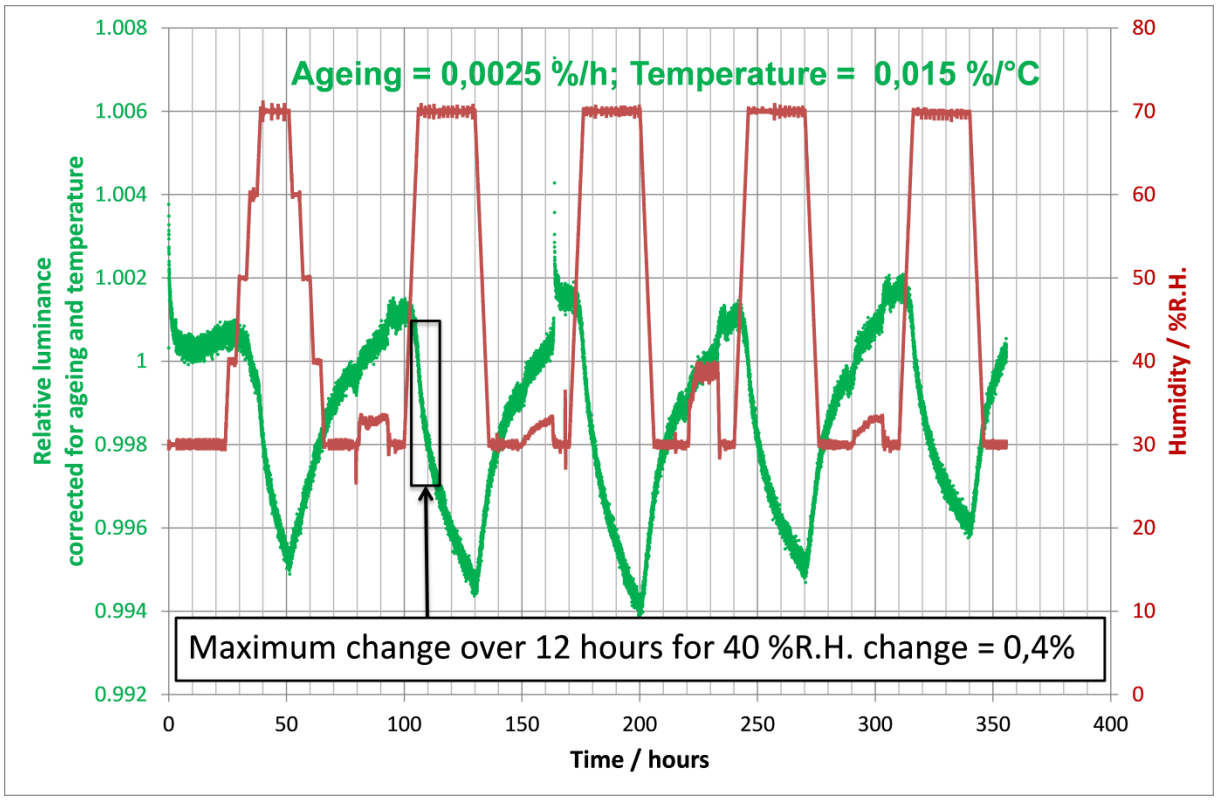

Figure 4 – Luminance variations shown in Figure 3, corrected for temperature and ageing effects. The humidity is shown in red (right vertical axis) for comparison

Although the effect of humidity is small, it is almost entirely due to the integrating sphere. The coating reflectance is known to change very slightly with humidity and the sphere has an amplifying effect. Without the integrating sphere, the effect of humidity is reduced to virtual insignificance, as shown in Figure 5.

Despite the extremely small variation with humidity shown in Figure 5, it is still clearly present. This was a surprise as LEDs are not usually considered at all sensitive to humidity. However, it is possible the humidity is changing thermal or electrical contact resistance (e.g. [Ramkumar 2007]) and affecting the LED in that way.

Both of the calibration sources use the same type of LED and control electronics yet had different temperature and ageing sensitivities, with more than a factor of 2 between them. This would indicate that care should be exercised in assigning a single sensitivity value to classes of instrument based on single-sample tests, even if they are technically of the same type.

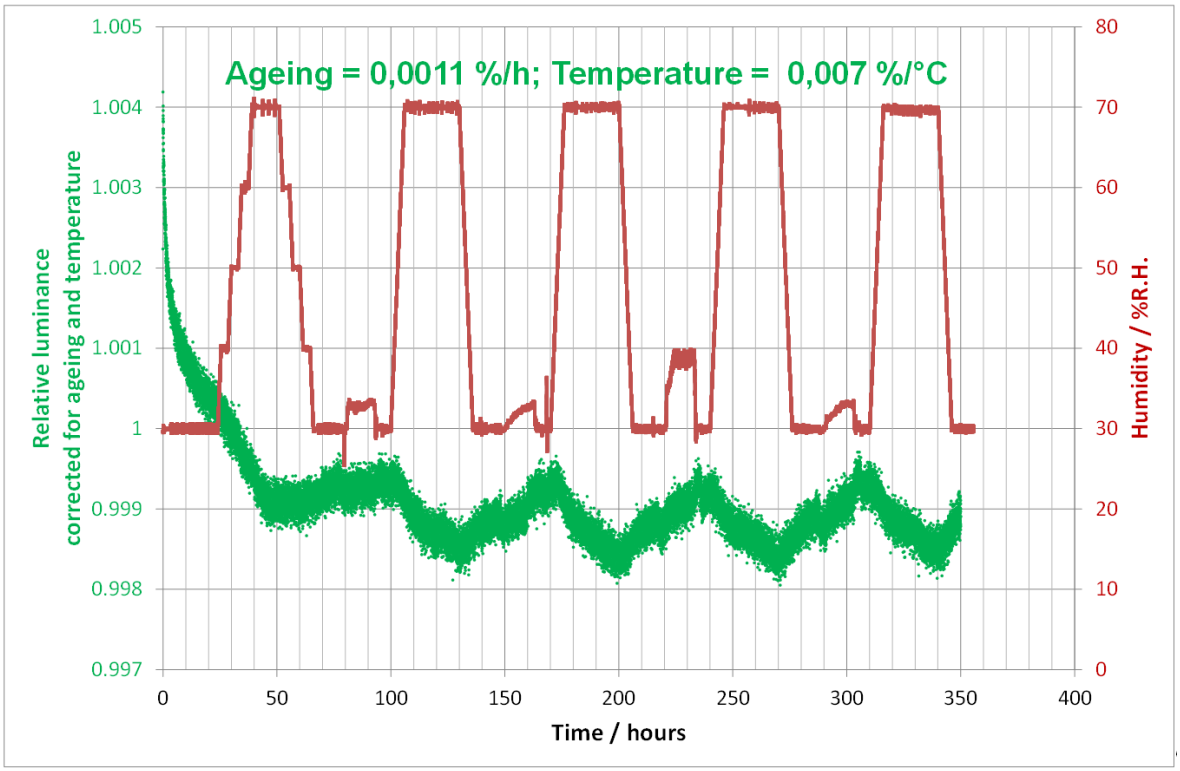

Figure 5 – Luminance variations from multiple cycle tests on a LED calibration standard without the integrating sphere, corrected for temperature and ageing effects (The humidity is shown in red (right vertical axis) for comparison.)

4 Conclusions

From this study, equipment would not be expected to endure extreme temperatures or humidities, except during packing and unpacking. However, high levels of mechanical shock should be expected during transport handling, especially when transferring from one mode of transport to another.

Environmental chamber tests can give misleading results on single cycles, especially when long periods of stable conditions are assumed to be equivalent to equilibrium. Multi-cycle testing shows that, in these studies, equilibrium was not achieved even with days under stable humidity conditions. Sensitivity coefficients, which are essential to evaluation of uncertainties or corrections, are easily obtained for temperature and ageing (time) changes but cannot be obtained for humidity variations. Some form of time-dependent treatment is therefore required for the treatment of uncertainties due to humidity and this study shows a simple “worst-case” treatment as an example.

References

CIE 2011. CIE 198:2011. Determination of measurement uncertainties in photometry. Vienna: CIE.

JCGM 2008. JCGM 100:2008. Evaluation of measurement data – guide to the expression of uncertainty in measurement. Available from http://www.bipm.org/utils/common/documents/jcgm/JCGM_100_2008_E.pdf (correct as accessed on 2014-09-18)

Ramkumar, S. M. and Srihari, K. 2007. Influence of PCB surface finish and thermal and temperature/humidity aging on the performance of a novel anisotropic conductive adhesive for lead-free surface mount assembly. Accessed from http://scholarworks.rit.edu/other/645 (correct as accessed on 2014-09-18)

MEASUREMENT UNCERTAINTY EVALUATION IN LUMINOUS FLUX METROLOGY USING INTEGRATING SPHERES

Rossi, G.[1], Migale, G.[2], Iacomussi, P.[1]
[1] INRIM, Torino, ITALY, [2] IMQ, Milano, ITALY
g.rossi@inrim.it

Abstract

The new standards for the photometric characterization of LED sources and luminaires require the evaluation of the measurement uncertainties for every measured photometric and colorimetric quantities. This request increases flexibility in the selection of instruments and in the definition of the measurement procedure, but requires the development of methodologies for the measurement uncertainty evaluation. Sometime industrial or testing house laboratories have great difficulties to follows the ISO-JCGM and CIE guidelines for uncertainty evaluation to correctly evaluate the influence of the available metrological characteristics of instruments and measurement procedures. This paper illustrates a simplified model for the evaluation of luminous flux with an integrating sphere. In order to validate the proposed model the preliminary results of an intercomparison between measurements carried out using two different goniophotometer systems are also showed.

Keywords: Photometry, Luminous Flux, Measurement uncertainty, Integrating sphere

1 Introduction

The European standard (CEN 2004) for the measurement of luminous flux of lamps and luminaires has been developed more then 10 years ago. At that time, the measurement uncertainty concept was well known in technical and scientific contexts, but its evaluation was practically an unknown task for industry and many testing-house laboratories. The JCGM guides (BIPM 2008a, BIPM 2008b) and the CIE technical report (CIE 2011) are powerful documents but their application is considered very difficult for every day work, especially for industrial photometric measurements.

For these reasons the technical group that developed the CEN standard (CEN 2004) chose to specify detailed quantitative requirements and tolerances on the metrological characteristic of instruments and on the operating, environmental and geometrical conditions. These requirements where obtained considering an undeclared, but realistic, uncertainty level. They were evaluated considering the main sources of measurement uncertainty and errors, qualitatively highlighted in the standard.

This approach has several drawbacks:

- The influence of the measurement procedure is completely underestimated. A good measurement procedure can overcome some lack in the metrological characteristic of the used instruments while increasing the number of measured parameters permits to quantify and apply correction factors. On the other hand, an inadequate procedure can increase the contribution in the uncertainty budget even of a well-suited instrument.
- Requirements for instruments and laboratories are based on the prevalent light sources and luminaires technologies on the market when the standard has been developed: new light sources or power supply devices may require different specifications, additional precautions or even a “softer” approach in their technical specifications. This requires the introduction of new standards, like in the case of LED modules and luminaires where two aligned standards will be soon published by CIE and CEN.
- Requirements should consider the more stringent conditions for a given class of products or sources. This was reasonable in the past when a small number of lamp and ballast types or categories was on the market. Nowadays with the same device name (i.e. LED drivers) so many products are available with a great dispersion of technical

characteristics, that it is possible to find luminaires with the luminous flux very stables for power line voltage variations, but that can vary at significant level with power line impedance (Zhao & Rietveld, 2012). To control this situation could be an unnecessary cost for an industrial laboratory (both in instrumentations and in measurement time) if the lab measures a well defined set of light sources or luminaires.

- The uncertainty value that could be obtained following the entire set of standard requirements is not declared in the standard and cannot be declared explicitly in test reports, as accreditation bodies requires (ISO/IEC 2005). The accredited laboratory shall evaluate its uncertainty following only its experience, scientific bibliography and guides, often considered too complex for industrial laboratories. These difficulties led to the result that in the test report often the measurement uncertainty is omitted and the measured values are given with an unrealistic too high number of significant digits or the customer requiring the text report has no information about the algorithm followed to obtain the measurement uncertainty value or about its reliability.
- Industrial laboratories use commercial measurement systems and commercial software with the advantage that instruments and measurement procedures are standard compliant. The laboratory has not the necessity to validate the software (acquisition, elaboration and text report editing) because the validation process is done or supposed to be done by the measurement system manufacture. The disadvantage is that, generally, the measurement software does not consider nor evalute the measurement uncertainty and the metrological characteristics of the used instruments are not known with the necessary accuracy and completeness. Without these peculiar data and those arising from the type of measured device it is difficult to develop a scientific and sound measurement model.

The new standards under development in CIE (TC 2-71) and in CEN (TC169-WG7) for the measurement of LED sources and luminaires follow a completely different approach: the evaluation of measurement uncertainty is the key point. As a matter of fact, all standard requirements and laboratory decisions in developing its own measurement procedure shall consider the measurement uncertainty level as a peculiarity of the laboratory. Standard requirements are a way to simplify the measurement model and its management and not to avoid its development. The laboratory measurement procedure, the selection of instruments and the environmental constrain shall be defined considering both the requirements and flexibilities of the standards and the uncertainty level goal of the laboratory. The use of correction factors, with known uncertainty, and/or peculiar procedure can compensate for some discrepancies in standard requirements without losing the possibility of writing in the test report that measurements complies with standard.

This new approach has two main advantages for industrial or testing house laboratories:

- The measurement costs can be correlated to the required uncertainty level. Measurement can be done for different aims: data to be published in catalogue, verification of production tolerances, pass/not pass testing of components or of the end products, verification of performance respect to coercive standards, i.e. to EU directives (EC 1998), verification of design expectations, research for new design solutions, studies for evaluating performances at different working conditions, comparison with measurement carried out in other laboratories. Each of these aims can require different measurement uncertainty for correct evaluation of the measurement results, and therefore instrumentations and procedures should the adapted to these conditions to minimize measurement cost and time.
- The selection of instruments, the laboratory layout, the definition of the steps in measurement procedure can be done according to the main aims of the laboratory or the type of product that will be measured. This possibility permits the realization of specialized laboratories with a lower number of constrains or with less heavy constrains if compared with a general purpose laboratory.

This new approach has advantages for the laboratory customers too:

- The laboratory can be selected according to the best compromise between measurement cost and measurement uncertainty, considering the aim of the measurement.

- Results obtained by different laboratories can be easily compared considering the influence of the measurement uncertainty, as in BIPM (2012).
- The correct physical interpretation of results is simplified and long discussion on small variation between results, but inside the measurement uncertainty interval of values are completely avoided.
- In problematic cases the selection of a laboratory with a better accuracy can resolve any dispute between manufactures and customers.

2 The development of a measurement model

In developing a measurement model (BIPM 2009) as required for an accredited laboratory some technical compromises should be considered:

- The parameters involved shall give a real contribution to the uncertainty level (e.g. all the parameters that have a contribution lower that 1/10 of the main ones should not be considered). When a parameter is considered in the model, not only the cost necessary to measure it, but also the cost of the calibration of the instrument necessary for its measurement and the cost for its historical management shall be considered. All this activities are justified only if giving a real improvement in the measurement accuracy.
- The model shall be simplified as much as possible (e.g. it shall give a realistic evaluation of the uncertainty value, preferably with a small overestimation).
- The cost to evaluate all the parameters of the measurement model shall be considered. Generally it is not economical to carry out a set of specific measurements for defining the numerical values of all the parameters required by the measurement model for each lamp or luminaire. An historical background and database could be sufficient to obtain realistic values of the measurement uncertainty. Ad hoc specific measurements carried out periodically and standard requirements shall simplify the management of the model.
- If possible correction factor should be considered to reduce the influence of same parameters, but it is an unproductive work spend time and resources for correcting parameters that have a very small influence in the measurement results and uncertainty.
- The real cost in evaluating the measurement uncertainty is not in the mathematical complexity of the measurement model, but in the way the single parameter values are obtained and justified.
- If the laboratory uses a commercial measurement systems, sometime the manufacture of the system does the planned maintenance of the system too, and in this activity the calibration of the reference sources or detectors is included. Generally the measurement system manufacture carries out the calibration using traceable reference standards and measurement conditions very similar to those adopted by the lab (i.e. same type of instruments). In this case the measurement uncertainty in the calibration certificate is greater than the typical value given by a national metrology institute, but the measurement model can be simplified because the influence of some parameters is already considered in the calibration uncertainty.

The parameters considers in the measurement model depends on the:

- Characteristics of the laboratory, like the metrological characteristics of the used instruments, the calibration method and interval, the number of measurements, the environmental and geometric conditions. These parameters can be considered constant for a given type of luminous source or luminaire.
- Characteristics of the device under test (DUT), like its short term stability, its repeatability between different switch on and off, the limit in the accuracy of its alignment in the correct measurement position.

An open question that standards should clearly answer is about the selection of parameters correlated to the DUT characteristics that shall be considered in the uncertainty model like, for example, light source repeatability between different switch on and off. If considered in the measurement model, this last parameter requires different complete switch on/off cycles (alignment of the DUT in the measurement position, switch on, stabilization, measurement,

switch off, cooling, safety remove) that could increase the real measurement time, if an integrating sphere is used.

When the measurement model is defined practically there are two different approaches (BIPM 2009) to obtain the measurement uncertainty:

- the GUM uncertainty framework (BIPM 2008a), that gives exact results if the measurement function is linear in the input quantities and the probability distributions of these quantities are Gaussian and often works sufficiently well for practical purposes if these conditions are not hold. This approach is relatively complex because requires the evaluation of sensitivity coefficients for each parameter of the measurement models but can be managed with simple spread sheet programs and gives a clear understanding of the parameters that have the greater importance in the uncertainty budget. This information is extremely useful when the obtained uncertainty level is not satisfactory and the strategy for improvement shall be defined.
- The Monte Carlo method (BIPM 2008b) establishes numerically the measurement uncertainty by making random draws from the probability distribution of the measurement model parameters. Its numerical accuracy can be mathematically controlled. This approach is more simple to understand, the acquisition software can be easily modified for its evaluation or the uncertainty value can also be obtained with same spread sheet programs.

3 The measurement model

The measurement of the luminous flux of a light source using an integrating sphere and spectral radiometric measurement was considered in a research program between INRIM, the Italian National Metrology Institute, and IMQ, the Italian most important certification body. The main aim of this research is to give support to the National Standardization Body (UNI) in developing guidelines for the evaluation of measurement uncertainty for photometric and colorimetric quantities in industrial laboratories.

The procedure for the measurement of the luminous flux considered in this research is a relative measurement carried out following the steps described in table 1. A reference calibrated lamp is used for the calibration of the integrating sphere while an non-calibrated auxiliary lamp is used to compensate the influence of the DUT inside the sphere.

The measurement model can be written as:

$$\Phi_{\mathrm{DUT}}(\lambda) = \Phi_{\mathrm{cal}}(\lambda)\,\frac{R_{\mathrm{d}}(\lambda)}{R_{\mathrm{a}}(\lambda)}\,\frac{R_{\mathrm{c}}(\lambda)}{R_{\mathrm{b}}(\lambda)} \tag{1}$$

where

$\Phi_{\mathrm{DUT}}(\lambda)$ is the measured spectral concentration at wavelength λ of the radiant flux of the lamps under measurement;

$\Phi_{\mathrm{cal}}(\lambda)$ is the spectral concentration at wavelength λ of the radiant flux of the reference lamps, from its calibration certificate ;

$R_{\mathrm{a}}(\lambda)$ is the measured value at wavelength λ with the experimental condition described in step 1 of table 1;

$R_{\mathrm{b}}(\lambda)$ is the measured value at wavelength λ with the experimental condition described in step 2 of table 1;

$R_{\mathrm{c}}(\lambda)$ is the measured value at wavelength λ with the experimental condition described in step 3 of table 1;

$R_{\mathrm{d}}(\lambda)$ is the measured value at wavelength λ with the experimental condition described in step 2 of table 1.

Table 1 – The measurement steps

Step	Measured quantity	Main light source	Conditions	
			Main light source	Auxiliary lamp
1	$R_{\mathrm{a}}(\lambda)$	Reference	ON	OFF
2	$R_{\mathrm{b}}(\lambda)$	Reference	OFF	ON
3	$R_{\mathrm{c}}(\lambda)$	DUT	OFF	ON
4	$R_{\mathrm{d}}(\lambda)$	DUT	ON	OFF

Considering the parameters in the uncertainty budget, $R_{\mathrm{a}}(\lambda)$ can be written as:

$$\begin{aligned} R_{\mathrm{a}}(\lambda) = {} & R_{\mathrm{a,i}}(\lambda)\; k_{\mathrm{a,la}}\; k_{\mathrm{a,ls}}\; k_{\mathrm{a,lr}}\; k_{\mathrm{a,lp}}(\lambda) \\ & k_{\mathrm{a,ac}} \\ & k_{\mathrm{a,sw}}(\lambda)\; k_{\mathrm{a,ssl}}(\lambda)\; k_{\mathrm{a,sr}}\; k_{\mathrm{a,sp}}\; k_{\mathrm{a,srr}}(\lambda) \\ & k_{\mathrm{a,sdc}}\; k_{\mathrm{a,snl}}(\lambda) \\ & k_{\mathrm{a,isr}}\; k_{\mathrm{a,iss}}\; k_{\mathrm{a,ise}}(\lambda) \end{aligned} \tag{2}$$

where

$R_{\mathrm{a,i}}(\lambda)$ is the indication of the sphere detector at wavelength λ with the experimental condition described in step 1 of table 1;

$k_{\mathrm{a,la}}$ is the correction factor to take into account for the ageing of the reference lamp;

$k_{\mathrm{a,ls}}$ is the correction factor to take into account the short term stability of the reference lamp;

$k_{\mathrm{a,lr}}$ is the correction factor to take into account the reproducibility of the reference lamps;

$k_{\mathrm{a,lp}}(\lambda)$ is the correction factor to take into account the influence of the actual power supply conditions of the lamp at wavelength λ;

$k_{\mathrm{a,ac}}$ is the correction factor to take into account the influence of laboratory ambient conditions;

$k_{\mathrm{a,sw}}(\lambda)$ is the correction factor to take into account the wavelength error of the spectroradiometer at wavelength λ;

$k_{\mathrm{a,ssl}}(\lambda)$ is the correction factor to take into account the stray light of the spectroradiometers at wavelength λ;

$k_{\mathrm{a,sr}}$ is the correction factor to take into account the reproducibility of the spectroradiometer;

$k_{\mathrm{a,sp}}$ is the correction factor to take into account the influence of polarised light in the spectroradiometer;

$k_{\mathrm{a,ssr}}(\lambda)$ is the correction factor to take into account the relative spectral responsivity of the spectroradiometer at wavelength λ;

$k_{\mathrm{a,sdc}}$ is the correction factor to take into account the dark current of the measurement system;

$k_{\mathrm{a,snl}}(\lambda)$ is the correction factor to take into account the spectroradiometer non linearity at wavelength λ;

$k_{\mathrm{a,isr}}$ is the correction factor to take into account the integrating sphere repeatability;

$k_{\mathrm{a,iss}}$ is the correction factor to take into account the integrating sphere stability;

$k_{\mathrm{a,ise}}(\lambda)$ is the correction factor to take into account the integrating sphere error (spatial non uniformity and self-absorption) at wavelength λ.

If it is possible to consider the measuring conditions equivalent to those used during the reference source calibration, the contribution of same parameters can be neglected because already evaluated in the calibration uncertainty. In this case $R_{\mathrm{a}}(\lambda)$ can be written as:

$$\begin{aligned} R_{\mathrm{a}}(\lambda) = {} & R_{\mathrm{a,i}}(\lambda)\; k_{\mathrm{a,la}} \\ & k_{\mathrm{a,ssl}}(\lambda)\; k_{\mathrm{a,sr}}\; k_{\mathrm{a,sp}}\; k_{\mathrm{a,srr}}(\lambda) \\ & k_{\mathrm{a,sdc}}\; k_{\mathrm{a,snl}}(\lambda) \\ & k_{\mathrm{isr}}\; k_{\mathrm{iss}} \end{aligned} \tag{2}$$

Following the same type of approximation and with obvious changes of symbols, the other three quantities can be written as:

$$\begin{aligned} R_{\mathrm{b}}(\lambda) \;=\; & R_{\mathrm{b,i}}(\lambda)\; k_{\mathrm{b,ls}} \\ & k_{\mathrm{b,sdc}}\; k_{\mathrm{b,snl}}(\lambda) \\ & k_{\mathrm{b,isr}}\; k_{\mathrm{b,iss}} \end{aligned} \tag{3}$$

$$\begin{aligned} R_{\mathrm{c}}(\lambda) \;=\; & R_{\mathrm{c,i}}(\lambda)\; k_{\mathrm{c,ls}} \\ & k_{\mathrm{c,sdc}}\; k_{\mathrm{c,snl}}(\lambda) \\ & k_{\mathrm{c,isr}}\; k_{\mathrm{c,iss}} \end{aligned} \tag{4}$$

$$\begin{aligned} R_{\mathrm{d}}(\lambda) \;=\; & R_{\mathrm{d,r}}(\lambda)\; k_{\mathrm{d,lr}}\; k_{\mathrm{d,lp}}(\lambda) \\ & k_{\mathrm{d,ac}} \\ & k_{\mathrm{d,sw}}(\lambda)\; k_{\mathrm{d,ssl}}(\lambda)\; k_{\mathrm{d,sr}}\; k_{\mathrm{d,sp}}\; k_{\mathrm{d,srr}}(\lambda) \\ & k_{\mathrm{d,sdc}}\; k_{\mathrm{d,snl}}(\lambda) \\ & k_{\mathrm{d,isr}}\; k_{\mathrm{d,iss}}\; k_{\mathrm{d,ise}}(\lambda) \end{aligned} \tag{5}$$

Like the stray light characteristics of the spectroradiometer, many parameters can be difficult to obtain or, practically, their measurement can be so complicated and time consuming that only a roughly information can be available from manufacture. In this case, the correction is numerically equal to 1 and only their uncertainty is considered in the measurement model.

Other parameters, like $k_{\mathrm{d,lr}}(\lambda)$, the reproducibility of the DUT, can be obtained from database or from previous measurement of the same type of lamps. Other parameters like the dark current of the measurement system (see figure 1) can be measured at the beginning or at the end of the spectral acquisition, practically without increasing the measurement time. Its values can also be useful to have a partial indication of the stability and correct working of the measurement systems.

The use of multiplicative parameters is not a limitation of the measurement model. Many parameters that conceptually are not multiplicative like the dark current can be easily transformed in the proposed form:

$$\begin{aligned} S_{\mathrm{i}}(\lambda) \;&=\; S_{\mathrm{M}}(\lambda) \;+ S_{\mathrm{dc}} \\ S_{\mathrm{M}}(\lambda) \;&=\; k_{\mathrm{sdc}}(\lambda)\; S_{\mathrm{i}}(\lambda) \\ k_{\mathrm{sdc}}(\lambda) \;&= 1 - \frac{S_{\mathrm{dc}}}{S_{\mathrm{i}}(\lambda)} \end{aligned} \tag{6}$$

where

$S_{\mathrm{i}}(\lambda)$ is the indication of the sphere detector at wavelength λ in any experimental condition;

$S_{\mathrm{M}}(\lambda)$ is the signal that should be measured at wavelength λ;

S_{dc} is the dark current of the measurement system;

$k_{\mathrm{sdc}}(\lambda)$ is the correction factor at wavelength λ to take into account the dark current of the measurement system.

In the above example the dark current in considered independent from the wavelength. As show in figure 1 its mean value can be used to correct the spectroradiometer indication. Also the parameters that represent the short term stability of the auxiliary and reference lamps can be considered independent from the wavelength and can be verified occasionally (figure 2). They are numerically equal to 1 and only their contribution in the uncertainty budget is considered.

When the values of parameters in the measurement model are known the evaluation of measurement uncertainty of the spectral concentration of the radiant flux is obtained following the GUM algorithms (BIPM 2008a) while the measurement uncertainty of the integrated quantity, the luminous flux, is obtained considering the correlation of the spectral data (Woolliams & Goodman, 2012). Alternatively the Monte Carlo approach can be followed.

If the aim is the measurement of the luminous flux, the influence of the correction factors that take into account the wavelength error, the bandwidth and the relative spectral responsivity of the spectroradiometer and the wavelength step can be evaluated considering the spectral distribution of typical light sources, as in table 2. With this type of sources and a wavelength step $\Delta\lambda$ = 5 nm the spectral deconvolution is not necessary because other correction are more important.

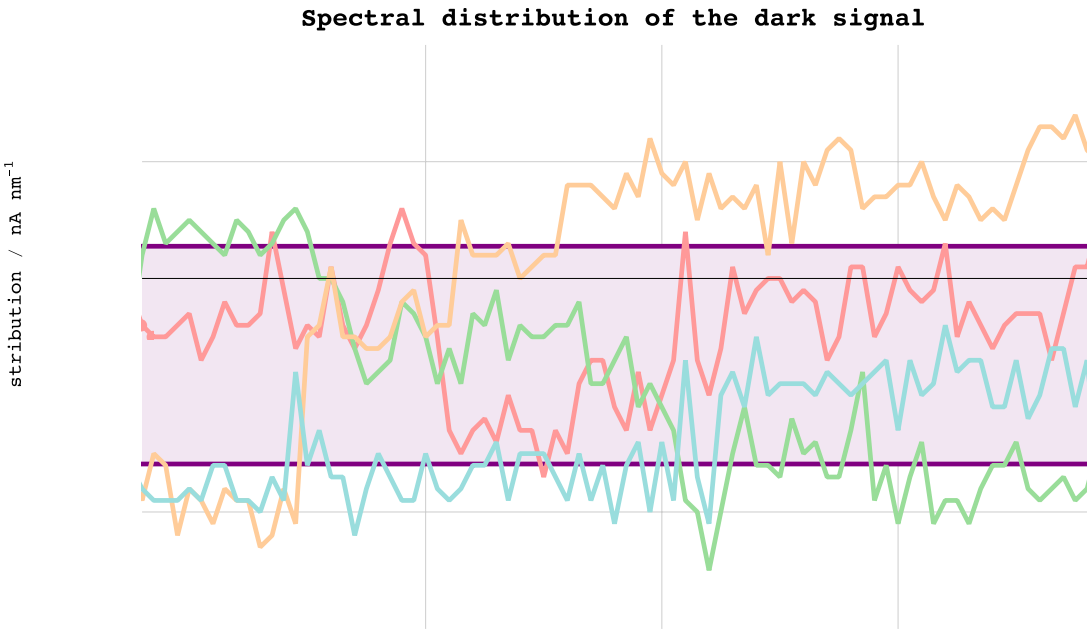

Figure 1 – Example of the measurement of the dark current. The mean value of the dark current (S_{dc} in blue) is practically independent from the wavelength and can be measured at the beginning or at the end of the spectral acquisition

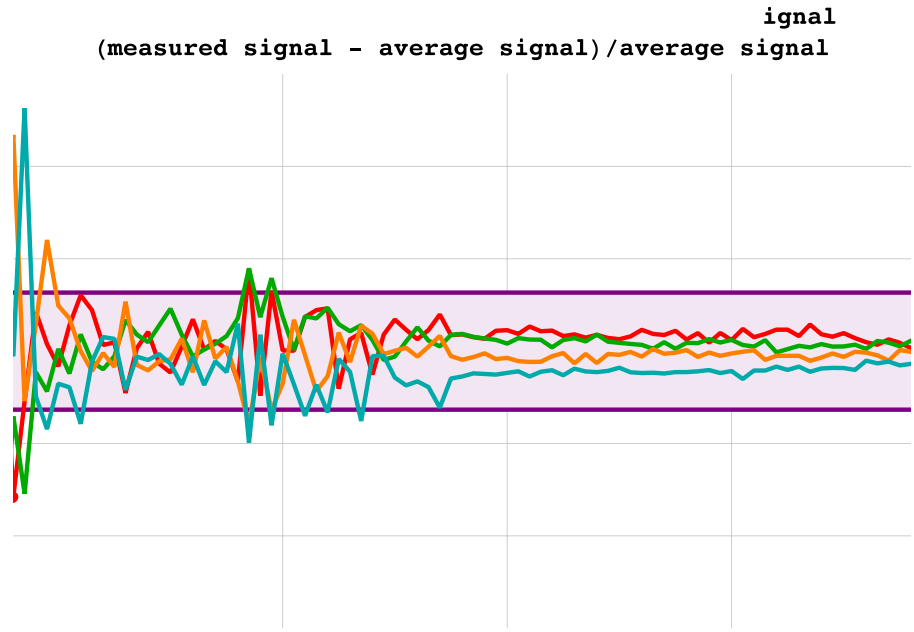

Figure 2 – Example of the short term stability of the auxiliary lamp. To highlight the wavelength influence without considering the increasing of energy within wavelength the difference between the measured signal and its average is normalized to the average signal.

Table 2 – Influence of the spectroradiometer parameters on the luminous flux for several types of lamps evaluated with a wavelength step $\Delta\lambda$ = 5 nm and a bandwidth of 5 nm

Lamp type	Difference between the luminous flux obtained from the spectral distribution	
	With deconvolution and without deconvolution	With a wavelength shift of ± 1 nm
	%	%
Halogen	0,00	0,7
Fluorescent	0,03	0,9
Metal Halide 3000 K	0,02	0,6
Metal Halide 4000 K	0,02	0,3
High Pressure Sodium	0,02	1,4

4 Comparison of results

The luminous flux of the set of lamps measured with the integrating sphere has been partially compared with two different goniophotometers, one at INRIM (radius of about 3 m, fixed lamp) and the other at IMQ (mirror type with a measuring distance of 15 m). At INRIM also the spectral distribution was measured at different angular directions. The comparison is not concluded yet but preliminary results show a measurement uncertainty from 3,5 % to 4 % for measurement carried out using the integrating sphere and from 1 % to 2.5 % for measurement carried out with the goniophotometers. The results between the different systems are compatible considering the measurement uncertainty, and this can be considered a validation method of the measurement model for the integrating sphere and of the management of the parameters in the uncertainty budget.

The main contribution in the measurement uncertainty rises from the spectral lamp calibration, the integrating sphere error due to different light distribution between the calibration lamp and the DUT, the wavelength accuracy of the spectroradiometer and its non-linearity.

5 Conclusions

This proposed measurement model show that several mathematical simplifications can be done and the influence of several parameters can be obtained considering information from historical database. Of course this is true if the standard requirements are satisfied.

Especially for LED, the light source short term stability and reproducibility are better than the measurement uncertainty so a small number of spectral acquisition is possible, minimizing the measurement time.

For industrial measurements when the measurement uncertainty is generally greater of 3 % spectral deconvolution and bandwidth (≤ 5 nm) are not the main sources of uncertainty. The sphere error can become very high with directional lamps or luminaires. In this case more measurements are required with the light source in different positions.

References

BIPM 2008a. JCGM 100:2008. Evaluation of measurement data – Guide to the expression of uncertainty in measurement (GUM). Paris: BIPM

BIPM 2008b. JCGM 100:2008. Evaluation of measurement data – Supplement 1 to the “Guide to the expression of uncertainty in measurement” – propagation of distributions using a Monte Carlo method. Paris: BIPM

BIPM 2009. JCGM 104:2009. Evaluation of measurement data – An introduction to the “Guide to the expression of uncertainty in measurement” and related documents. Paris: BIPM

BIPM 2012. JCGM 106:2012. Evaluation of measurement data – The role of measurement uncertainty in conformity assssment. Paris: BIPM

CEN 2004. EN 13032-1:2004+A1:2012. Light and lighting: Measurement and presentation of photometric data of lamps and luminaires - Part 1: Measurement and file format. Brussels: CEN

CIE 2011. CIE 198:2011. Determination of Measurement Uncertainties in Photometry. Vienna: CIE

EC 1998. COMMISSION DIRECTIVE 98/11/EC. Commission Directive 98/11/EC of 27 January 1998 implementing Council Directive 92/75/EEC with regard to energy labelling of household lamps. Brussels: EC

ISO/IEC 2005. ISO/IEC 17025: 2005. General requirements for the competence of testing and calibration laboratories. Geneva: ISO

WOOLLIAMS, E., GOODMAN, T. 2012. Determining the uncertainty associated with an integrated quantity calculated from correlated spectral data. Poster at CIE Conference, Hangzhou, China, 17-21 Sept 2012. Vienna: CIE

ZHAO, D., RIETVELD, G.. 2012. The Influence of Source Impedance in Electrical Characterization of Solid State Lighting Sources. Proceedings of 2012 Conference on Precision Electromagnetic Measurements, 1-6, July, 2012 ISBN: 978-1-4673-0441-2,

ACCURACY, REPRODUCIBILITY AND REPEATABILITY OF FAST METHODS FOR HEAD LAMP EVALUATION

Marutzky, M.[1], Kleinert, B.[1], Heinrichs, A.[1], Schwanz, B.[1], Bogdanow, S.[1]
[1] Ingenieurgesellschaft Auto und Verkehr GmbH, Gifhorn, GERMANY
michael.marutzky@iav.de

Abstract

Fast luminance camera-based methods for the collection of the light intensity distribution (LID) are an alternative to far field photo-goniometer measurements in the industrial development process. The mentioned alternative becomes interesting when examining dynamic vehicle head lamps which enable various LID. We built up a set-up for fast measurements of LID in IAV's Light- and Driver Assistance Hall, estimated the error budget, proved the measurability in a measurement systems analysis, and compared with the far field photo-goniometer.

Keywords: head lamp evaluation, camera based measurement, photo-goniometer, geometrical reduction

1 Introduction

For vehicle head lamp evaluations, usually the light intensity distribution (LID) is collected on a far field photo-goniometer. This method is highly accepted, and also measurements for homologation are conducted with photo-goniometers. On a photo-goniometer, the single component can be measured, and the measurement time is in the range of hours when a reasonable angle resolution and accuracy is aimed. However, adaptive head lamps enable more and more complex variable light distributions. For example, the "Matrix-beam" head lamp of Audi realises its dynamic light distributions with 25 LED enabling 966 million light distributions [PANDER, J, 2013]. Of course, only a fraction of the light distributions are relevant, but clearly a trend of increasing complexity is given. Thus, for a comprehensive examination of a head lamp's performance, or for the evaluation of a special situation, a fast measurement method with sufficient accuracy is needed. A solution could be luminance camera-based methods. Therefore, we developed a set-up in IAV's Light and Driver-Assistance Hall which enables indirect measurements of the LID on a screen (cp. [Schwanengel, C, 2005]) in variable working distance, and measurements under "reduced geometry" which is method we presented in [MARUTZKY, M, 2012].

The topic of this study is now to reveal the uncertainties of the mentioned camera based methods, and to proof that the measurability of the set-up is given, i.e. the measurements are reproducible, repeatable, and stable. In order to do this, we pick out two very common evaluation methods: - the evaluation on basis of the lux isolines on a virtual street, simulated from the measured LID, - the evaluation on the ECE test table. In the following, we show that such evaluations indeed can be repeatable and reproducible done with the camera based method in sufficient accuracy.

2 Measurement methods, measurement environment, and evaluation criterions

2.1 Far field photo-goniometer

The far field photo-goniometer is a well-known and accepted instrument, so here we set a detailed description aside. For this study, we assume goniometric angles of type A. In order to be able to make comparison between the different methods, we apply the same angle range and the same angle grid given at our set-up for the camera-based methods stated below (see 2.3, 2.4). The output from such measurement is the LID $I(\vartheta,\varphi)$ which is the basis for the light evaluation (cp. 2.5).

2.2 IAV's Light and Driver-Assistance Hall

IAV's Light and Driver-Assistance Hall is a measurement environment which enables repeatable reference conditions. In this hall, examinations of the single component but also on the whole vehicle can be done, and small sceneries can be built up. The walls of the hall are prepared specially so that incident light is absorbed and dispersed effectively. Light traps are placed in suitable positions, and the large dimensions of the hall effects that stray light fades away. With such efforts, the measurement described in 2.2 and 2.4 can be done with small fail light level on the screens and the measurement ground.

The hall can be darkened so that the residual light level is below the detection limit of the used photometer class L from Optronik and the luminance camera LMK98-4 colour from TechnoTeam. Additionally, user defined day- and twilight states can be realized by a day-light simulation.

2.3 Indirect measurement of LID on screens in 10 m and 25 m working distance

This measurement method was described by TechnoTeam [SCHWANENGEL, C, 2005]. Here, the head lamp illuminates a test screen, and the luminance distribution on the screen is collected with the luminance camera and transformed into the LID:

$$I\left(L(pixX, pixY), k, z, \vartheta, \varphi\right) = \frac{L(pixX, pixY)}{k} \cos\vartheta \cos\varphi z^2 \left(\tan^2\vartheta + \tan^2\varphi + 1\right)^2 \quad (1)$$

It is: I light intensity, L luminance, $pixX,pixY$ the pixel coordinates on the imaged screen, $k=L/E$ the luminance coefficient of the screen, z the working distance head lamp – screen with z || reference axis of head lamp and z ⊥ on the screen, ϑ horizontal angle, and φ vertical angle.

2.4 Method of geometric reduction

This is a method we invented ourselves as a quick benchmark tool which can also applied directly on vehicle. The aim of this method is to measure the light distribution of a vehicle head lamp directly on the pavement near to mounting position. The problem is that a low or high beam distribution is spatial unlimited. For a repeatable measurement under well-defined condition a closed ambience, i.e. a hall, is indispensable. A closed ambience naturally is spatial limited. A solution is this method of geometric reduction. It is described in detail in [MARUTZKY, M, 2012]. In principle, the head lamp respectively the vehicle is tilted by a small defined angle φ', e.g. *1.5* deg. With this, the light rays which would touch the ground in large distance to the lamp are drawn within the dimensions of the measurement ground. A measurement area of *200* m x *50* m is reduced to *34* m x *15* m. Similar to 2.3, the reduced luminance distribution on the measurement ground is collected by a luminance camera and the LID is calculated:

$$I\left(L(pixX, pixY), k_{||}(\alpha_i), h, \vartheta, \phi^*\right) = \frac{L(pixX, pixY)}{k_{||}(\alpha_i)} \cos\vartheta \cos\phi^* h^2 \left(\tan^2\vartheta + \cot^2\phi^* + \tan^2\vartheta \cot^2\phi^* + 1\right)^2 \quad (2)$$

Mathematical, the equation is identical to (1). The difference is that (1) is in dependence of z, but (2) is in dependence of h with is the height of the reference point of the head lamp above the measurement ground. Also, $\varphi^* = -(\varphi+\varphi°+\varphi')$ includes besides the goniometric vertical angle φ the legal prescribed incline of the cut-off $\varphi°$ (normally *1* % = *0.57* deg.) and the additional downtilt φ', for example *1.5* deg. The luminance coefficient $k_{||}$ generally depends on the angle of incidence, the observation, and the angle between the plane of incidence and the plane of observation. The camera can be placed above the head lamp and so $k_{||}$ degrades and is only dependent on the angle of incidence α_i . The angles of incidence are very small in the far field, for example around *0.6* deg. at *60* m distance (cp. 2.5) to the head lamp. As the determination of $k_{||}$ is very difficult at α_i smaller than *1* deg., a downtilt of the head lamp of *1.5* deg. increases α_i approximately by *1.5* deg. which makes it possible to determine $k_{||}$ accurately. Also the measured luminances increase compared to the luminances without downtilt, because the distances the light rays have to pass are reduced. As result the signal to noise ratio is improved.

2.5 Light assessment

Usually, the measured LID is used as input for light simulations, and the light assessment is done on the output of this light simulations.

Very common is to simulate the light flux and the illuminance on a virtual road under the assumption that the head lamp is in mounting position. Often a car manufacturer has defined an own assessment system where the position of certain lux isolines or the ratios of the light flux in certain zones on the road are considered. A general assessment system was defined by CIE TC 4-45. A crude assessment criterion is to consider the position of the 3 lux isoline on the road. Near to this position, the cut off will usually touch the ground, and so it is used as rough criterion for the detection range. At least, handling which such a criterion, different head lamps can be compared in benchmark. Because of the simpleness and the relative significance of this criterion we will later also consider the position of the 3 lux isoline in the measurement systems analysis stated below.

The other assessment we will focus on is the evaluation of the illuminance distribution on the "ECE test table", a virtual screen in distance to the head lamp, cp. ECE-R 112. On this test table, specific minimum and maximum values of the illuminance has to be fulfilled in certain zones and points. The head will pass or will not pass this evaluation which is part of the homologation tests in the ECE region. Below, we will observe the especially "B50L"-point, in this point the glare on an oncoming driver is evaluated and so a small maximum illuminance value is specified. The measure this small value in an accurate, repeatable, and reproducible way is a touch-stone for our test bench.

3 Error budget and error calculation

In the following part, the most important errors are pointed out and analysed.

3.1 General error sources

3.1.1 Stray light level

In the darkened hall, when the head lamp is turned off, the stray light level is below the detection limit of the used photometric measurement devices, i.e. <0.0001 lux. When the head lamp is turned on for the measurement, stray light occurs from reflections on the ground, walls, and the ceiling. This is reduced by a special preparation of the walls and the outfit with light traps. The residual stray light level on the screen is about 0.01 lux. So the stray light level is low enough to prove the small maximum illuminance values in the order of 0.1 lux above the cut-off.

3.1.2 Temperature stability

Due to its large volume, the hall is thermally very inert. After the operation temperatures of the measurement equipment and the head lamp come to an equilibrium, temperature changes between $+18$ °C and $+23$ °C lead not to an observable change in the results. Therefore we estimate the influence of a temperature change of 5 K on the measured photometric values to be <1%.

3.1.3 Stability of the power source

The power source has to be constant with maximum change in current of 0.005 A when a halogen lamp based vehicle head lamp is operated. Then the change in the measured photometric value will be <0.1%. Suitable measurement devices have to be in use to prove the constant operation.

3.2 Estimation of the photometric error

In order to estimate the error in the light intensity I, the eq. (1) resp. (2) are expansed into the linear term and the error square sum is calculated ("error propagation"):

$$\frac{\Delta I}{I} = \frac{1}{I}\sqrt{\sum_i \left(\frac{\partial I(\mathbf{x_0})}{\partial x_i} \Delta x_i \right)^2} \tag{3}$$

For the indirect screen method (cp. 2.3) with screen in 25 m resp. 10 m working distance we assume the following uncertainties: $dL/L = 0.03$, $dk/k = 0.04$, $dz = 0.02$ m, $d\varphi = 0.05$ deg. at $\varphi = 10$ deg. resp. 3.5 deg., $d\vartheta = 0.05$ deg. at $\vartheta = 30$ deg. resp. 10 deg. Thus for the screen method the expected photometric uncertainty is $\Delta I/I=0.05$ (5%).

For the far field photo-goniometer, the error source k, the luminance coefficient of the screen, misses. As result, expected photometric uncertainty for the far field photo-goniometer is $\Delta I/I=0.03$ (3%).

Coming to the measurements on the test ground in "reduced geometry": as described in 2.4, it is difficult to determine $k_{||}$ at small angles of incidence. In our estimation we considered that for the different measurement points different illumination and observation distances occur. At the current state of our development, we would not like to estimate the uncertainty in $k_{||}$ better than $\Delta k_{||}/ k_{||} = 0.08$ (8%). So, for the method of reduced geometry we expect $\Delta I/I=0.1$ (10%) at the current state of development.

3.3 Effect of the photometric uncertainty on the light evaluation

A photometric uncertainty of 5% at the screen compared to 3% on the far field photo-goniometer is acceptable when the ECE-conformity has to be checked, since also the ECE regularities tolerates deviations from 10% up to 30% depending on the test point (cp. ECE-R 112). But it has to be proved that the sensitivity of the camera-based method is sufficient for the low illuminances above the cut-off. This will be done in chapter 4 for the screen method. The method of geometrical reduction is more an instrument for benchmarks than a tool to check the legal conformity.

As we explained in 2.5 the light assessment via the simulated lux isolines on the virtual screen is very usual, and we wanted to have a special look on the isoline. Typically the 3 lux isoline is located around $d=60$ m in front of the head lamp. Also we assume a typical mounting height of the head lamp of $h=0.65$ m, In table 1, we estimate geometrical with $I = Er^2$, $E =$, $I=const.$, $r^2 = d^2 + h^2$ (Fig. 1) the effect of an error in I of 3%, 5%, and 10% on the isoline.

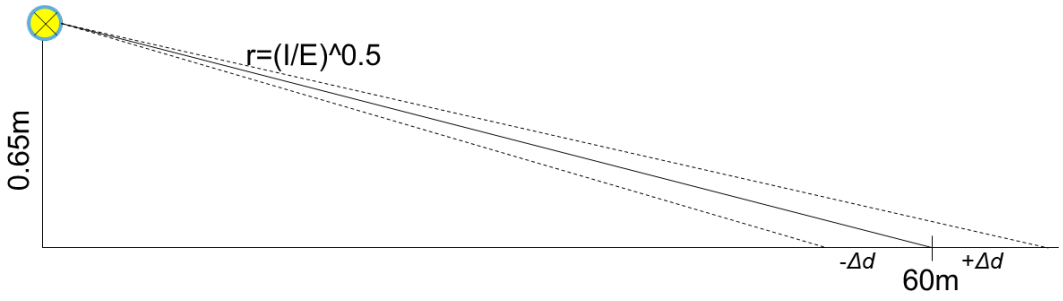

Figure 1 – Illustration of the effect of the uncertainty in I on the uncertainty Δd of the 3 lux isoline at $d=60$ m

Table 1 – Effect of the photometric uncertainty on the uncertainty of position of the *3* lux isoline at *d=60* m

method	photometric uncertainty	*d* (position of isoline)	uncertainty $\pm\Delta d$	$\Delta d/d$
far field goniometer	*3*%	*60* m	*1.2* m	*2*%
screen method	*5*%	*60* m	*1.6* m	*2.7*%
„reduced geometry“	*10*%	*60* m	*2.4* m	*4*%

3.4 Considerations on the working distance and the square law

The theoretical basis for all examined methods, the far field photo-goniometer, the indirect measurement on the screen, and the measurement under reduced geometry, is the photometric square law $I=Er^2$. This means that we approximate the luminous plane of the head lamp with a point light source when we measure the LID. The approximation becomes better and better when the working distance becomes larger. Usually, for the ECE type approval on the far field photo-goniometer a working distance of *25* m is chosen. Therefore, in order to be comparable to this configuration, we also used *25* m working distance in the measurement systems analysis stated below.

We also favour a working distance of *10* m, because here we get a larger goniometric angle range. Theoretical the mentioned approximation is less exact than at *25* m. Standards like prEN 13032:2013 recommend working distances $r > 15 \times D$ (D dimension of the luminous plane). At $r = 10$ m, this would allow to measure luminous planes up to *0.7* m which is not exceeded by serial vehicle head lamps, even the recent LED based head lamps.

The discussion becomes very interesting when we look at the method of reduced geometry. Here we have a variable working distance between *35* m which is “better” than the usual *25* m and *5* m which is less than the recommendation. But in fact in mounting position in the vehicle the rays from the different positions of the luminous plane will not intersect at *25* m but in any other distance on the street. So possibly in reduced geometry we are closer to mounting geometry. In order to find an approach to an answer we make a geometrical plausibility consideration: let us regard a ray from the reference point which touches the photometric sensor in a distance *r* under an angle α. This ray will contribute to $I(\alpha)$. Another ray from the luminous plane in a distance *d* to the reference point will also touch the same photometric sensor, but under the angle $\alpha+\Delta\alpha$ (Fig. 2). This ray will also be erroneously assigned to $I(\alpha)$ although it belongs to $I(\alpha+\Delta\alpha)$. Roughly it is to expect that the error becomes more relevant the larger is $\Delta\alpha$. In Fig. 3 we assume $d=0.1$ m and plot the difference between $\Delta\alpha$ for the real situation in the vehicle on the street and $\Delta\alpha$ for the respective test method. We compare the method of geometrical reduction and the far field photo-goniometer with working distance. According to the rough assumption, the method of reduced geometry approximates the real conditions better than the goniometer in the near field up to *15* m. In the middle field, around *25* m, the goniometer gives a better approximation. In the far field, both methods equals. This confirms our opinion, the method or reduced geometry is suitable for benchmarks of the far field, e.g. for the position of the isoline.

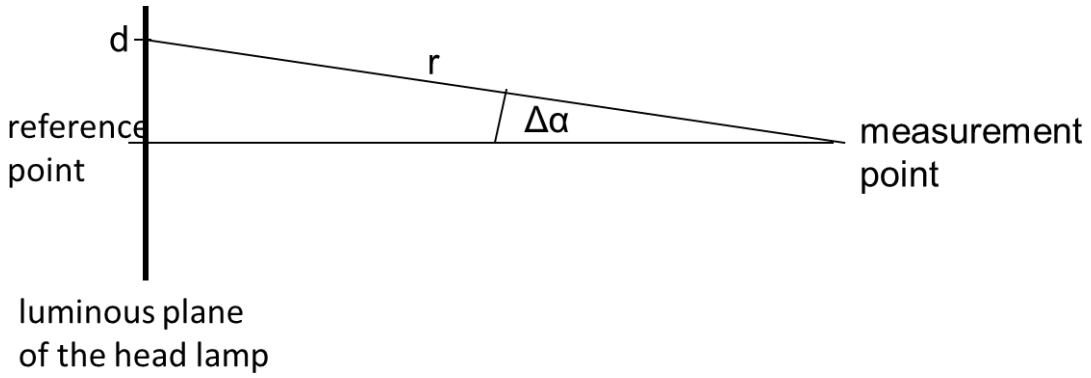

Figure 2 – Angle difference between a ray from the reference point to the measurement point and a ray from position *d* on the luminous plane

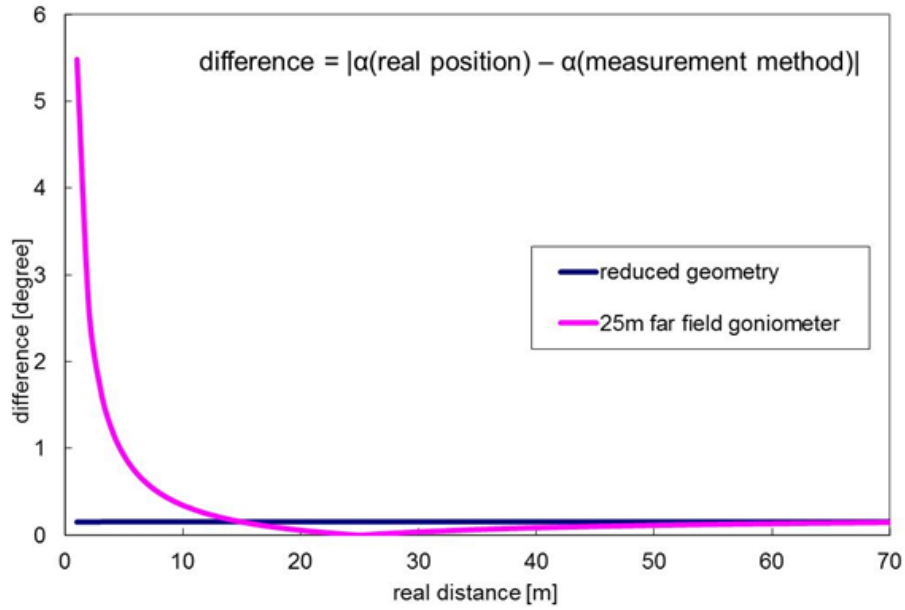

Figure 3 – Differences of $\Delta\alpha$ between the situation in the real position in the vehicle on the street and the respective measurement method in dependence to the distance of the measurement point on the real street, cp. Fig. 2

3.5 Effect of angle related uncertainties and angle resolution

At the photo-goniometer, the angle grid is variable. The tightest possible angle grid is typically around 0.01 deg. For the camera-based methods the angle grid is given through the measurement geometry and the camera objective lens. In this study we get 0.015 deg. (25 mm objective lens) for the screen configuration with working distance, and 0.05 deg. (8 mm objective lens) for the screen configuration with working distance. For the configuration for the measurement in reduced geometry, we also get a mesh with 0.05 deg. In table 2 is shown how this affects the grid resolution on the virtual road when looking again at the 3 lux isoline at $d=60$ m.

Table 1 – Impact of the angle resolution on the position of isoline at ~*60* m.

method	angle resolution	d (position of *3* lux isoline)	spatial resolution Δs at $d=60$ m
far field photo-goniometer (maximum)	*0.01* deg.	*60* m	*1* m
far field photo-goniometer, 25 m screen	*0.015* deg.	*60* m	*1.5* m
far field photo-goniometer, 10 m screen, „reduced geometry“	*0.05* deg.	*60* m	*5.3* m

For the calculation of the uncertainty in I we gave an uncertainty of the goniometric angle $d\varphi=0.05$ deg. *and* $d\vartheta = 0.05$ deg. This uncertainty refers to the error which occurs when the cut-off is aimed for adjustment of the head lamp on the set-up. Another error arises from a possible displacement of the luminance camera. Though the luminance is independent of the distance, and the reflection properties of the screen is Lambert-like in the relevant angle range, but errors can occur at the assignment of the pixel to the goniometric angles. This is reduced to a minimum with a calibration measurement, and the residual uncertainty is negligible, namely *0.002* deg. for the *25* m working distance and *0.004* deg. for the *10* m working distance. This calibration measurement also captures the aberration of the objective lens which is especially for the 8 mm objective lens visible.

4 Measurement systems analysis

After we have summarized the expected errors and uncertainties in chapter 3, here we prove now that our set-up in measurement hall is indeed able to measure. We focus on the indirect measurement in *25* m working distance, because this is the configuration for measurements in highest accuracy.

4.1 Requirements

In order to prove the measurability of a measurement tool in mass production, mostly various statistical characteristic values are deduced. For a pragmatic, simple, and clear treatment we only consider mean values and standard deviations and check if they are plausible and range in the expected uncertainties estimated in chapter 3. For this, we again focus on the ECE test table and on the illuminance distribution on the virtual road.

4.2 Accuracy and stability

The test sample, a halogen-lamp based low beam head lamp, is mounted one time on the set-up and adjusted. The lamp is burned in for 30 min. Without touching the head lamp and the set-up any more, 40 measurements were made, every 30 s one measurement. From this 40 measurement, the mean value and the standard deviation are calculated. In order to prove the stability of the system, the first and the last ten values are averaged, and is checked that their mean value equals to the total mean value of all 40 tries. The operating voltage and current is logged every second to prove the stability of the power source.

The result is illustrated in Figs. 4 and 5. No drift is visible, and the variation is marginal. The system is also sensitive at low intensities in the order of *0.1* lux and the value at B50L could be measured.

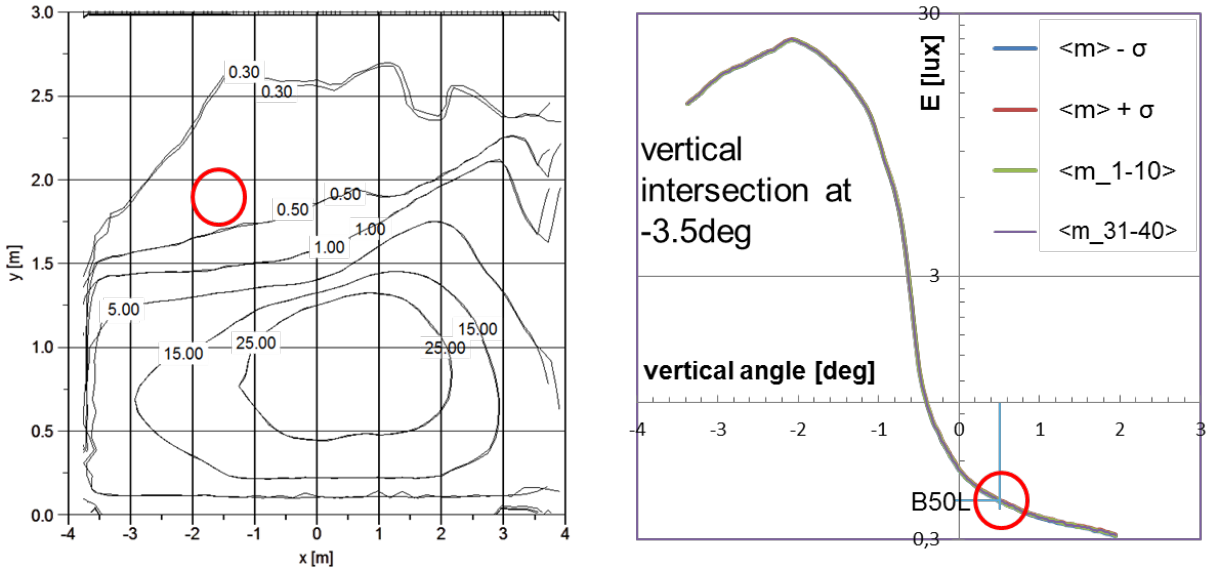

Figure 4 – Test run head lamp is mounted one time and 40 measurements were made. On the left side, the illuminance on the ECE test table is shown, the limits are given from the standard deviation. The red circle marks the B50L which results to E(B50L) = *(0.422±0.002)* lux (dev. *0.5*%).

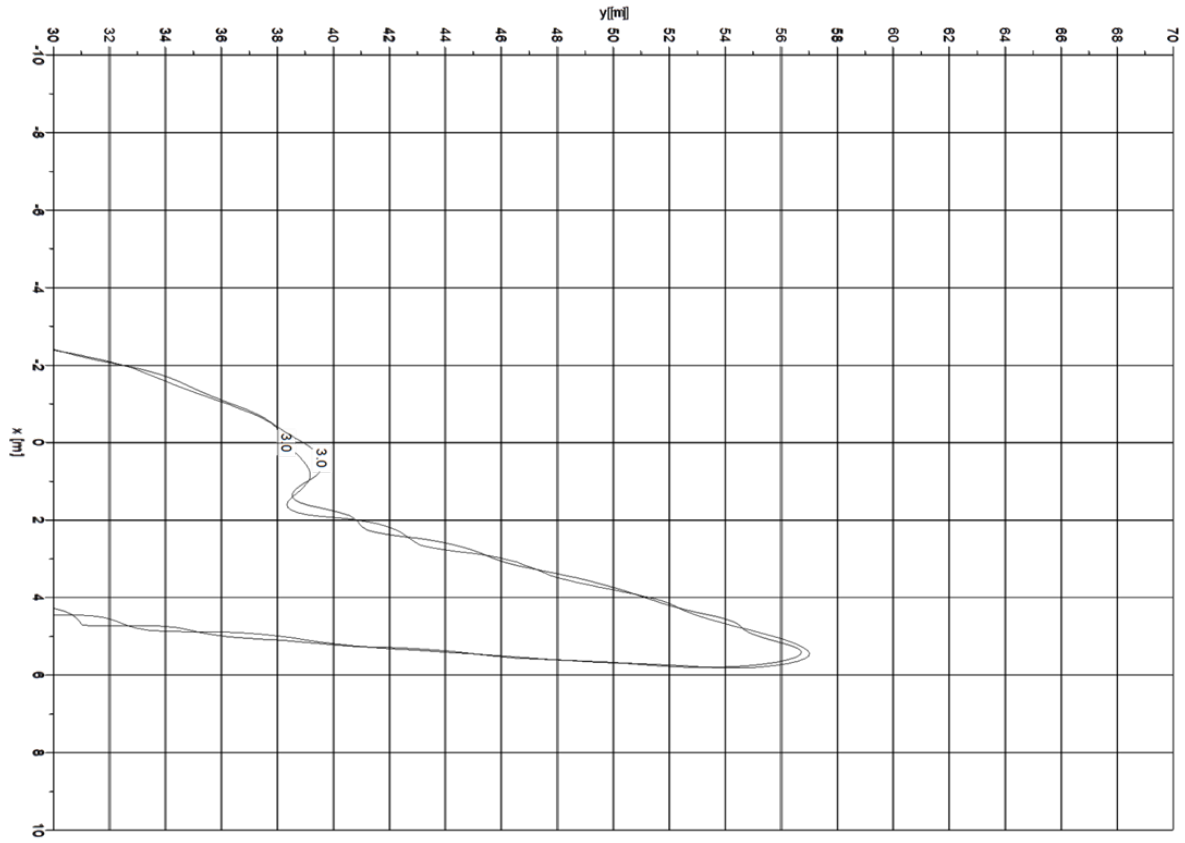

Figure 5 – Test run head lamp is mounted one time and 40 measurements were made. The *3*lux isoline on the virtual road is displayed, the limits are given by the standard deviation. The variation is marginal.

4.3 Repeatability

For this test run, one test engineer mounts and adjusts the head lamp three times. Every time, one measurement is taken. With this procedure, we get the tolerances from our set-up. The result is depicted in Figs. 6 and 7. We get E(B50L)=(*0.424±0.008*)lux, (deviation *2*%), and for the isoline a standard deviation of *±2* m. This corresponds to the expected uncertainties.

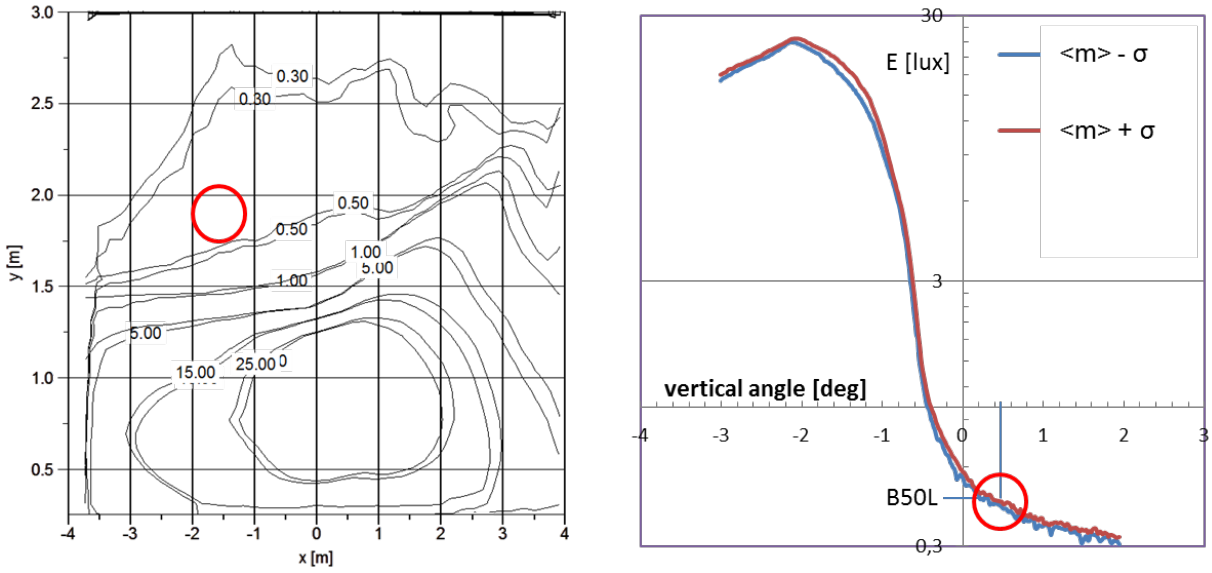

Figure 6 – Test run head lamp is mounted and measured times by the same person. On the left side, the illuminance on the ECE test table is shown, the limits are given from the standard deviation. The red circle marks the B50L which results to E(B50L) = (*0.424±0.008*)lux (dev. *2*%).

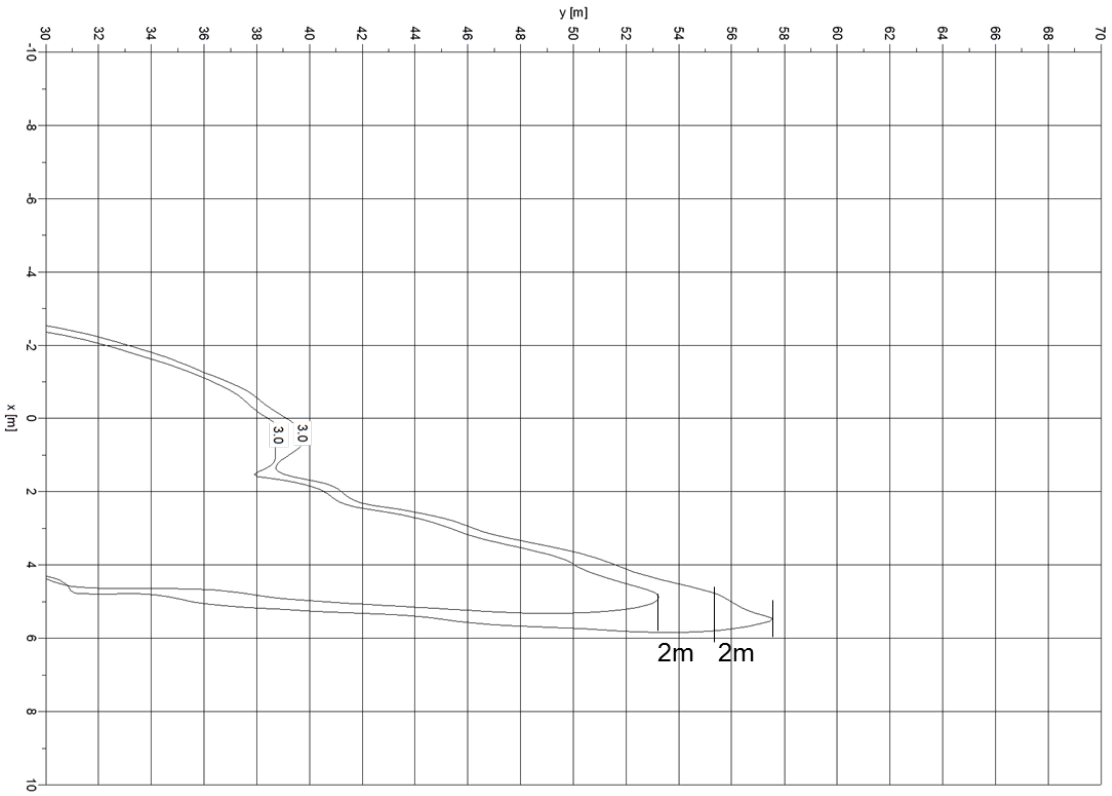

Figure 7 - Test run head lamp is mounted and measured three times by the same person. The *3* lux isoline on the virtual road is displayed, the limits are given by the standard deviation.

4.4 Reproduciblity

Now the head lamp is mounted, adjusted and measured 3 times, every time from another test engineer in order examine the subjective influence of the test engineer on the test procedure. The result is E(B50L)=(0.421 ± 0.003)lux, (deviation <1%), and the range of the isoline was measured to 55 m for every try. Probably by chance this is better than for the repeatability, but we see that the influence of the test engineer is not significant.

5 Summary

The error budget for a set-up in IAV's Light and Driver-Assistance Hall for fast camera-based measurements of the LID was manifested and discussed. The measurability of the set-up was proven.

Whereas the method of reduced geometry seems to be a suitable benchmark tool for the far field, the indirect measurement on the screen in is accurate and sensitive enough to check if the ECE requirements are fulfilled.

As result, the presented method can be applied within the industrial development process which will save time and with it costs.

References

PANDER, J, 2013, Jahresrückblick 2013- Einfach helle, Spiegelonline, http://ml.spiegel.de/article.do?id=940064, last download October 2014

SCHWANENGEL, C, 2005, Spatially resolved luminance measuring compared with illuminance measurements of automotive headlamps, Proceedings 6th ISAL

MARUTZKY, M, 2012, Bewertung der Abblendlicht-Fernfeldverteilung in einem geschlossenen Raum durch geometrische Verkürzung, Proceedings Licht

ACCURATE DETERMINATION OF THE NEAR-FIELD ILLUMINANCE FROM NARROW-BEAM LED ARRAYS USING RAY FILES

Jacobs, V.A.[1,2], Ryckaert, W.[2], Rombauts, P.[1], Hanselaer, P.[2]
[1] Department of Electric Engineering and Energy Technology, Vrije Universiteit Brussel, Brussels, BELGIUM,
[2] Light&Lighting Laboratory Ghent, Department of Electrical Engineering, KU Leuven, Heverlee (Leuven), BELGIUM
valery.ann.jacobs@vub.ac.be

Abstract

Most lighting manufacturers represent the angular distribution of the flux of their light sources by a far-field representation, also known as luminous intensity distribution (LID.) For spatially extended sources however, the inverse square law is only valid beyond the limiting photometric distance. By consequence, this distribution does not allow for accurate illuminances to be determined in the near-field region of the source. This problem is even more pronounced for arrays of LEDs with focusing optics creating narrow beams. We gathered a ray-file of several LED arrays using a near-field luminance goniophotometer. This paper reports on measurements and simulations using ray-tracing. It shows that a far-field representation cannot be used to calculate illuminance values in the near-field. In contrast, a near-field representation allows the calculation of accurate illuminance values at any target point, irrespective of the distance to the source and its luminous intensity distribution.

Keywords: Light emitting diodes, Optical system design, Optical engineering, Photometry, Illumination.

1 Introduction

Luminaires are conventionally modeled using a far-field representation in which the spatial extent of the luminaire is, by definition, irrelevant and the source is approximated by its photometric center. To calculate this far-field representation, a photometer revolves around a light source at a large and fixed distance to the source, and illuminance values are measured in a set of angular directions. The far-field intensity of the luminaire in each direction, also called the *luminous intensity distribution* (LID) can be calculated using the traditional relationship between intensity and illuminance—also called the inverse-square-law—which states that illuminance decreases with the square of the distance to the source. (Walsh, 1926) It is implicitly assumed that the spatial extent of the detector is also negligible with respect to the distance between the source and detector, and can thus be represented by a point.

$$I = \frac{E \cdot R^2}{\cos \alpha_{rec}}, \tag{1}$$

where

- I is the luminous intensity distribution;
- E is the measured illuminance by a detector;
- R is the distance between the source and detector;
- α_{rec} is the polar angle between the local surface normal describing the orientation of the photometer and the direction vector from the detector towards the photometric center of the source.

For Lambertian light sources, a far-field representation yields accurate results from a distance of at least five times the maximal dimension of the source.(Stannard & Brass, 1990) This distance is often called the *limiting photometric distance*.(Moerman & Holmes, 1981) Applying the inverse-square-law at a distance smaller than the limiting photometric distance, can generate serious errors in the intensity when determining the LID in a goniometer and in the

illuminance when using correct intensity data but calculating back to at distance in the near-field.

For non-Lambertian sources, the limiting photometric distance depends on the beam width and the specific LID of the source. Two problems arise for such sources. First, the determination of the limiting photometric distance is not evident using a far-field goniophotometer. At least two measurements at different, yet large, distances should be performed and compared, which is impractical. If the measurement distance is lower than the limiting photometric distance, the far-field intensity — as calculated from the measured illuminance — could be called an '*apparent intensity*' and will depend on the measurement distance.(Moerman & Holmes, 1981; Rombauts, 1992) When increasing the measurement distance, the error between this apparent intensity and the far-field intensity will decrease. Whenever the difference between two measurements is smaller than a predefined threshold, the far-field region is said to be reached. (Sun, Chien, Moreno, Hsieh, & Lo, 2009) However, different criteria are used: in general, the threshold of 1% is only measured along the optical axis of the luminaire, while other metrics use a weighted average in a set of angular directions.(Moreno, Sun, & Ivanov, 2009) Second, far-field intensities are often used to calculate illuminance values on a working plane, which can lie at a distance much smaller than the limiting photometric distance. Calculations based on the far-field intensity will be erroneous.

The above-mentioned problems become more pronounced for luminaires composed of LED arrays, with focusing optics creating narrow beams, and having large non-luminous areas between the LEDs. (V. Jacobs, Forment, Rombauts, & Hanselaer, 2014) Typical examples of luminaires incorporating arrays of individual LEDs focused at close distance are e.g. surgical luminaires, road lighting and decorative lighting. This paper shows that any discussion to determine the limiting photometric distance and the associated error sources can be avoided by introducing a near-field representation of a luminaire, which has become available now.

2 Test source and method

In this paper, a narrow-beam LED array is used as test source. It consists of 2 cool-white power LEDs (Luxeon K2) combined with a focusing lens and mounted on an aluminum plate. (Figure 1) By bending the aluminum support, the beams of the LEDs can be focused to a point along the optical axis of the array, thus resulting in a *focused* array. A *parallel* array occurs when both sources are lying in one plane, and the optical axes of the individual sources are parallel.

The LED array is mounted in a near-field luminance goniometer, in which an illuminance meter and a luminance camera revolve around the light source at a fixed distance. The luminance camera captures luminance maps, from which a list of rays is extracted (also called ray set or ray file). Each ray of this list is characterized by a spatial starting point, a direction of propagation and a luminous flux.

As opposed to the far-field LID, these ray-files offer a near-field representation of the light source. This representation can be used to represent extended light-sources with any spatial and angular luminance distribution. A ray-file can be imported in specific ray-tracing software. After ray-tracing, accurate illuminance values can be calculated at any distance and position with respect to the source.

Figure 1 – The LEDs of the array used in the experiments, are rotated by bending the aluminum support. The distance between the centers of the LEDs (D_{Array}) is 0.32m.

3 Results and discussion

The simulation software TracePro is used to trace the rays of a parallel and focused LED array and to determine illuminance in the near- and far-field. (Figure 2) Illuminance values are determined on planes, along the optical axis of the LED array, and while varying the angle w.r.t. the optical axis. All measurements are performed at distances in the near- and far-field. The double overbar notation for α and R indicate these values are taken w.r.t. the photometric center of the array.

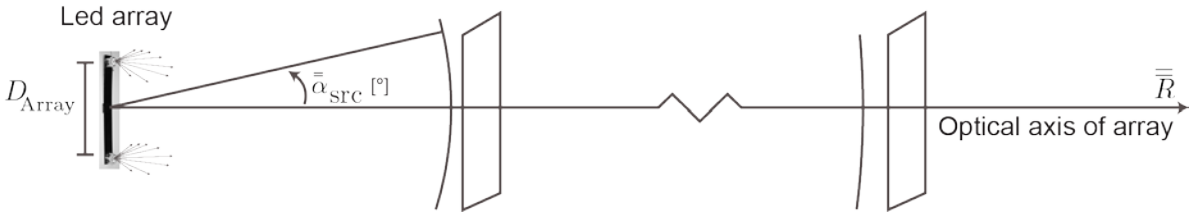

Figure 2 – This paper reports on measurements on LED arrays: a) on illuminance distributions on planes at various distances, b) along the optical axis of the array, and c) while varying the angle w.r.t. the optical axis for several distances to the source.

3.1 Illuminance on a plane

Figure 3 shows the illuminance for a parallel array of two LEDs in four planes, corresponding to four distances. Their distance varies from 2.2 times the size of the array, to 25 times this size, which spans a range from 0.7m to 8m. At short distances, two individual illuminance peaks are observed, corresponding to the individual LEDs. From a certain distance between 5 and 11 times the size of the array, only one broader peak is observed. At larger distances, the illuminance of this peak decreases, while the peak becomes more and more broad. This behavior is expected in the far-field region.

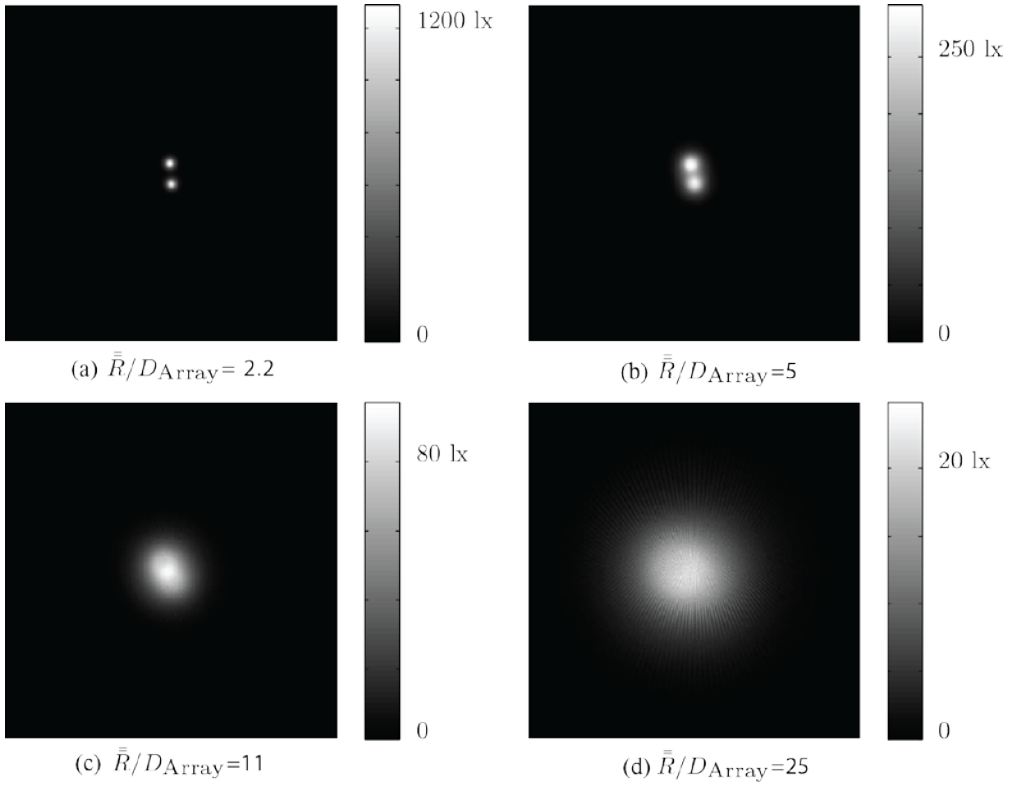

Figure 3 – Simulated illuminances in a plane of 5x5m^2 at various test distances below the parallel LED array. At short distances, 2 separate peaks can be observed, while at larger distances, only 1 broader peak is observed.

3.2 Illuminance along the optical axis of the array

The left panel in Figure 4 shows the illuminance of the same source along the optical axis. Notably, the illuminance along the optical axis first increases and then decreases again. Unlike illuminance in the near-field, the behavior at large distance to the source seems to correspond again to an inverse square law.

The right panel in Figure 4 shows the illuminance of a focused array along the optical axis. A maximum illuminance is reached at a distance of about 5 times the size of the array. Notably, the maximum illuminance is much higher compared to the parallel array, Clearly, this is because a high illuminance occurs near the focal point, where the optical axes of the individual LEDs intersect. At higher distances, illuminance decreases rapidly. For focused sources a more narrow illuminance peak is found.

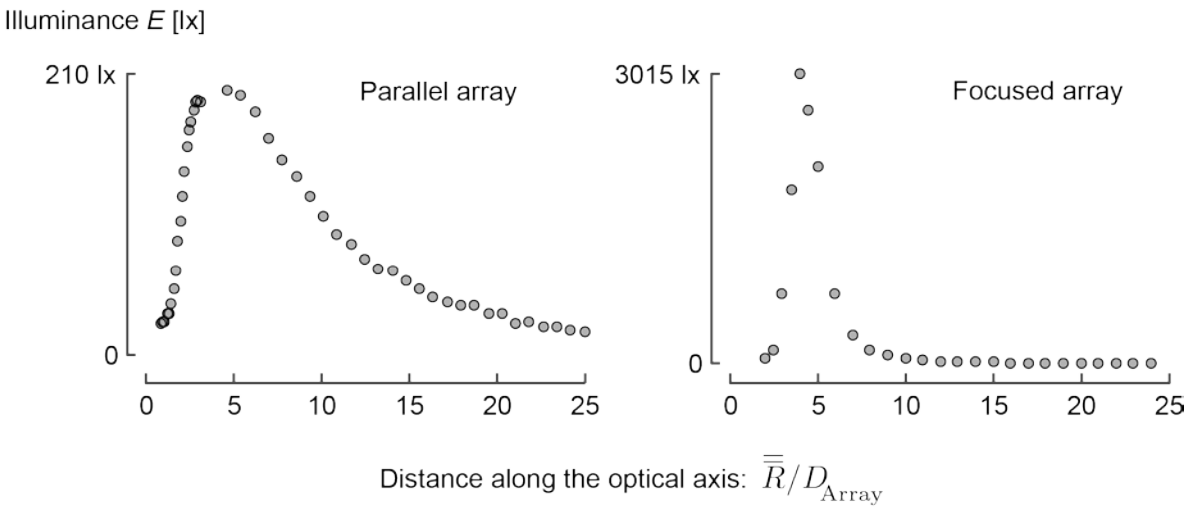

Figure 4 – The illuminance along the optical axis ($\bar{\bar{\alpha}}_{src} = 0$) of a parallel array (left panel) and a focused array (right panel) at distances from 2.2 to 25 times the size of the array.

3.3 Angular variation of illuminance

The angular variation of the illuminance in the near- and far-field of a parallel array is displayed in Figure 5. The upper panel displays the illuminance that is measured using a photometer at a radial distance of 2 and 4 times the size of the array, and moving the detector in a set of angles around the source. The x-axis covers a measurement range from -30° to +30°. In accordance to Figure 4, the illuminance at the optical axis (where $\bar{\bar{\alpha}}_{src} = 0$) first increases with increasing distance and in accordance to Figure 3, two individual peaks can be observed in the angular illuminance distribution. The lower panel displays the angular variation of illuminance at larger distances of 8 and 11 times the array size. This corresponds more to a far-field behavior: only one peak is observed and the illuminance along the optical axis decreases with increasing distance.

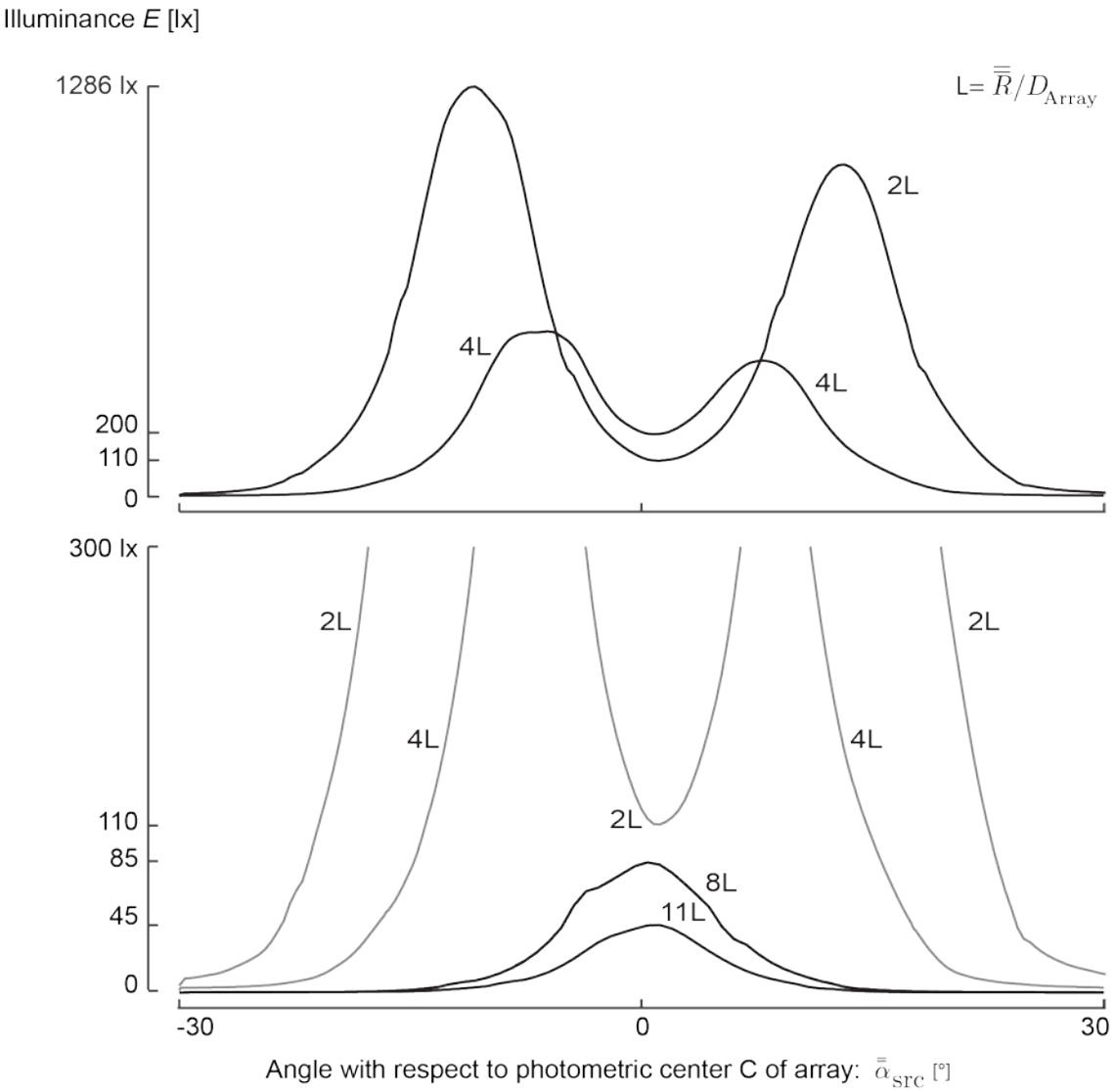

Figure 5 – The angular variation of the illuminance of a parallel array is measured using a photometer at radial distances of 2 and 4 times (upper panel) and 8 and 11 times (lower panel) the size of the LED array.

3.4 Comparing illuminances from the near- and far field

The angular distribution of illuminance for focused and parallel arrays at various distances to the source is simulated and compared in Figure 6. Illuminances are simulated at close distance (3 times the size of the array) and at large distance (25 times the size of the array).To facilitate comparison at different distances, all curves are normalized to their individual maximum. The left panel shows the results when the illuminance is measured along the polar angle ranging from -50° to +50°. The measurement distance is close to the source, at 3 times the size of the array. The grey line in the left panel indicates only one maximum illuminance is found. Deriving the far-field intensity from a measurement of illuminance at a distance this close to the source, would indicate the beam is parallel.

Similarly, the black line in the left panel corresponds to a parallel array. However, if this were truly the LID, the two peaks would suggest the array is focused.

Vice versa, the right panel in Figure 6 displays the illuminance distribution at a far larger distance of 25 times the diameter of the array. As opposed to the left panel, the focused array now displays two peaks, as expected for its LID, while the parallel array displays only one central peak. These findings clearly indicate the importance of the measurement distance

when determining an LID. Erroneous illuminances would be derived from a LID determined in the near-field of the array, while a LID determined in the far-field cannot be used to calculate illuminances in the near-field.

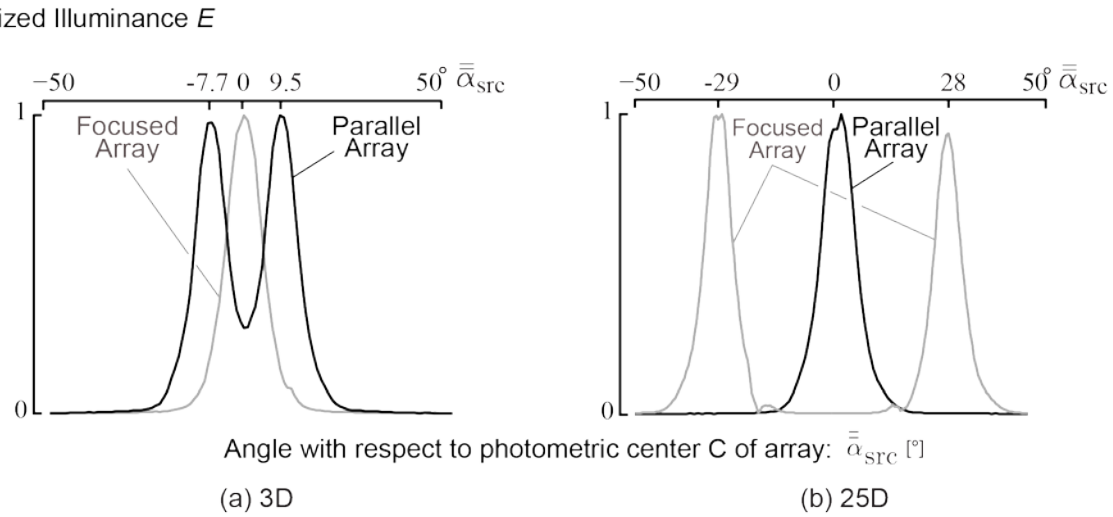

Figure 6 – Illuminance for a focused and parallel array, as determined from simulations at (a) 3 times the size of the array, and (b) 25 times the size of the array.

4 Conclusions

The near-field representation of any luminaire can be obtained from measurements using a near-field luminance goniometer. Simulations using ray-tracing software allow the calculation of accurate illuminance values at any target point, irrespective of the distance to the source and its luminous intensity distribution. Moreover, by selecting only parallel rays from the ray-file, the true far-field intensity can be calculated. This near-field approach makes any discussions to determine the far-field photometric distance superfluous.

For the parallel and the focused LED arrays considered in this paper, good agreement is found between the measured illuminance values and those obtained by simulations from the ray-file. This agreement is found for any distance of the plane of analysis with respect to the LED array. Moreover, the inadequacy of a far-field representation to obtain illuminance values in the near-field is illustrated.

References

Jacobs, V., Forment, S., Rombauts, P., & Hanselaer, P. (2014). Near-field and far-field goniophotometry of narrow-beam LED arrays. *Lighting Research and Technology*. doi:10.1177/1477153514530139

Moerman, J. J. B., & Holmes, J. G. (1981). The choice of test distance to control errors in the photometry of round projectors focused at a long distance. *Lighting Research and Technology*, *13*(2), 87–95. doi:10.1177/096032718101300205

Moreno, I., Sun, C.-C., & Ivanov, R. (2009). Far-field condition for light-emitting diode arrays. *Applied Optics*, *48*(6), 1190–7. Retrieved from http://www.ncbi.nlm.nih.gov/pubmed/23567581

Rombauts, P. (1992). *Phenomenology and characterisation of spatial distribution and reflection of light. Application to residential area lighting and reflector design.* Vrije Universiteit Brussel.

Stannard, S., & Brass, J. (1990). Application Distance Photometry. *J. Illum. Eng. Soc.*, *19*, 39–46.

Sun, C.-C., Chien, W.-T., Moreno, I., Hsieh, C.-C., & Lo, Y.-C. (2009). Analysis of the far-field region of LEDs. *Optics Express*, *17*(16), 13918–27. Retrieved from http://www.ncbi.nlm.nih.gov/pubmed/19654799

Walsh, J. W. T. (1926). Photometry, 96.

LIGHT EMITTING DIODES – FACTORS TO BE CONSIDERED IN SUCCESSFUL CONFORMITY TESTING

Schneider, M.[1]
[1] OSRAM Opto Semiconductors GmbH, Regensburg, GERMANY
markus.schneider@osram-os.com

Abstract

The conformity testing of LED packages is often reduced to the conformity assessment of group limits or ranges rather than the assessment of the measured values. The main influencing factors for a successful conformity testing are described with the chromaticity coordinates as an example.

Keywords: Photometry, LED package, binning, test conditions

1 Introduction

Conformity testing of light emitting diodes (LEDs, LED packages) in practical cases often means the confirmation of the bin information, either by the LED manufacturers themselves or by a 2nd party, e.g. customers. The bin information of LEDs defines a certain expectation for a measurement result that might be obtained at any stage of the value creation chain. The later a measurement is performed in this chain, the larger are usually the differences in the measurement conditions, e. g. the forward current I_F, the temperature T_X at any reference point X, or the presence of additional optically effective components. Considering certain aspects, a conformity test can be done anyway, but accuracy will be limited by the involved (additional) uncertainties and/or corrections – which are also subject to uncertainties.

2 LED binning

Due to unavoidable variations in the production processes from the growth of the epitaxial layers until the finished good – the LED package – , LEDs are usually 100 % finally tested and classed in terms of e.g. forward voltage V_F, light output and colour. The photometric quantity describing the light output is normally either the luminous flux Φ_v or the luminous intensity I_v. In special cases also their energetic equivalents might be used.

The colour is usually expressed by the dominant wavelength λ_{dom} in the case of LEDs with highly saturated colours or the chromaticity coordinates $(x; y)$ in the case of white LEDs or LEDs with low saturation [CIE2007].

Each of these so-called binning quantities is classed into specific groups or ranks and one bin is defined by a unique set of one group per each binning quantity. For one-dimensional quantities like V_F or Φ_v, a group corresponds to an acceptance interval, for two-dimensional like $(x; y)$, a group is defined by an acceptance area.

Consequently, binning reduces the information from individual values to ranges, and conformity assessment is then given by the confirmation of the bin information.

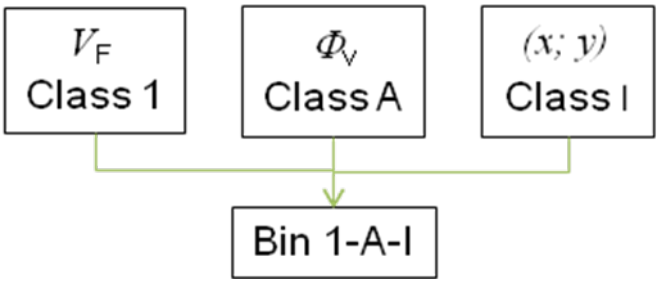

Figure 1 – Example of a bin definition

3 Conformity Testing

3.1 Test Conditions

The binning of LEDs is done at well-defined testing conditions. This comprises not only the settings of the rated forward current $I_{F,r}$ and the ambient temperature T_a, but also a well-defined ambience of the device under test (DUT) and a well-defined timing of the measurement sequence. The latter aspects are especially important if the DUT is tested at high currents (or current densities), since the operating of the LED for testing purposes leads already to a heating of the LED chip, especially of its optically active regions. The ambience of a LED package during final testing is given by a dedicated test fixture, which usually provides a very poor, but strongly reproducible thermal interface.

All electro-optical LED properties depend on temperature; therefore any change of the chip temperature during or due to the measurement influences the measurement's result. In order to minimize this influence, the measurement should be taken in a time as short as possible. Additionally, testing a device under repeatability or reproducibility conditions [GUM2008] requires the measurements to start and to stop always at the same times relative to the start of power consumption. In figure 2, these times correspond to t_1 and t_2 for the voltage measurement, and t_1 and t_3 for the optical measurement, each of them relative to the time t_0 when the power supply/consumption of the DUT starts. Depending on the specific package design, a time period $t_3 - t_0$ in the order of 10 ms to 50 ms is necessary to minimise the influence of the DUT's ambience on the heating of its optically active components (chip, phosphor) and therefore on the measurement results. A time period $t_1 - t_0$ in the order of 1 ms to 5 ms enables an initial thermodynamically quasi stable state since they are typical times for the heat propagation through the die.

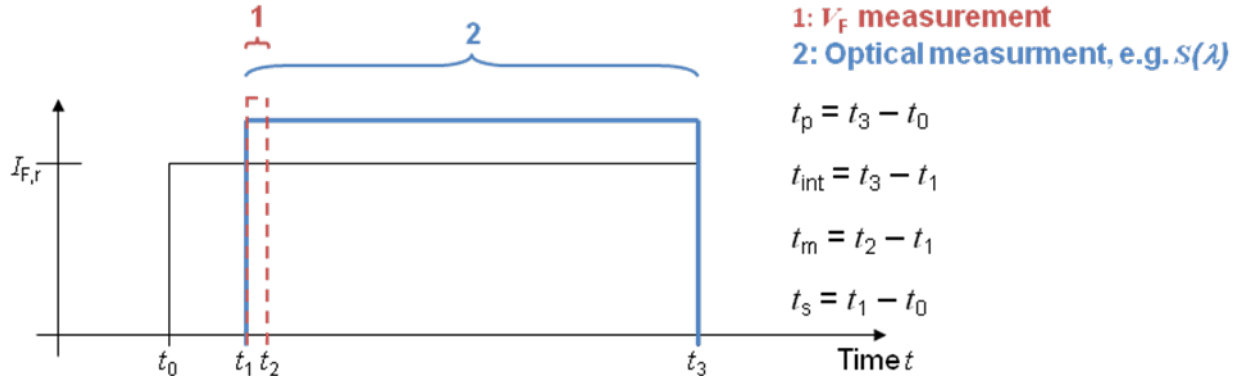

Figure 2 – Timing chart of a typical final test measurement; t_{int} is the integration time of e.g. a spectrometre, t_m is the integration time of the voltage measurement. Instead of a single current pulse also a train of pulses can be used.

Once the LED package has been assembled to any kind of PCB with passive or active cooling, this changes have to be considered in the interpretation and comparison of measurement results, even if all other parameters have been chosen identical (current, temperature, timing).

For more details one can refer to [DIN5032-9] and the up-coming reports of CIE's TCs 2-63 and 2-64 [TC2-63, TC2-64].

3.2 Example

The following example deals with the conformity test of LEDs, which have been assigned to a certain white group based on the final test results: Accordingly, the *(x; y)* coordinates shall be in the marked area in figure 3a). LEDs taken from two test lots (at production site, tested at different days) have been retested in a lab under repeatability conditions and the obtained *(x; y)* values are plotted in figure 3b). The *(x; y)* values show an offset to the expected white group area, but figures 3c) and d) also show that the area covered by the re-measured *(x; y)* values corresponds to the *area* of the initially assigned white group.

If one considers the four measurements (lot 1 and 2 at production site and at lab site, respectively), then we can state within each of these 4 measurements repeatability conditions. Repeatability conditions also apply to the measurements of Lot 1 and 2 *at the lab site*, because they were measured at the same test station by the same person under identical test conditions within a short time. The measurements of lot 1 and 2 at production site were taken with a temporal distance of several weeks – consequently, a comparison of the values from production site of both lots to each other and a comparison to the values taken by the re-measurement at the lab site may only be done under reproducibility conditions [GUM2008].

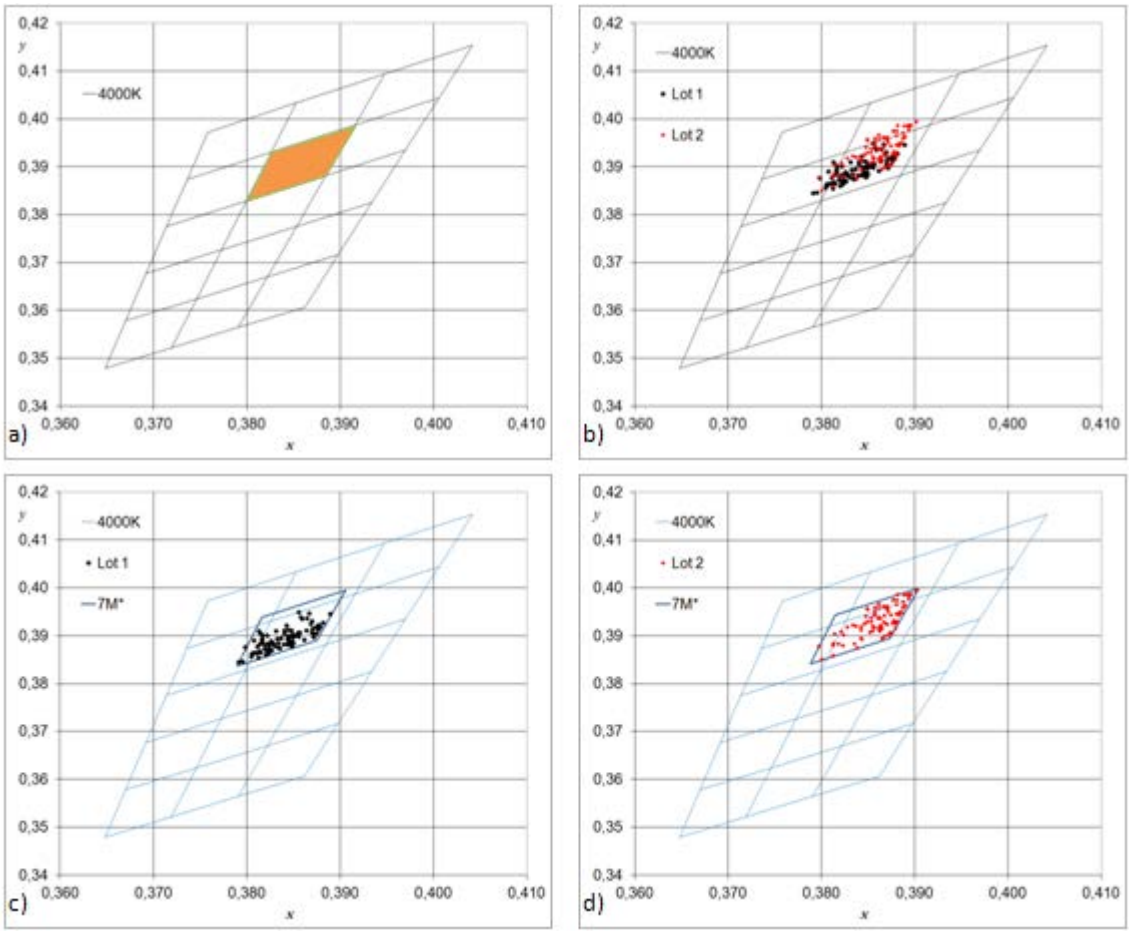

Figure 3 – a) bin assignment due to measurement results at final test; b) re-measurement results at lab site; c) data of Lot 1; d) data of Lot 2. The shifted white groups in c) and d) indicate that the covered area is conserved, but its location is slightly displaced.

Due to the repeatability conditions for each individual lot, the area covered by the *(x; y)* values is conserved (figure 3c) and 3d)). Nevertheless, as a consequence of the reproducibility conditions, a slight displacement of the re-measured white groups (figure 3c) and d)) can be

observed. The displacement of the corresponding areas can be calculated as $(\Delta x; \Delta y)$ = (-0,0010; 0,0008) for lot 1 and $(\Delta x; \Delta y)$ = (-0,0011; 0,0013) for lot 2.

Due to these displacements, values outside the original white group can be observed. This observation raises the question: Can conformity with the original white group information be stated?

This question can only be answered by taking into account the measurement precision: In the case of the presented example, a measurement precision under reproducibility conditions (measurement reproducibility) must be considered due to the different measurement locations and systems [GUM2008]. Under otherwise unchanged measurement conditions its values are 0,005 for the quantities x and y, respectively, and a coverage factor k = 3. Consequently, small deviations to the originally measured values which define the assignment to a certain white group must be accepted and are indeed unavoidable due to the always present measurement uncertainties. In the presented case – which is indeed a general representation and also transferable to the other measured grouping quantities – the conformity of the declared white group can be stated within the tolerance limit and because all test systems used are part of the same metrological traceability chain.

If the different used test systems are not part of the same metrological traceability chain, then additional contributions (systematic and random) to the combined measurement uncertainty must be considered to identify possible reasons of deviations between the different measurements. Of course, it is preferable if the measurement results are additionally metrological comparable [VIM2012], i.e. there is a common reference in the traceability chains.

In the case of different measurement conditions, e.g. the LED packages are assembled to the final application environment or pre-stages thereof, additional parameters have to be taken into account: optical components usually influence the spectral distribution emitted by the LED packages or operating conditions (DC pulsed or PWM), leading to systematic chromaticity shifts or light output offsets. Therefore, if the conformity test bases on measurements at a higher level of integration, a conformity assessment of LED packages can only be done if these shifts and offsets are well-known. Since they base again on measurements or any kind of simulations, they are also subject to uncertainties which need to be considered.

4 Conclusion

For a successful conformity assessment, it is necessary to take the measurements at very well specified conditions. They do not only comprise the obvious parameters like forward current and ambient conditions, but also a well defined timing of the measurements and thermal ambience of the LED under test. If the test is done at a higher integration level (a later stage in the value creation chain), the additionally necessary corrections and/or correction factors need to be determined in order to do not (falsely) fail a conformity test due to omitted corrections.

References

CIE2007. CIE 127:2007.Measurement of LEDs. Vienna: CIE.

DIN5032-9. Lichtmessung — Teil 9: Messung der lichttechnischen Größen von inkohärent strahlenden Halbleiterlichtquellen.

Photometry — Part 9: Measurement of the photometric quantities of incoherent emitting semiconductor lightsources.

GUM2008. JCGM 100:2008. Evaluation of measurement data – Guide to the expression of uncertainty in measurement.

VIM2012. JCGM 200:2012. International vocabulary of metrology – Basic and general concepts and associated terms (VIM). 2012.

TC2-63. CIE Technical Committee 2-63. Technical Report. Optical Measurement of High-Power LEDs. To be published.

TC2-64. CIE Technical Committee 2-64. High-Speed Testing Methods for LEDs. To be published.

REALIZATION OF PHOTOMETRIC UNITS WITHOUT V(λ) FILTERS AND THEIR DISSEMINATION TO LED LIGHTING APPLICATIONS

Poikonen, T.[1], Pulli, T.[2], Dönsberg, T.[2], Baumgartner, H.[1,2], Vaskuri, A.[2], Sildoja, M.[2], Manoocheri, F.[1,2], Kärhä, P.[1,2], Ikonen, E.[1,2]

[1] Centre for Metrology and Accreditation (MIKES), P.O. Box 9, FI-02151 Espoo, FINLAND
[2] Metrology Research Institute, Aalto University, P.O. Box 13000, FI-00076 Aalto, FINLAND
tuomas.poikonen@mikes.fi

Abstract

We have developed a novel method for realization of photometric units of spectrally limited light sources, such as light emitting diodes (LEDs), using the Predictable Quantum-Efficient Detector (PQED) without $V(\lambda)$-filter. In the measurements, the Brewster-window of PQED is replaced with a precision aperture and nitrogen-flow through the detector. The photometric weighting is carried out numerically, for which a spectral measurement of the source is needed. The new PQED-method was compared with a conventional reference photometer by measuring the illuminance of a stable white LED-lamp. The difference in the measured illuminance values was 0.35 %. The expanded uncertainties of the PQED-method and the photometer method are 0.25 % and 0.50 % (k = 2), respectively. The developed method allows photometers and luxmeters to be calibrated directly against the primary standard of optical power. A further advantage of using a white LED-lamp as the calibration source, instead of illuminant A, is that the spectral mismatch errors of luxmeters and photometers are reduced to 1/3 on average, when measuring general white LED-lighting.

Keywords: photometer, $V(\lambda)$-filter, PQED, light-emitting diode, illuminance, calibration

1 Objective

Incandescent standard lamps with standard illuminant A spectrum are widely used in photometric calibrations. However, the mass production of such lamps is being phased out globally. Energy-saving lamps based on LEDs are widely available on the market, and consumers buy them to replace incandescent lamps. Eventually, manufacturing of incandescent lamps will disappear. As a result, incandescent measurement standard lamps may not be available, or they become very expensive.

Therefore, it is important to investigate the possibility to replace conventional standard lamps with new LED-technology. Possibilities for such standard sources look promising, as the luminous flux of certain types of commercial LEDs has been shown to be stable within 0.2 % over a time period of 20,000 hours of operation [1]. Furthermore, the illuminance measurement uncertainty of a $V(\lambda)$-filtered photometer increases in LED lighting applications relative to incandescent lighting, when the photometer has been calibrated using an incandescent standard lamp as the calibration source. This is due to the complicated spectra of white LEDs and supports the objective that LED-based standard sources should be used for calibration of photometers for general LED lighting.

2 Methods

We have developed a novel method for the realization of photometric units of LED-based light sources using the PQED [2]. A significant advantage of using the PQED for illuminance and luminous intensity measurements of LEDs is that the PQED-based method does not need any filters, whereas the $V(\lambda)$-filter of conventional photometers causes their most significant uncertainty components. The photometric weighting in the PQED-based method is taken into account numerically in the spectral mismatch correction. The PQED is equipped with a precision aperture, and utilizes dry nitrogen flow to avoid dust from entering the detector [3]. The method has been demonstrated by illuminance measurements of blue and red narrow-band LEDs with 0.18 % standard uncertainty [2]. Preliminary measurements of white LED sources have given similarly low uncertainties. The illuminance of a commercial E27-base

LED-lamp was measured with both methods by operating the lamp with DC-voltage to improve the stability of its luminous output. The difference in the measured illuminance values between the two methods was 0.35 %. The preliminary expanded uncertainties of the PQED-method and the photometer method are 0.25 % and 0.50 % (k = 2), respectively. By utilizing the PQED and an LED-based standard source in the calibration of $V(\lambda)$-filtered photometers, it is possible to reduce the uncertainty in measurements of LED-based lighting due to primary realization of units.

3 Analysis of spectral errors

We carried out analysis of spectral mismatch errors of three $V(\lambda)$-filtered photometers in the case of 24 warm-white LED lamps of different types (Figure 1). For each lamp, the spectral mismatch errors were calculated by comparing two calibration methods. The first method consisted of calibrating the photometers using an incandescent standard lamp and a $V(\lambda)$-filtered reference photometer. The second method consisted of using an LED standard source and a PQED as the reference detector. The same 24 spectrally different LED lamps were tested as the calibration source in the analysis. The blue and phosphor peaks of the LED lamps were between 440 – 468 nm and 568 – 618 nm, respectively. Two of the LED lamps had an additional red peak at 630 nm.

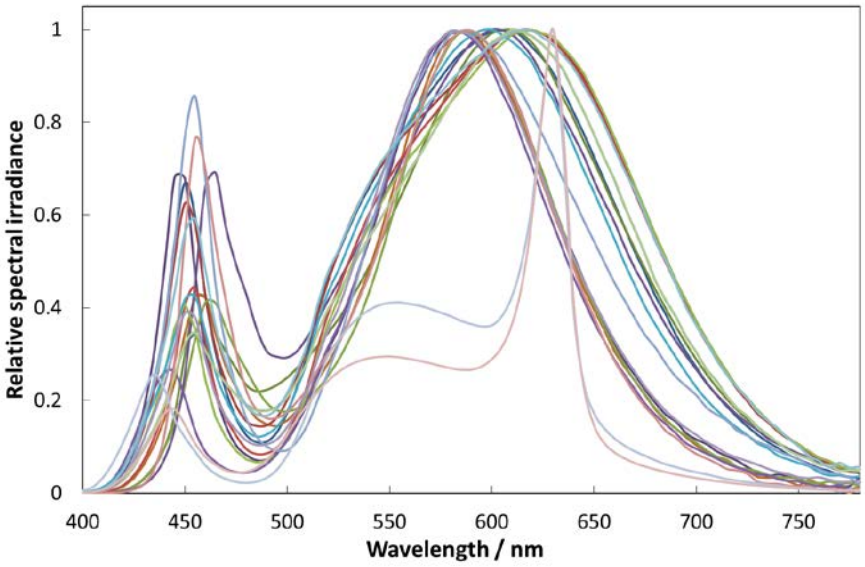

Figure 1 – Relative spectral irradiances of the LED-lamps used in the analysis of spectral mismatch errors

The three photometers used in the analysis are high quality instruments with spectral quality factors f_1' between 1.97 % and 2.20 % [4]. Spectral mismatch errors up to 0.8 % were obtained for the photometers, and for the 24 different LED-lamps, when using an incandescent calibration source in the analysis. The spectral errors were reduced to less than 0.3 %, when using any of the 24 LED-lamps as the calibration source in the analysis. The spectral mismatch errors of the photometers were found to be relatively insensitive to the change of the LED calibration source, even though their spectral properties were different.

4 Conclusions

The results demonstrate the advantages of replacing incandescent standard lamps with LED-based standard sources, when calibrating photometers for measurement of LED lighting. The spectral errors are reduced by a factor of three. The uncertainties of photometer calibrations are further reduced by using an LED-based calibration standard and the PQED without $V(\lambda)$-filter as a reference. In both the PQED-based method and the traditional photometry, the accuracy of the wavelength scale is one of the largest contributions to the uncertainty [2,4]. The wavelength scale of the spectroradiometer used for measuring the spectrum of the LED

standard source can be conveniently calibrated using laser lines, but the wavelength scale uncertainty in the spectral responsivity of conventional photometers is more problematic.

References

1. Kärhä, P. et al. 2014. Natural and accelerated ageing of solid state lamps. In Proceedings of NEWRAD 2014 conference, 310-311.

2. Dönsberg, T. et al. 2014. New source and detector technology for the realization of photometric units. 6 p. - Accepted to Metrologia.

3. Dönsberg, T. et al. 2014. A primary standard of optical power based on induced-junction silicon photodiodes operated at room temperature. *Metrologia* 51, 197-202.

4. Poikonen, T. et al. 2009. Uncertainty analysis of photometer quality factor f_1'. *Metrologia* 40 75-80.